Tokyo Bay storm surge barrier: A conceptual design of the moveable barrier

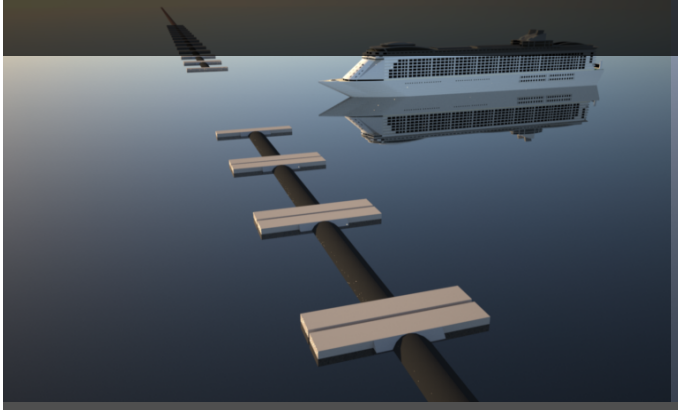

Kaichen Tian

October 2014

TU Delft
Delft University of Technology

Graduate:

K. Tian BSc
Student ID: 1547305
E: *kt4182@hotmail.com*
T: +31641402541

Pauwmolen 87
2645GC Delfgauw
The Netherlands

Educational institution:

Delft University of Technology
Faculty of Civil Engineering and Geosciences
Section Hydraulic Engineering

Stevinweg 1
2628CN Delft
The Netherlands

Graduation committee:

Prof. dr. ir. S.N. Jonkman — Delft University of Technology
Ir. A. van der Toorn — Delft University of Technology
Dr. ir. P.C.J. Hoogenboom — Delft University of Technology
Dr. Ir. M. Esteban — The University of Tokyo

Trademarks:

Preface

This is the final report for the thesis titled 'conceptual design of a storm surge barrier in Tokyo Bay'. The thesis is part of the Master's program Hydraulic Engineering, specialization Hydraulic Structures and has been completed at Delft University of Technology. The report describes the design process for the moveable barrier section of a storm surge barrier in Tokyo Bay, Japan. Part of the report structure and assumptions are based on the master thesis done by Peter A.L. Vries (Vries 2014)

I would like to express sincere gratitude to all of the members of my graduation committee, consisting of prof. dr. ir. S.N. Jonkman, ir. A. van der Toorn, dr. ir. P.C.J. Hoogenboom and dr. ir. M. Esteban, for their valuable input and support concerning this thesis. Furthermore, I would like to thank mister Hiroshi Takagi for providing help during my research.

Last but not least, I would like to thank my family, all my friends, (ex-)roommates and everyone who supported me for their support and mental coaching.

Kaichen Tian

Delft, October 2014

Abstract

Typhoons and tsunamis are dangerous phenomena for our society and Japan has been exposed to both of these hazards. The risks of these hazards are getting bigger and bigger due to the growing population in the cities near these 'dangerous' coasts. This thesis focuses on the design of a storm surge barrier located in Tokyo bay to reduce the flooding risk of Tokyo and its surrounding areas.based on a global-to-detailed approach.

The research starts with the analysis of the risk of Tokyo and its surrounding area to tsunamis and typhoons. Past existing investigations have shown that both large tsunamis and typhoons can cause considerable water level rises inside the bay. But since the chance of a large tsunamis to occur at Tokyo Bay is very small, while typhoons have a much higher frequency of occurrence. Together with the possible typhoon intensification and sea level rise in the future, it can be considered as the main threat for the Tokyo and Kanagawa region and therefor decisive for the design of the storm surge barrier.

The design process starts with drafting a design framework consisting choosing the most suitable barrier location and compiling of the corresponding functional requirements and boundary conditions. The span between Yokosuka and Futtsu is considered as the most suitable location for the placement of a barrier because of its short span and small 'to be closed off' area. As for the requirements, the design typhoon is chosen to be the Ise-Wan typhoon (1959). Also the barrier have to contain a navigation channel that is sufficient for future navigation and in order to maintain the ecological value of the bay, it is also desirable to maintain as much as possible water exchange between the bay and the sea.

The first design step considers the total barrier as a system. Considering the conservation of the environmental value of the Bay and the large depth of the chosen location, a barrier that is partly closure dam and partly moveable barrier is the considered most suitable for the situation. It is chosen to place the moveable barrier above the under water dam at the deepest part of the span due to the large soil volume saving and thus cost saving. It also reveals that due to the large retention capacity of the bay, the navigation channel can be left permanently open without exceeding the acceptable water level rise inside the bay when the other parts of he barrier are fully retaining.

The next design step will be focused on the moveable barrier part of the storm surge barrier. It is presumed that earthquakes will be critical for this project the during the chosen design life. As the foundation of the moveable barrier is recognized as critical point of the design, traditional bottom founded barriers are being compared with a new conceptual barrier type, floating barriers. The floating moveable barrier has shown great potential regarding earthquake resistance due its independence of the stability of the under water dam and the small energy transfer from seabed to the moveable barrier during earthquake conditions. and is therefor chosen for further design. Considering the cost and the preferred weight and size of the gate for a floating moveable barrier, it appears that the inflatable rubber gate is the most suitable gate type.

During the third design step a preliminary design for a floating moveable barrier is drafted to find the required main dimensions. The maximum water level rise at the seaside of the barrier during design typhoon condition is 2.25 m from the MSL. Since the moveable barrier is floating on water, it rises together with the storm surge, maintaining a minimum crest height of 1.75 m above surge level during the design typhoon condition after a SLR of 1 m. The maximum gap height between the floating barrier and the under water dam has been chosen to be 5 m. By placing maximum 5 floating moveable barriers, this gap can be left permanently open together with the navigation channel without the water level rise inside the protected area exceed its acceptable limit. It is chosen to have the floating barrier fixed with 7 mooring chains each side of the floating barrier. The number and type of mooring chains are chosen such that the floating barrier will still be kept in its position during the design typhoon scenario even after one of the mooring chains is broken.

In the last step of the design process a detailed analysis will be made on the earthquake resistance of the floating moveable barrier regarding dynamic resonance. An analytical dynamic model has been made for the floating barrier and its natural frequencies has been checked with the frequency spectrum of several past Japanese earthquakes. Based on the results from dynamic model no clear conclusion can be made on the dynamic stability of the floating barrier under earthquake condition. But since the resonance frequencies are really low and together with the contribution of the water damping, sag in the mooring lines and the short duration of the earthquakes, the maximum displacement of the floating barrier is expected to be limited. To validate this reasoning more research regarding the dynamic behaviour of the floating barrier is needed.

Overall the floating moveable barrier has been considered as a technically feasible design and it has shown great potential in its effectiveness regarding the earthquake resistance and flexibility in maintenance and replacement. For further research on this concept it is recommended to create a more detailed numerical dynamic model of the barrier to check its behaviour under both earthquake and storm conditions including the contribution of the water damping and the sag of the mooring lines. Other recommendations are the anchor design and the economical feasibility analysis of this type of barrier. Also it is interesting to investigate whether the gap between the floating barrier and the under water dam will lead to erosion problem of the under water dam and what the possible measures are to solve this problem.

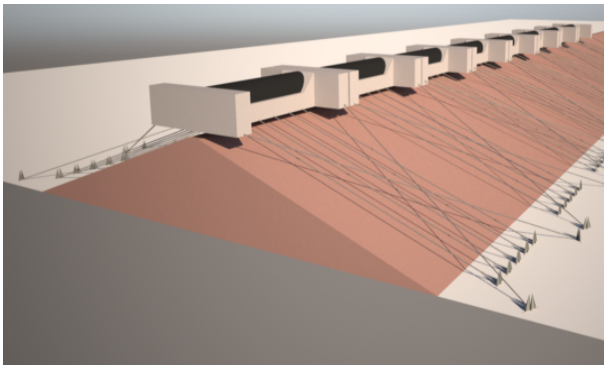

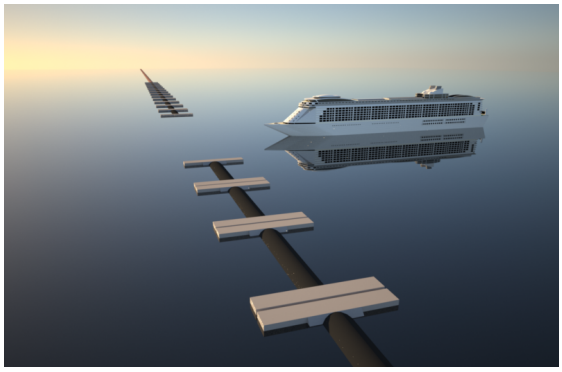

TABLE OF CONTENT

1 INTRODUCTION

Typhoons and tsunamis are dangerous phenomena for our society and Japan has been exposed to both of these hazards. The risks of these hazards are getting bigger and bigger due to the growing population in the cities near these 'dangerous' coasts. From the past we have noticed that the impact of such hazards can be enormous. Very well known examples are the recent tsunami of 2011 in Japan and the typhoon Vera in Ise Bay (Japan) in 1959. Figure 1 shows the vulnerable coastlines in the world that are at risk for tsunamis and Figure 2 show the origins and tracks of the tropical typhoons together with the different names used around the world.

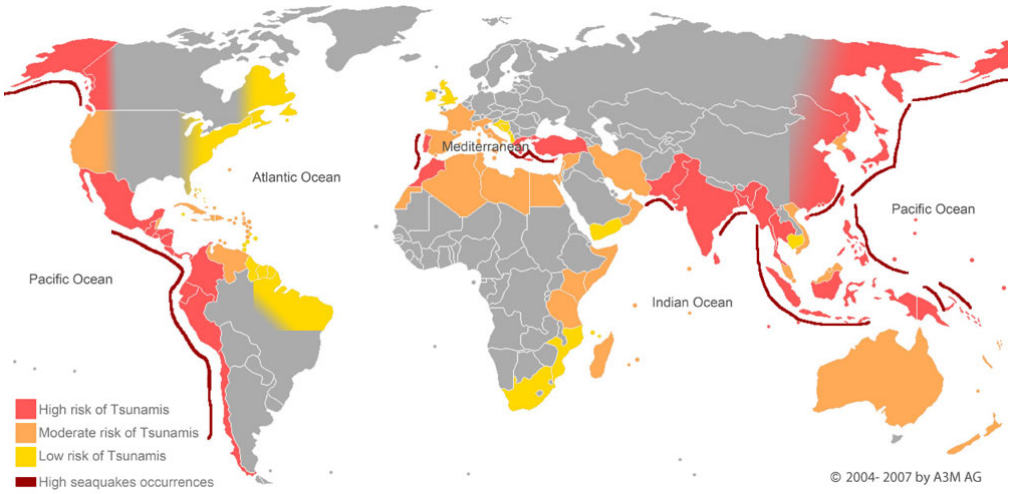

FIGURE 1: MAP OF COASTLINES AND THEIR TSUNAMI RISKS (A3M MOBILE PERSONAL PROTECTION GMBH 2012)

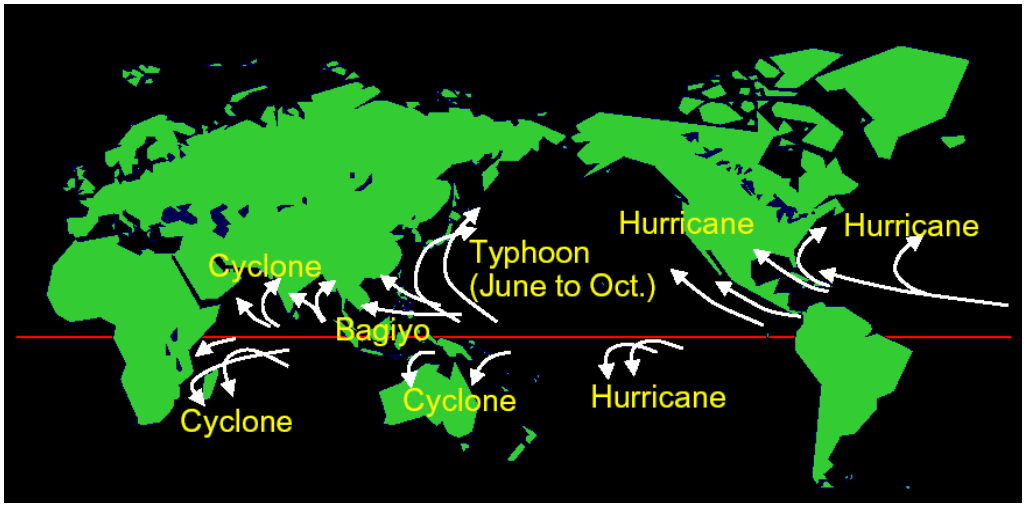

FIGURE 2: ORIGINS AND TRACKS OF TROPICAL TYPHOONS TOGETHER WITH DIFFERENT NAMES AROUND THE WORLD (KLAVER 2005)

1.1 Future problems

1.1.1 TSUNAMI

It can cause many problems in the future when no measures are taken to protect us from the tsunamis, which will hinder the development of our prosperity. Places where tsunamis often occur will be difficult to inhabit and every time a tsunami occurs, many casualties will take place during the event. Lives will be lost and buildings will be destroyed. This will lead to a lot of reconstructions and rescheduling. Due to the tsunami in 2011 in Japan, 15889 people lost their lives (National police agency of Japan 2014), many have lost their homes and buildings and structures have to be reconstructed. This tragedy may happen again if no measures are taken. Since the Tokyo area is the densest populated area in Japan, therefor it is important to analyse the risk of the Tokyo's exposure to tsunami hazards and take measures if it is needed.

1.1.2 TYPHOONS

Due the climate change, sea level rise (Church 2013) and more intense typhoons (Yasuda 2010) have been predicted for the future and the current coastal protections in Tokyo might not be sufficient for these future changes. Since a considerable large part of the population and national wealth of Japan is concentrated in Tokyo, which results in a high risk, it is important and necessary to protect this area from the possible typhoon hazards.

Both tsunami and typhoon will have social effects on the society. The idea that his kind of hazard can strike without sufficient protection will cause fear among the people. It will reduce the general happiness of the population, which will act as an unstable factor for the society.

1.2 Objective

The ambition of this research is to maintain/improve the safety conditions of the Tokyo and its surrounding area against flooding due to typhoons and tsunamis. Therefor the main objective of this thesis is to analysis the risk of Tokyo and its surrounding area to the typhoons and tsunamis and design of a storm surge barrier to reduce the this risk in the future.

1.3 Research questions

1.3.1 MAIN QUESTION

What is a technically feasible design for s storm surge barrier in the Tokyo Bay to reduce the flood risk in Tokyo and its surrounding area in the future?

1.3.2 SUB QUESTIONS

1. What is the main threat that caused the largest flood risk in Tokyo and its surrounding area?
2. What other measures are there to reduce the flood risk?
3. What are the advantages of constructing a storm surge barrier compared to the other measures?
4. What are the requirements for the construction of a storm surge barrier in the Tokyo Bay?
5. What are the technical challenges of the construction of a storm surge barrier in the Tokyo Bay and how can they be solved?
6. What is the influence of earthquakes on the strength/stability of the storm surge barrier?

1.4 Research approach

This thesis focuses on the design of a storm surge barrier located in Tokyo bay to reduce the flooding risk of Tokyo and its surrounding areas. First both the threat of typhoon and tsunami on the Tokyo area will be analysed based on the existing investigations. Based on this analysis the corresponding requirements for the storm surge barrier will be determined. The focus of this thesis will be on the design from a conceptual level to a detailed level using several design steps. In this way different design aspect can be assessed thoroughly based on the applicability to the situation.

1.5 Report structure

This document is the main report of the master thesis 'Tokyo Bay storm surge barrier: A conceptual design of the moveable barrier'. It gives an overview of the thoughts and decisions of the auteur during the research and design process. Background information and extensive calculations are separated from this main report and are presented in the appendices. The structure of this report is schematically presented in Table 1.

First background information is given for Japan and Tokyo in chapter 2. It contains the social background of Japan and some site specific information of Tokyo Bay. Also an short description of the typhoon and tsunami history of Japan will be given.

In chapter 3 an analysis has been done for the threat of both typhoon and tsunami on Tokyo and its surrounding area based on existing investigations. Also several possible protection measures beside the construction of a storm surge barrier will be presented qualitatively and the choice of further investigation on the storm surge barrier solution will be elaborated.

In chapter 4 the important cost drivers for a storm surge barrier will be recognized and the most suitable barrier location will be determined based on these cost drivers.

Subsequently the framework in which the storm surge barrier should be designed is drafted in chapter 5. This consists of the requirements and the boundary conditions. The combination of the requirements and boundary conditions serves as the input for the design steps.

The design process is based on a general-to-detailed design approach. Chapter 6 marks as the start of this design process. This first design step investigates the total barrier as a system, including both moveable barrier and closure dam. The distribution between closure dam and moveable barrier will be determined. Also it will be checked if it is possible to keep the navigation channel permanent open during storm conditions. Next in chapter 6 it will focus on the moveable barrier. In this chapter the foundation type of the barrier will be chosen (floating or bottom founded). This is due to the recognition of the earthquake resistance of the moveable barrier as the decisive factor for the total cost of the moveable barrier. Based on the chosen foundation type, the most suitable gate type for the moveable barrier will be chosen using a Multi Criteria Analysis. In chapter 7 a preliminary design is presented for the chosen barrier type from the previous design steps (floating moveable barrier). This preliminary design aims on giving a feel for the required dimensions and revealing the technical challenges.

In chapter 8 a check of the earthquake resistance of the floating moveable barrier regarding the resonance occurrence will be performed. The earthquake ground motion frequencies and amplitudes will be analysed and compared to the natural frequencies of the floating barrier obtained from a simplified dynamic model.

Chapter 9 contains conclusions and recommendations for future research.

TABLE 1: REPORT STRUCTURE

Introduction	Chapter 1 Introduction	
	Chapter 2 Background information Japan and Tokyo	
Analysis	Chapter 3 Analysis future tsunami/typhoon hazards in Tokyo Bay	Tsunami hazard
		Typhoon hazard
		Protection measures
Design framework	Chapter 4 Barrier location	
	Chapter 5 Requirements and boundary conditions	
Design process	Chapter 6 System level design: Total barrier system	Distribution of retaining structure
		Water level inside the bay with permanent open navigation channel
	Chapter 7 Subsystem level design: Moveable barrier system	Foundation type assessment
		Gate type assessment
	Chapter 8 Preliminary design Floating moveable barrier	Floating caisson design
		Mooring lines design
		Inflatable rubber gate
		Anchors
Check earthquake resistance	Chapter 9 Earthquake resistance floating barrier	Earthquake ground motion frequencies and amplitudes
		Dynamic model floating barrier
		Comparison natural frequency range floating barrier and earthquake frequencies.
Conclusion	Chapter 10 Conlusion and recommendation	

2 JAPAN AND TOKYO

In this chapter a global overview of Japans and Tokyo's current state regarding it's exposure to tsunamis and typhoons will be given. First a brief description will be given about Japan, Tokyo Bay and Tokyo and their geological character. After that some background information regarding the tsunami and typhoon conditions in Japan will be given

2.1 Natural and social condition

Japan is and island country located in the north-western part of the Pacific Ocean. It is separated from the Eurasian continent by the Sea of Japan and the East China Sea. Japan has a total land area of approximately 378,000 km² and nearly 80% among the area is mountainous and unsuitable for agriculture, industrial or residential use. The majority of the population and the most activities are concentrated in numerous small and narrow plains that are mainly located along the coasts. The coastline is in total 35,000 km in length and has various configurations: plain beaches, bays and peninsulas.

The Japanese population counted in 2008 128 million people, of which the majority resides in the urban areas along the coast. In 2005, the population density consisted on average 343 persons per km². Due the high population density in the coastal areas, Japan has a high risk of coastal natural disasters: tsunami and storm surge. For example, a storm surge of 3.5 m was generated in the Ise bay by the Typhoon Ise-wan in 1959, which has led to unprecedented damage including more than 5,000 people killed or missing (PIANC 2010).

The Japanese economy is also well developed in the coastal areas. Since Japan has only limited natural resources and therefore the economy mainly depends on foreign imports, this has led to well developed industries, especially around ports.

2.2 Tokyo bay

Tokyo bay, also known as Edo bay, lies in the southern Kanto region of Japan, which spans the coast of Tokyo, Kanagawa Prefecture and Chiba Prefecture. It is connected to the Pacific Ocean by the Uraga Channel and is both the most populated and largest industrialized area in Japan. In Figure 3 is the Tokyo Bay shown on map.

FIGURE 3: MAP TOKYO BAY (GOOGLE MAPS SD)

2.2.1 GEOGRAPHY

Tokyo bay is surrounded by the Boso Penisula in Chiba Prefecture to the east and the Miura Peninsula in Kanagawa Prefecture to the west. The shore of the Tokyo bay is subjected to rapid marine erosion and consists of a diluvial plateau. Sediments on the shore of the bay make for a smooth, continuous shoreline.

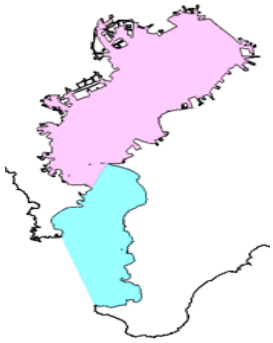

FIGURE 4: BOUNDARY TOKYO BAY (WIKIPEDIA SD)

2.2.2 BOUNDARIES

In a narrow sense, Tokyo Bay is the red part of Figure 4. This area covers about 922 km^2. In a broader sense, Tokyo Bay includes the Uraga Channel, which is the red part plus the blue part in Figure 4. The area of including the Uraga channel covers 1,500 km^2.

2.2.3 DEPTH

Nakanose, which is the shoal between Cape Futtsu in Chiba Prefecture and Cape Honmaku in Yokohama, has a depth of 20 m. Simple submarine topography can be found North of this area and has a depth of 40 m. Areas south of Nakanose are significantly deeper moving towards the Pacific Ocean. See Figure 5 for impression.

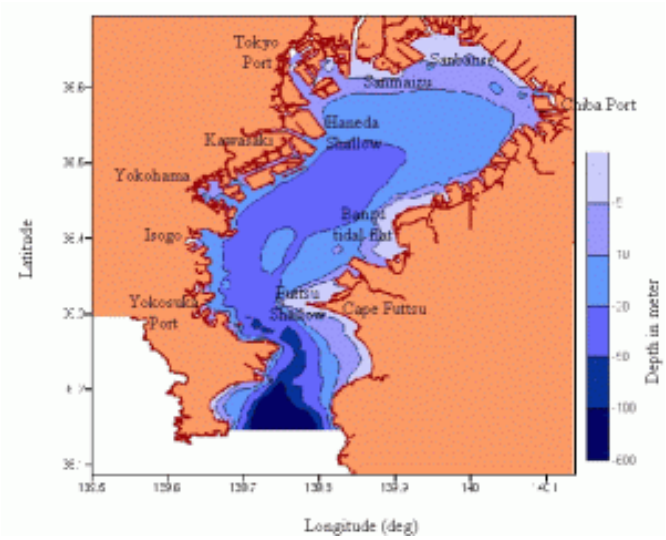

FIGURE 5: DEPTH MAP TOKYO BAY (EXTRA.SPRINGERS.COM SD)

2.2.4 ISLANDS

Sarushima is the only natural island in Tokyo Bay. It is located at Yokosuka in Kanagawa Prefecture. Beside Sarushima, there are many artificial island in the Tokyo Bay, which are Odaiba, Hakkei Island, Heiwa, Katsushima, Showa, Keihin and Higashiogi Island. Part of these artificial islands were built as naval fortification in the Meiji and Taisho period, while others are used for housing or rubbish dump.

2.2.5 RIVERS

Several rivers, which flow into the Tokyo Bay, provide water for residential and industrial areas along the bay. These rivers are listed below.

- The Tama and Arakawa rivers flow into the bay in Tokyo.
- The Edo River flows into the bay between Tokyo and Chiba Prefecture.
- The Obitsu and Yoro rivers flow into the bay in Chiba Prefecture

2.2.6 LAND RECLAMATION

Land reclamation along the Tokyo Bay has been carried out since a long time. Areas with a depth less than 5 m are simplest to carry out landfill, whereby the sand from the floor of Tokyo is used for the reclamation. The reclaimed land area in Tokyo Bay is approximately 249 km^2 (Wikipedia sd).

2.2.7 BRIDGES

The Tokyo Bay Aqua-line Bridge connects Kawasaki and kisararu by crossing the Tokyo Bay. Also the Tokyo-Wan Ferry crosses the bay toward the Uraga Channel between Kurihama in Yokosuka and Kanaya in Futtsu on the Chiba side.

2.2.8 FISHING

In the past Tokyo Bay was a rich center for fishing industry, but due to the industrialization in the early 20th century and the construction of the Keihin and Keiyo industrial zones after the WOII, the fishing industry inside the Tokyo Bay is almost completely ceased.

2.2.9 PORTS

Numerous important Japanese ports are located in the Tokyo Bay. They are not only one of the busiest port in Japan, but also in the Asia-Pacific region. These ports are listed below.

- The Port of Yokohama
- The Port of Chiba
- The Port of Tokyo
- The Port of Kawasaki
- The Port of Yokosuka
- The Port of Kisarazu

2.2.10 INDUSTRIAL ZONES

Industrial zones on Tokyo Bay started developing as early as in the mid 19th century. The Keihin Industrial Zone was built on reclaimed land in Kanagawa Prefecture to the south of Tokyo. After WOII, this was expanded to the Keiyo Industrial Zone in Chiba Prefecture along the north and east coasts of the Tokyo Bay, which has resulted in the largest industrialized area in Japan.

2.2.11 MILITARY FACILITIES

Naval bases of the United States Forces Japan and the Japan Maritime Self-Defense Force is located at the Port of Yokosuka.

2.3 Tokyo

Tokyo city has a population of around 13 million inhabitants and is the city with the greatest GDP in the world with a gross output of 1479 billion dollars (Pricewaterhouse Coopers 2009). Together with adjacent cities such as Yokohama and Kawasaki it forms what it is called the 'greater Tokyo', having a total population of more than 35 million people, making it the largest megalopolis in the world. In the Tokyo area, an estimated 116 square kilometres of land lies below sea level, which counts 1.76 million inhabitants in that area, see Figure 6. This makes Tokyo very vulnerable for inundation if the existing coastal protection fails.

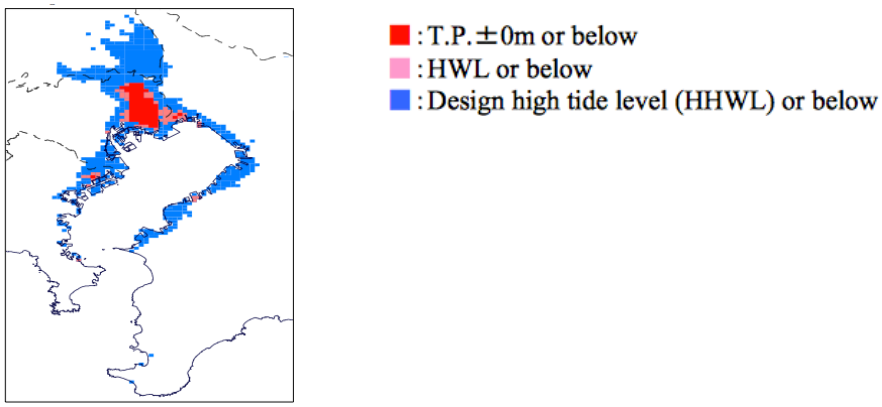

FIGURE 6: ELEVATION MAP TOKYO (MLIT SD)

2.4 Tsunami in Japan

Japan is situated in the circum-Pacific volcanic belt of the 'Pacific Ring of Fire' and subduction zones in which big earthquakes occur are formed by four earth's crusts of the Eurasian Plate, the North American Plate, the Pacific Plate and the Philippine Sea Plate encountering under the Japanese islands and surrounding sea, as shown in Figure 7. In Japanese history, tsunamis, which are generated by big earthquakes along these subduction zones, occurred repeatedly. The earliest record in the Japanese history of tsunami disaster is an event in the year 684, which was caused by the Hakuo-Nankai Earthquake. The most recent tsunami was generated by the Tohoku earthquake in 2011. This earthquake was also the largest recorded earthquake in the Japanese history.

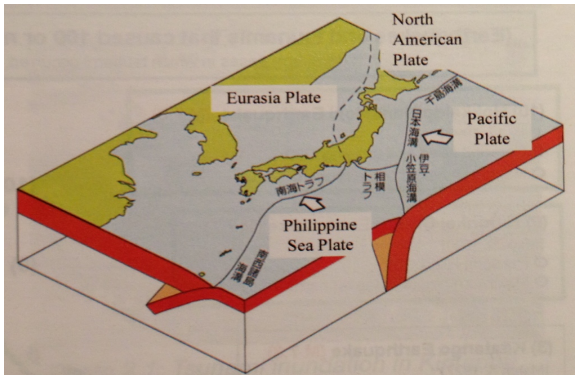

FIGURE 7: TECTONIC PLATES SUROUNDING JAPAN (PIANC 2010)

2.4.1 2011 TOHOKU EARTHQUAKE

On March 11, 2011 at 14:46 local time, a large earthquake occurred 130 km offshore the north-eastern coast of Japan. According to estimates, this earthquake was of magnitude 9.0 on the Richter scale, which makes it the largest earthquake ever recorded in Japan. The Japan Meteorological Agency issued a tsunami warning three minutes after the main earthquake. Soon after that, a tsunami of 2.6 to 7.7 m was recorded by the GPS mounted buoys at a spot of 100-200 m in water depth off the Tohoku coast. Six hours after the earthquake of March 11, a nuclear emergency at Fukushima Daiichi nuclear power plant was reported by the International Atomic Energy Agency. On March 12 and at 15:30 local time, a first hydrogen explosion took place, which was followed by two more explosions on the 14th and 15th of March. As result of those events, a large emission of radiation occurred that has reached 400 millisievert per hour, which is 1.5 million times more than the radiation that a normal human being is supposed to be exposed per hour. A detailed description of the 2011 Tohoku earthquake can be found in Appendix 1.

2.5 Typhoon in Japan

The typical typhoon season in Japan is between June and October. Typhoons are initially generated in the tropical regions. They are gradually weakened as they move north (in the northern hemisphere) due to the force caused by the Earth's rotation. The cause of this weakening process is the decrease in the sea surface temperature as the typhoon moves north; this will eventually result in the short falling of the vapour supply due to the energy loss caused by friction. This vapour supply will be completely cut off after the typhoon hits land.

2.5.1 TYPHOON PATHS FOR JAPAN

Typhoons are driven by high altitude winds. In low latitude regions, east winds are generally prevalent in high altitudes, therefore the typhoon will move west while gradually veering north. This changes when the typhoon comes to mid-latitude regions where west winds become dominant, the course of the typhoon will change towards northeast, see Figure 8.

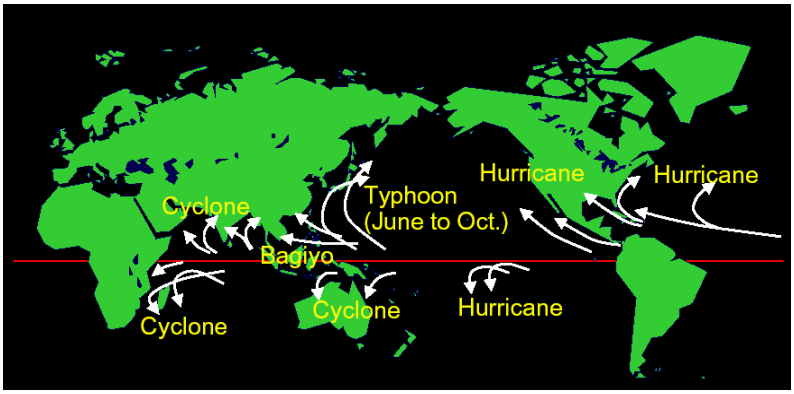

FIGURE 8: ORIGINS AND TRACKS OF TROPICAL TYPHOONS TOGETHER WITH DIFFERENT NAMES AROUND THE WORLD (KLAVER 2005)

However in August the movement of the typhoon can be unstable due to the weak west winds in high altitude. The typhoons can therefore meander and cause unexpected damage. These high altitude west winds become stronger after September, which leads to an arc form movement of the typhoon from southern seas towards Japan. Disastrous typhoons in the past such as the Muroto Typhoon (1934) and the Ise Bay Typhoon (1959) followed this specific course. These tropical typhoons lose their tropical characteristics after it curves into the northeastern direction and comes in contact with a colder environment. This leads to expansion of the circulation, decrease of the maximum wind speed, increase of the translational (forward) speed and increase of the asymmetry of the distribution of the winds, rainfall and temperature.

2.5.2 NUMBER OF TYPHOON LANDINGS PER YEAR IN JAPAN

Twenty-seven typhoons are developed every year in the Northwest Pacific basin on average, from which two or three of these hit Japan. In an extreme year this number can increase to ten typhoons, which was the case in 2004, see Figure 9.

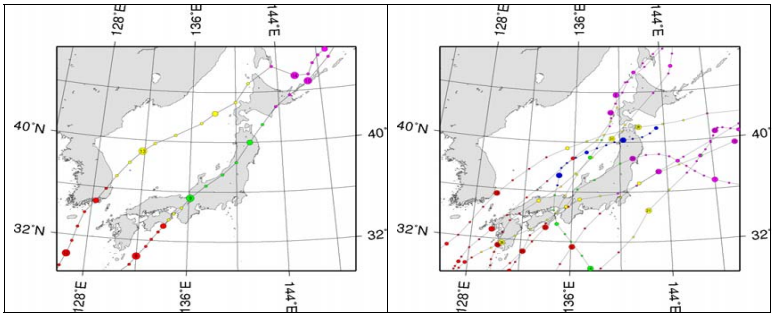

FIGURE 9: NUMBER OF TYPHOON LANDING ON JAPAN. FOR A NORMAL YEAR TWO TYPHOONS (IN 2003 LEFT) AND FORA N EXTREME YEAR TEN (KLAVER 2005)

2.6 Summary

Japan has a total land area of approximately 378,000 km². The Japanese population counted in 2008 128 million people, of which the majority resides in the urban areas along the coast. Also the Japanese economy is also well developed in the coastal areas.

Tokyo bay lies in the southern Kanto region of Japan, which spans the coast of Tokyo, Kanagawa Prefecture and Chiba Prefecture. Including the Uraga channel, Tokyo Bay covers an area of 1500 km². Numerous important Japanese ports are located in the Tokyo Bay. The most important ports are port of Tokyo, port of Yokohama and port of Chiba.

Tokyo city has a population of around 13 million inhabitants and is the city with the greatest GDP in the world with a gross output of 1.479 billion dollars. Together with adjacent cities such as Yokohama and Kawasaki it forms what it is called the 'greater Tokyo', having a total population of more than 35 million people, making it the largest megalopolis in the world. In the Tokyo area, an estimated 116 square kilometres of land lies below sea level, which counts 1.76 million inhabitants in that area,

Japan is situated in the circum-Pacific volcanic belt of the 'Pacific Ring of Fire' where big earthquakes occur. In Japanese history, tsunamis, which are generated by big earthquakes along these subduction zones, occurred repeatedly. The typical typhoon season in Japan is between June and October. Twenty-seven typhoons are developed every year in the Northwest Pacific basin on average, from which two or three of these hit Japan. In an extreme year this number can increase to ten typhoons, which was the case in 2004.

3 ANALYSIS FUTURE TSUNAMI/TYPHOON HAZARDS TOKYO BAY

In this chapter threat of tsunamis and typhoons for the Tokyo and Kanagawa region will be analysed. First the likelihood of the occurrence of a large tsunami at Tokyo Bay will be discussed. Also results of an existing simulation of a tsunami at Tokyo will be presented. After that the possible typhoon intensification and sea level rise in the future due to the climate change will be discussed together with some simulation results regarding the flood damage on Tokyo and the effectiveness of the construction of a storm surge barrier in the middle of the bay. At the end of this chapter the possible protection measures will be considered and elaborated.

3.1 Tsunami

Tokyo Bay is vulnerable to a tsunami originating from the Tokai region, which is located 100 – 150 km southwest of the Boso Peninsula and the so called 'Genroku' earthquakes, located in the south of the Kanto region. The likelihood of these future tsunamis will be elaborated followed by a simulation of a tsunami caused by a Genroku type of earthquake done by the Tokyo Metropolitan Government.

3.1.1 LIKELIHOOD OF FUTURE TSUNAMIS IN TOKYO BAY.

In the Tokai region the Philippine Plate is sliding under the Eurasia Plate. A sharp-edged peninsula that juts into the sea is being pushed down several millimetres a year under a process called crustal deformation. A catastrophic quake can be produced as the result of the pressure release of this crustal deformation, which can cause the land to jump up several meters. This kind of quake occurs every 150 or so. Since the last one was in 1857, scientists at the Earthquake Research Committee predicted an 87% chance of a massive quake registering 8 or more on the Richter Scale hitting this region before 2040 (Hays 2009).

As for the Genroku type of earthquakes in Kanto, since its location is directly in front of the mouth of Tokyo Bay, many scientists belief this kind of earthquake would cause the largest tsunamis in Tokyo Bay. The original Genroku earthquake has a magnitude of 8.2 Ms. The return period of such an earthquake is considered to be 2300 years (personal communication Hiroshi Takagi, Associate Professor at the Tokyo Institute of Technology). The Genroku Kanto earthquake originally happened in 1703, therefore the occurrence of such an earthquake within the design period of the barrier is considered to be very small. But given the great economical value of Tokyo, a tsunami protection safety of 1/2300 year is reasonable. The Tokyo Metropolitan Government has made a tsunami simulation for the Tokyo Bay using the Genroku Kanto earthquake in 1703 as reference. This simulation will be described in the next paragraph.

3.1.2 TSUNAMI SIMULATIONS

The Tokyo Metropolitan Government (Takagi 2013) has done 2 tsunami simulations for the Tokyo Bay. One generated by a 1703 Genroku type of earthquake, and one by a M7.3 earthquake in the north part of Tokyo Bay directly before Tokyo city, both using a high water level of T.P. +0.966 m (Tokyo peil). The result water level around Tokyo city for both cases is given in Figure 10 and Figure 11. The maximum given tsunami height is 2.61 m above mean sea level in Shinagawa.

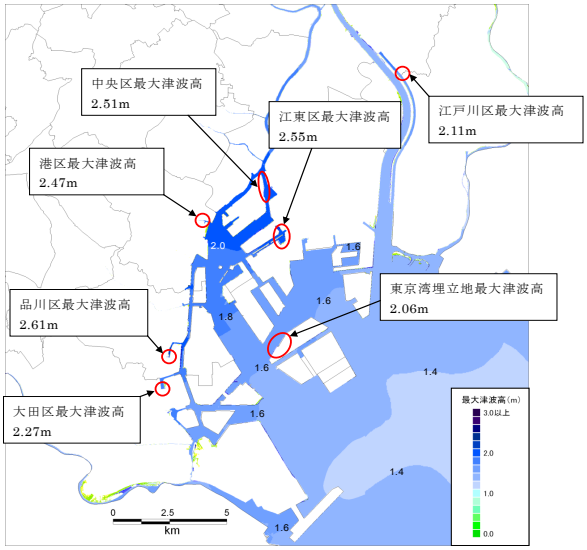

FIGURE 10: TSUNAMI HEIGHT TOKYO USING GENROKU EARTHQUAKE AS REFERENCE. (TAKAGI 2013)

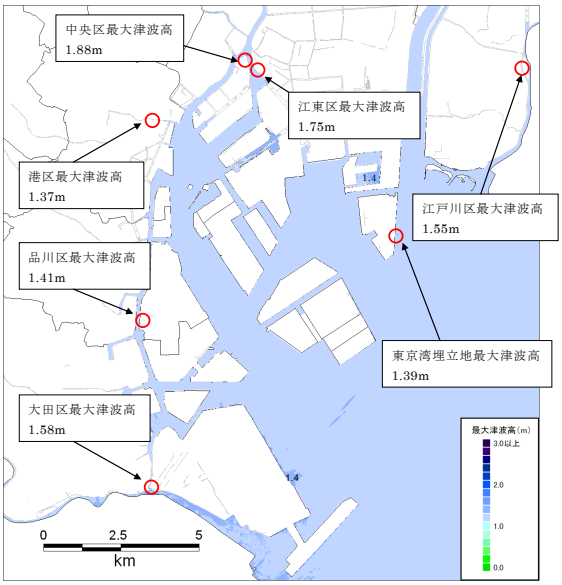

FIGURE 11: TSUNAMI HEIGHT TOKYO USING M7.3 EARTHQUAKE IN THE NORTH PART OF TOKYO BAY (TAKAGI 2013)

Except for the Tokyo Metropolitan Government, the same simulation for the Genroku earthquake induced tsunami is also done by Y. Wu (Wu 2012). Also the results of this simulation has shown relatively small water heights in the Bay during the tsunami. The results of this simulations are shown in Figure 12.

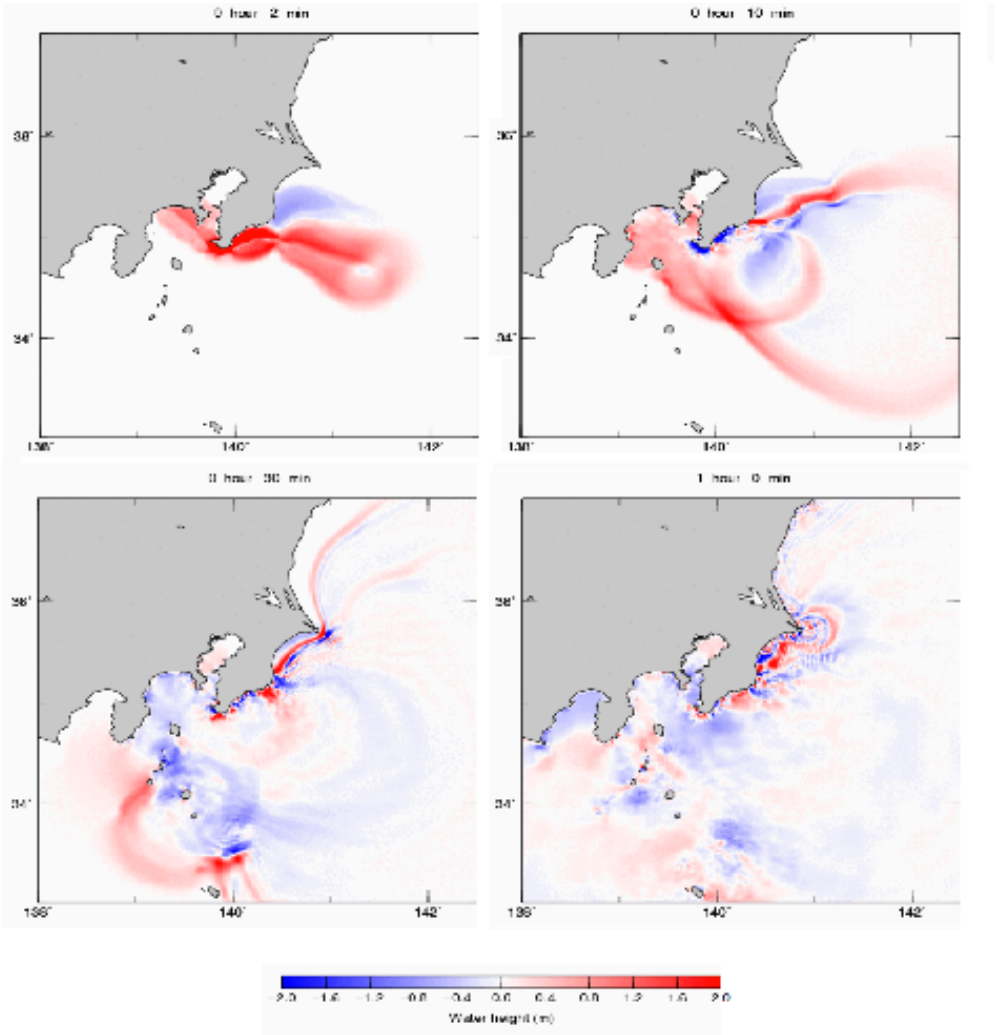

FIGURE 12: SNAPSHOT TSUNAMI WAVE OF 2 MINUTES, 10 MINUTES, 30 MINUTES AND 1 HOUR AFTER THE EARTHQUAKE.

3.1.3 CONCLUSION

Despite both simulations have shown a considerable water level elevation inside the bay caused by tsunamis, the chance of occurrence of such a tsunami is very small and the duration of the tsunami is really short. Also the chance of a tsunami attack during the maximum water level of the spring tide is considered negligible small. Therefor based on the result of the simulation it can be concluded that the risk caused by a tsunami attack on Tokyo and Kanagawa region is negligible small and the water level elevation caused by the tsunami won't be decisive for the design of the protection measure.

3.2 Typhoon

As the climate changes and the sea level rises, Tokyo is getting more and more vulnerable for the hazards caused by typhoons. In this paragraph future risk of the typhoon risk for Tokyo will be elaborated based on existing research followed by simulations done for several disaster scenarios.

3.2.1 TYPHOON INTENSIFICATION AND SEA LEVEL RISE DUE TO CLIMATE CHANGE

Global warming is a topical issue. Since high surface temperature is needed to generate tropical typhoons and the heat from the evaporation of seawater is the source of their strength, future increase in global temperature could lead to an increase of intensity of these typhoons. In the past several years, research has been done on this topic. Yasuda (Yasuda 2010) has provided a probability distribution function of the central pressure, outlining the present and future expected distribution of typhoon intensity in the Tokyo Bay area. This distribution is reproduced by Hoshino (Hoshino 2013) and is shown in Figure 13.

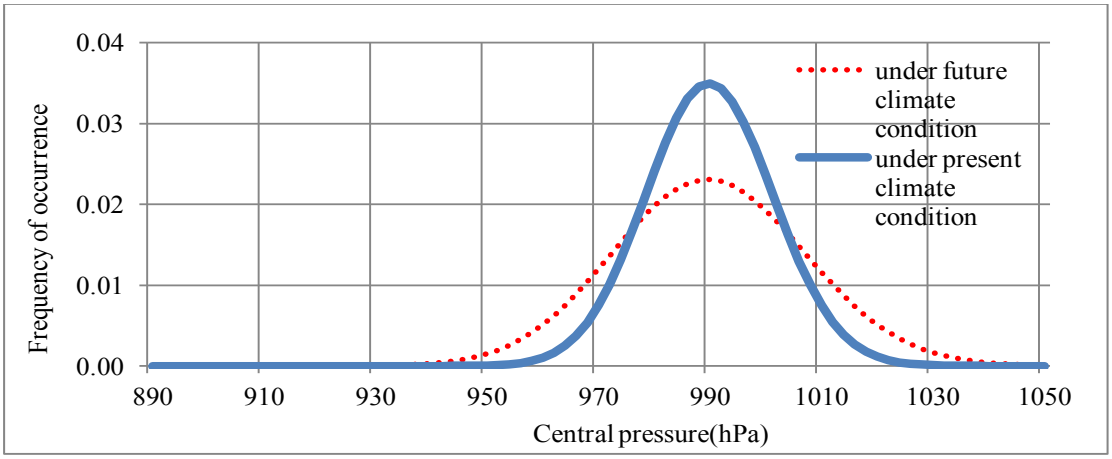

FIGURE 13: PROBABILITY DISTRIBUTION CENTRAL PRESSURE TOKYO BAY AREA (YASUDA 2010)

Beside intensification of the tropical typhoons, sea level rise is also a potential factor that could increase the chance of inundation in the low-lying areas around Tokyo Bay. The global sea level rose by an average around 1.7mm per year in the last century and satellite observations has shown that this has been increased to 3.7 mm per year since 2007. The IPCC 5AR (Church 2013) has shown a future projection of a worst scenario global sea level rise between 0.52 and 0.98 m higher than at present by the end of the 21st century. But recently many researchers believe that the sea level rise by 2100 is likely to exceed this range. This is because the IPCC 5AR has only comprised simple mass balance estimates of the contribution from the Greenland and Antartic ice sheets. Vermeer and Rahmstorf (Vermeer en Rahmstorf 2009) have argued a more extreme scenario of a sea level rise between the 0.81 and 1.90 m by the year 2100.

Despite the fact that the cities that are located around Tokyo Bay are generally well protected against storm surges by an extensive network of coastal structures, the effects of sea level rise, combined with increases in storm surges, could lead to increases in the chance of inundation and increase of the flooded areas.

3.2.2 COASTAL AND RIVER PROTECTION

The Tokyo Bay has 150 km coastal dikes and 157 km river dikes, which 89% and 78% are sufficient respectively for the current design dike height (MLIT sd), see Figure 14 and Figure 15.

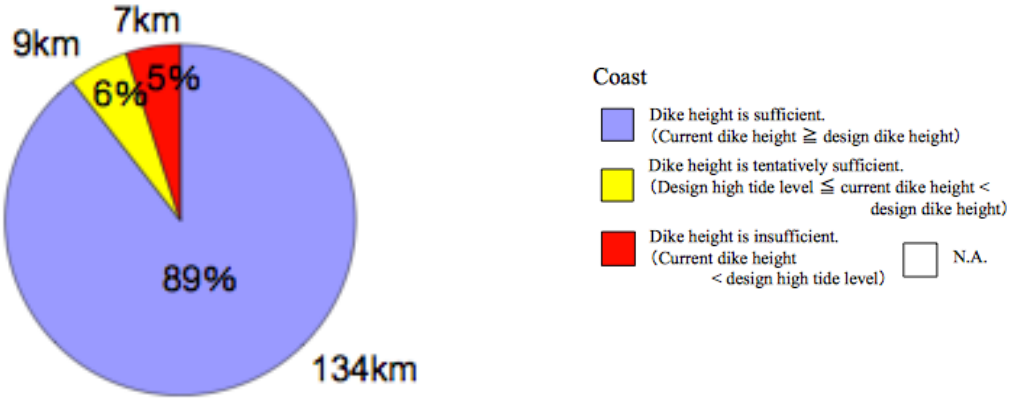

FIGURE 14: COASTAL DIKE HEIGHT (MLIT SD)

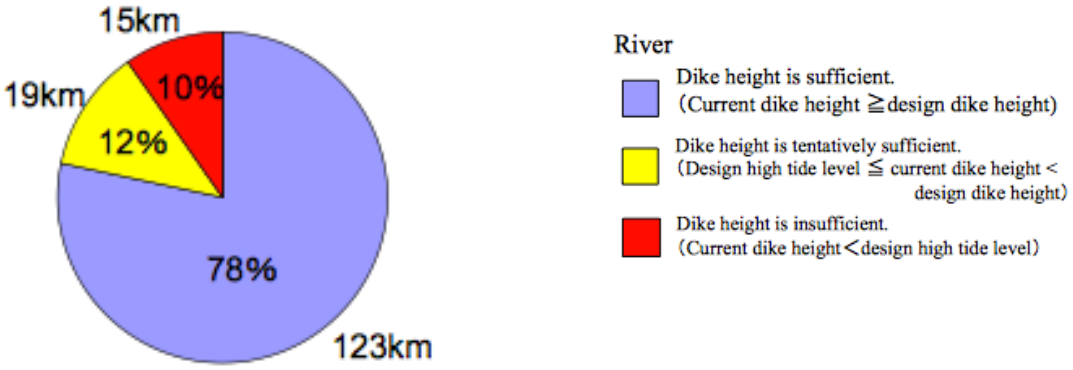

FIGURE 15: RIVER DIKE HEIGHT (MLIT SD)

Of these dikes, 62% and 73% respectively of the coastal and river dike possesses earthquake resistance measures, see Figure 16 and Figure 17. In Figure 18 the age of the current coastal dikes is shown.

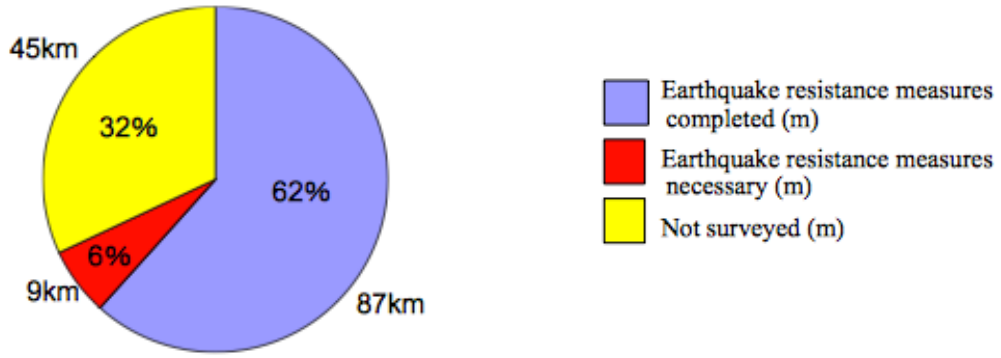

FIGURE 16: EARTHQUAKE RESISTANCE COASTAL DIKES (MLIT SD)

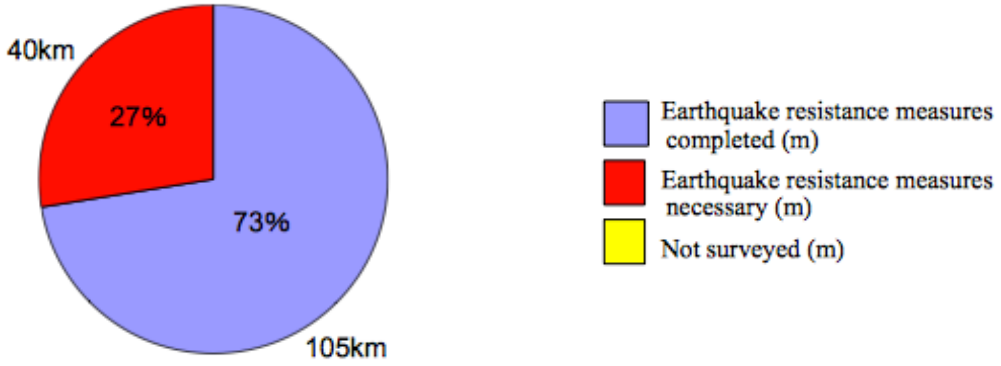

FIGURE 17: EARTHQUAKE RESISTANCE RIVER DIKES (MLIT SD)

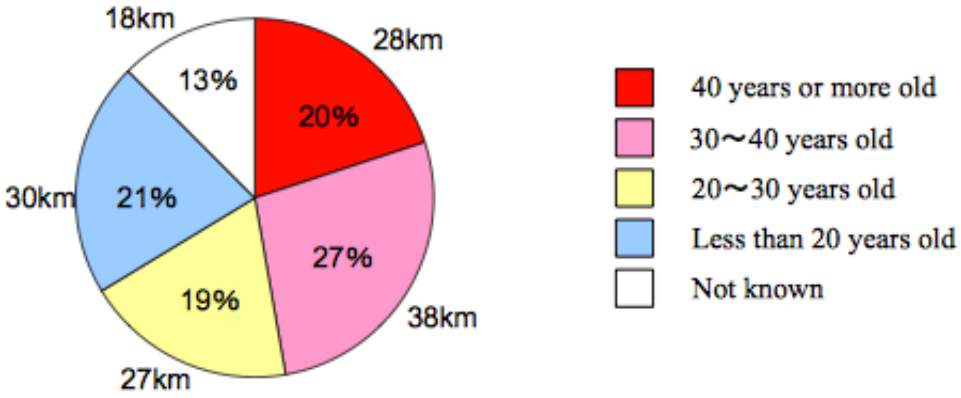

FIGURE 18: AGE CURRENT COASTAL DIKES (MLIT SD)

3.2.3 TYPHOONS SIMULATION ON PRESENT AND FUTURE SCENARIOS ON TOKYO BAY

In the past years numbers of simulations has been done by the Japanese about the typhoon impact on Tokyo Bay. Recent research by S. Hoshino (Hoshino 2013) has also included the effect of the climate change and sea level rise into their simulation, showing results for both present and future scenarios, clearly illustrates the conceivable disaster that could be magnified by these effects. This simulation will be elaborated in this paragraph.

3.2.3.1 The simulation

For this simulation the typhoon of October 1917 is used as reference, which is the worst typhoon to affect Tokyo Bay in the last 100 years. By using this typhoon they have obtained water level elevation for a 1 in 100 year event for present and different future scenarios for different locations in Tokyo Bay. These locations are shown in Figure 19 and Table 2.

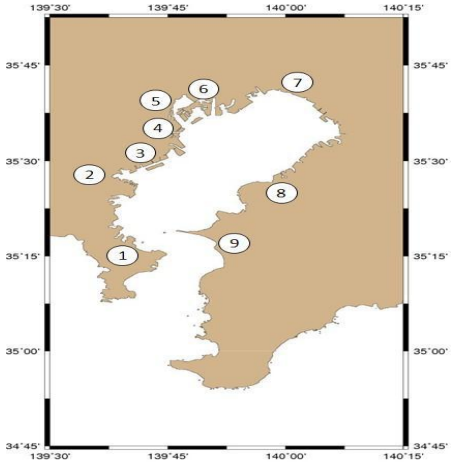

FIGURE 19: LOCATIONS OF INTEREST TOKYO BAY SIMULATION (HOSHINO 2013)

TABLE 2: LOCATIONS OF INTEREST TOKYO BAY SIMULATION (HOSHINO 2013)

No	Location	Prefecture
1	Yokosuka	Kanagawa
2	Yokohama	
3	Kawasaki	
4	Samezu	Tokyo
5	Shibaura	
6	Toyosu	
7	Funabashi	Chiba
8	Sodegaura	
9	Futtsu	

For the simulation four different future scenarios have been separated regarding the global sea level rise with the proportional central pressure of the typhoon in 2100. A summary of the simulated scenarios is given in Table 3. A more comprehensive description of the simulation is found in Appendix 2.

TABLE 3: SIMULATED SEA LEVEL RISE SCENARIOS (HOSHINO 2013)

P_0 (Taisho 1917 typhoon)	P_0 (2100, 1 in 100 year storm)	r_{max}	Sea level rise
952.7	933.9	Probability distribution function according to Yasuda et al. (2010b), 10 computations for each scenario	0(cm)
			28(cm)
			59(cm)
			190(cm)

The simulated path of the typhoon is approximately a straight line. The eye of the storm did not through the center of Tokyo Bay, but west of it. This is to ascertain the worst scenario for a 1 in 100 year typhoon. The course of the simulated typhoon is shown in Figure 20.

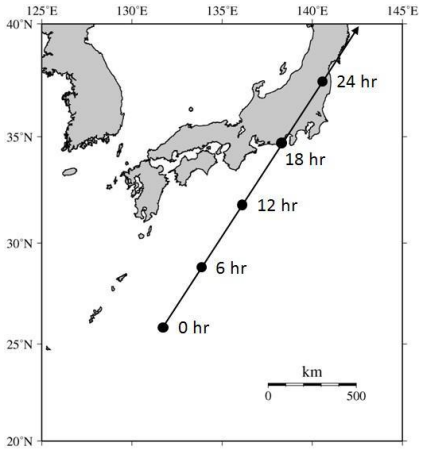

FIGURE 20: PATH SIMULATED TYPHOON (HOSHINO 2013)

3.2.3.2 Results

The results shown in Figure 21 give the water levels that could be expected for a 1 in 100 year typhoon by the year 2100 at the 9 points of interest after taking into account the intensification of the typhoons due to climate change and a sea level rise of 0.59 m. The vertical axis of the graph represents the frequency of occurrence and the horizontal axis the final water level. The dotted line in this graph shows the level of the current coastal defence in each of these locations. Note water levels are given as probability distribution dependent on the radius of maximum wind speed, which does not have a deterministic value. In the simulation done by S. Hoshino (Hoshino 2013) these values are defined using the stochastic parameters provided by Yasuda (Yasuda 2010).

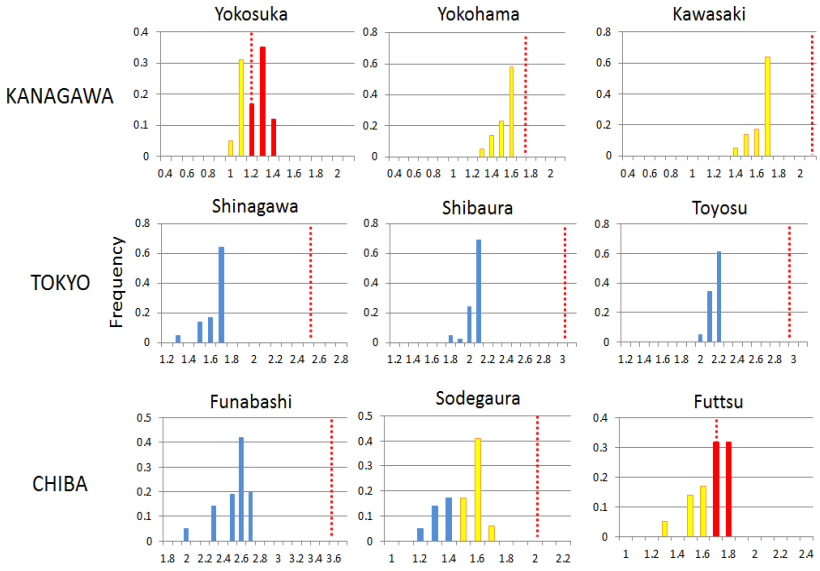

FIGURE 21: FINAL WATER LEVEL BY YEAR 2100 WITH TYPHOON INTENSIFICATION AND A SEA LEVEL RISE OF 0.59 M (HOSHINO 2013)

In the results of this simulation 2 failure cases of the coastal defense are considered, they are listed below. See also Figure 22:

- Case A, the probability that the storm surge will reach a level of at least 50 cm below the top of the defenses.
- Case B, the probability of the storm surge being higher than the protection structures.

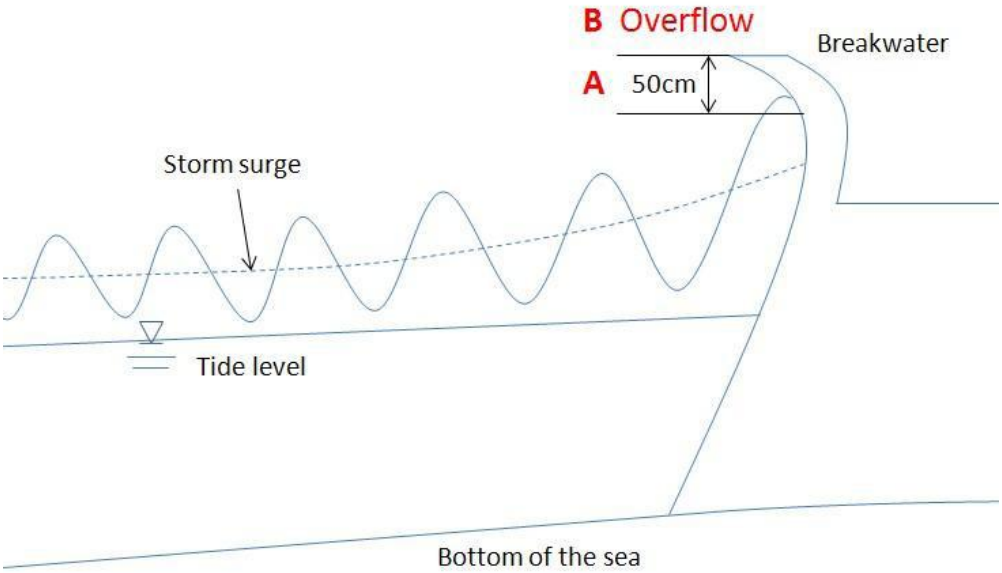

FIGURE 22: CASES A AND B (HOSHINO 2013)

The probability of each case being reached for each location is presented in Table 4 and Figure 23 shows the cumulative overtopping probabilities for all sea level rise scenarios for case B.

TABLE 4: PROBABILITY (%) THAT THE STORM SURGE HEIGHT BECOMES HIGHER THAN CASE A AND B (HOSHINO 2013)

Sea level rise	0cm		28cm		59cm		190cm	
Level of Storm Surge Height	A	B	A	B	A	B	A	B
Yokosuka	12	0	95	0	100	64	100	100
Yokohama	0	0	58	0	100	0	100	100
Kawasaki	0	0	64	0	100	0	100	100
Samezu	0	0	0	0	0	0	100	100
Shibaura	0	0	0	0	0	0	100	100
Toyosu	0	0	0	0	0	0	100	100
Funabashi	0	0	0	0	0	0	100	81
Sodegaura	0	0	0	0	64	0	100	100
Futtsu	0	00	81	0	100	64	100	100

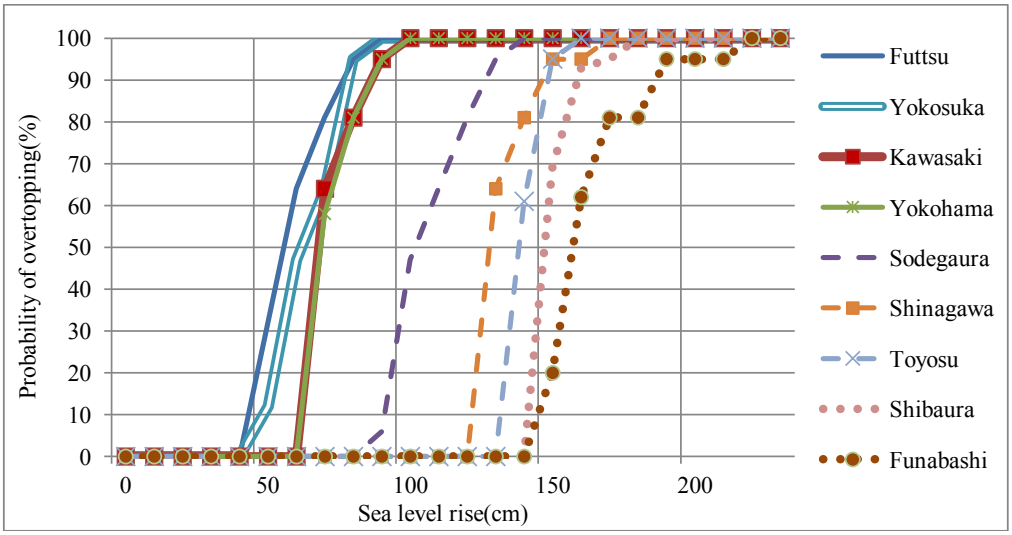

FIGURE 23: CUMMULATIVE OVERTOPPING PROBABILITY OF SEA DEFENSES (CASE B) IN EACH SEA LEVEL RISE SCENARIO FOR A 1 IN 100 YEAR TYPHOON BY THE YEAR 2100 (HOSHINO 2013)

3.2.3.3 Economic damage

Tokyo city has a population of around 13 million inhabitants and is the city with the greatest GDP in the world with a gross output of 1479 billion dollars. Together with adjacent cities such as Yokohama and Kawasaki it forms what it is called the 'greater Tokyo', having a total population of more than 35 million people, making it the largest megalopolis in the world. Therefor a typhoon flooding of the area will not only have a great impact on the Japanese economy, but also the world economy. S. Hoshino's work (Hoshino 2013) has also analysed the economical damage of Tokyo after inundation. The potential areas at risk of inundation along Tokyo Bay in Tokyo, Kanagawa and Chiba prefectures are shown in Figure 25, Figure 24 and Figure 26. The maps are based on elevation maps of Tokyo Bay and include the effect of the intensification of the future typhoons together with a sea level rise of 0.59 m and 1.90 m. The extent of the inundation area after dyke failure is represented by two contour lines. The thick blue line represents the future scenario with a sea level rise of 0.59 m and the light blue line represents the scenario with 1.90 m sea level rise. The maximum water levels shown in the maps are considered to take place at maximum high tide (+ 0.966 T.P.) and have included the mean expected storm surge height and the sea level rise for each scenario. The water levels are expressed at Tokyo Pail (T.P.). Due to the relative small population density in Chiba, the economic damage analysis has only included the Tokyo and Kanagawa prefectures, which the latter includes Yokohama and Kawasaki.

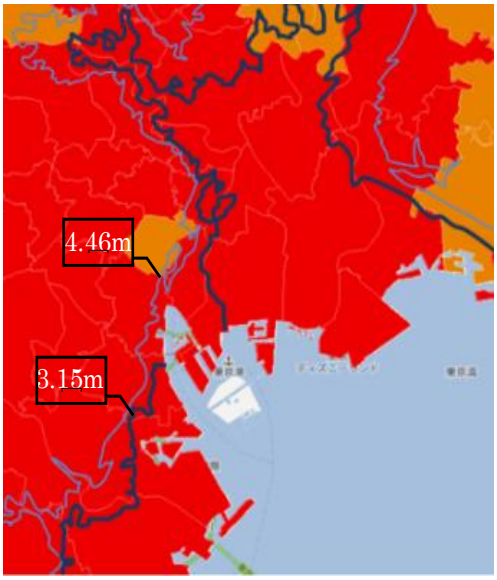

FIGURE 25: INNUNDATION AREA TOKYO FOR 1 IN 100 YEAR TYPHOON BY YEAR 2100 FOR 0.59 AND 1.90 M SEA LEVEL RISE (HOSHINO 2013)

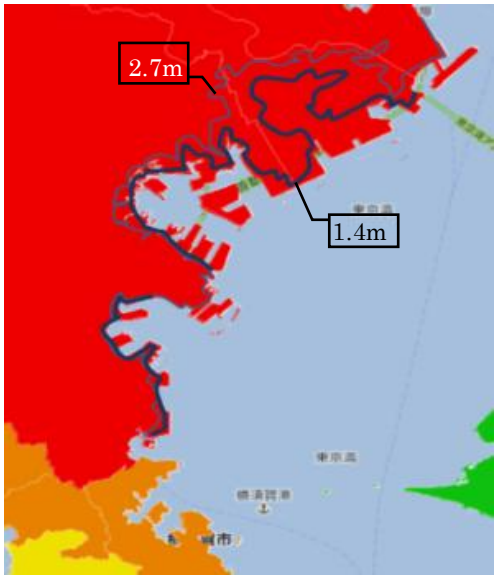

FIGURE 24: INNUNDATION AREA KANAGAWA FOR 1 IN 100 YEAR TYPHOON BY YEAR 2100 FOR 0.59 AND 1.90 M SEA LEVEL RISE (HOSHINO 2013)

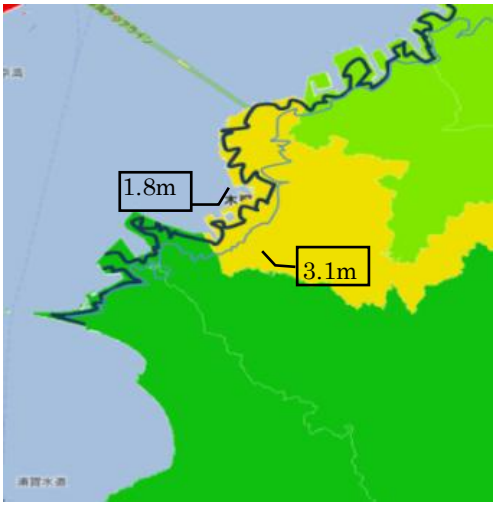

FIGURE 26: INNUNDATION AREA CHIBA FOR 1 IN 100 YEAR TYPHOON BY YEAR 2100 FOR 0.59 AND 1.90 M SEA LEVEL RISE (HOSHINO 2013)

The economic damage in the Tokyo and Kanagawa prefectures is calculated by adding up all the damage in the inundated areas (Hoshino 2013). Figure 27 shows the damage for inundation levels up to +4.5 m T.P. in Tokyo and +4.0 m T.P. in Kanagawa. In the figure the 0 m indicates no dyke failures and therefor the area inside the dyke would be dry. It is

important to note that some areas in Tokyo are under mean sea level; so even at present they will suffer damage if the dyke break.

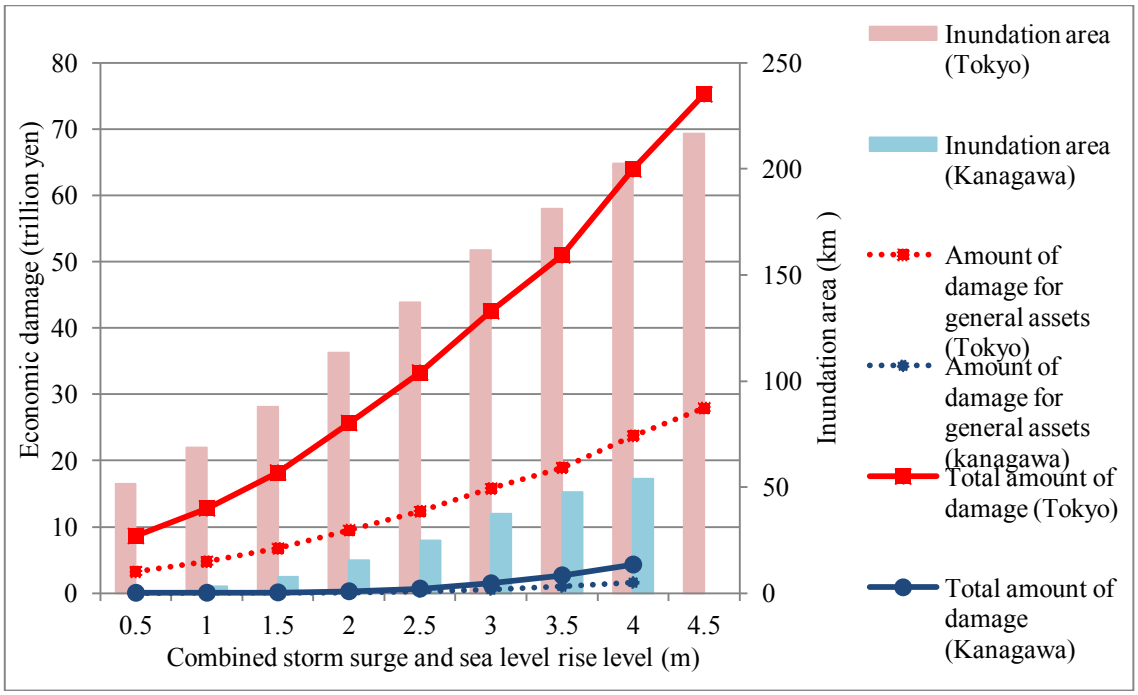

FIGURE 27: ECONOMIC DAMAGE TOKYO AND KANAGAWA FOR DIFFERENT INNUNDATION LEVELS (HOSHINO 2013)

3.2.4 CONCLUSION

From the analysis and simulation results presented in this paragraph, it can be concluded Typhoons can be considered as the main threat for the Tokyo and Kanagawa region. The possible intensification of the typhoons in the future and the sea level rise due to climate change makes the current coastal defence of the area insufficient for a large typhoon in the future. Together with the frequent occurrence of the typhoon in the area, it makes it the main threat for the Tokyo and Kanagawa region and therefor decisive for the design of the possible protection measure.

3.3 Protection measures

In this paragraph, three possible protection measures will be elaborated qualitatively for the prevailing situation in Tokyo. These three considered protection measures are:

- No measure
- Raise/build coastal dykes
- Storm surge barrier

3.3.1 NO MEASURE

By taking no measures, the incurred risk by Tokyo and Kanagawa is assumed to be the same as given in Figure 27.

3.3.2 RAISE/BUILD COASTAL DYKES

The cost of raising costal dykes for a 1 in 100 year typhoon and a sea level rise of 1.9 m has also been investigated by S. Hoshino (Hoshino 2013). This estimation has been done for the following sub-measures:

- Raise dyke heights
- Build new dykes
- Anti-earthquake reinforcements
- Raise ground level

These measures are investigated for the Tokyo, Kawasaki and Yokohama. They are undertaken such that the risk levels in the 2100 are similar to those in 2010 for a 1.9 m sea level rise scenario. A summary of the adaption measure components and cost for each region is given in Table 5 and the total costs of adapting old dykes or building new dykes is given in Table 6. A more comprehensive description of the cost estimation of the raising/building of coastal dykes is given in Appendix 3.

TABLE 5: SUMMARY OF ADAPTION MEASURE COMPONENTS FOR EACH LOCATION, FOR A 1.9 M SEA LEVEL RISE SCENARIO (1 JAPANESE YEN = 0.0072 EURO) (HOSHINO 2013).

		Measures for coastal dykes (bn yen)			Measures for areas outside dykes (bn yen)
Prefecture	Location	① Raise dykes height	② Build new dykes	③ Anti-earthquake Reinforcement	④ Raise the ground level
Tokyo	Tokyo port	0.58	6.01	97.43	19.51
Kanagawa	Kawasaki port	0.22	3.63	59.78	67.79
	Yokohama port	×	5.78	94.77	34.52

TABLE 6: TOTAL COSTS OF ADAPTING OLD DYKES OR BUILDING NEW ONES FOR A 1.9 M SEA LEVEL RISE SCENARIO (1 JAPANESE YEN = 0.0072 EURO) (HOSHINO 2013).

	①+③+④ Adapting old dykes (bn yen)	②+③+④ Building new dykes (bn yen)
Tokyo	117.5	123.0
Kanagawa	257.1	266.3

3.3.3 STORM SURGE BARRIER

Another possible measure to reduce the risk level of Tokyo and Kanagawa region due to typhoon intensification and sea level rise is to construct a storm surge barrier. By this measure, the coastal protection length will be greatly reduced, saving a lot of indirect influenced and measures for the surrounding areas of the coastal dykes. A simulation done by Takeshi Ito in 1964 has shown great potential of constructing a storm surge barrier. The brief description of this simulation will be presented in the next paragraph.

3.3.3.1 Typhoon barrier simulation Tokyo Bay

In 1964 a simulation has been done by Takeshi Ito (Ito en Hino 1964) for the storm surge height reduction by a typhoon barrier in Tokyo Bay. The simulated typhoon is the typhoon that has caused the most sever damage for the Japanese history, named the Ise-Bay Typhoon in 1959.

3.3.3.1.1 The model configuration

The path of the typhoon is assumed to proceed northward along a course parallel to the axis of the Tokyo Bay with a propagation speed of 73 km/h. The eye of the storm is assumed to be 40 km west of Tokyo, see Figure 28. The considered worst-case scenario course is the A-course and only this course will be considered in this report. This is to ensure a worst-case scenario for this typhoon. The simulated barrier is constructed across the central part of Tokyo Bay, having a length of circa 18 km, see Figure 29[20]. An permanent open navigation channel is included in the barrier model. A series of simulations with different permanent opening width had been carried out and are listed below:

- No barrier
- Central opening width 2000 m
- Central opening width 1000 m
- Central opening width 500 m

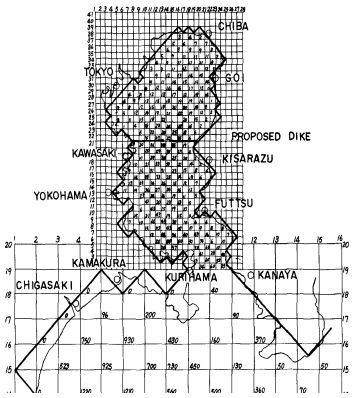

FIGURE 29: LOCATION SIMULATED BARRIER (ITO EN HINO 1964)

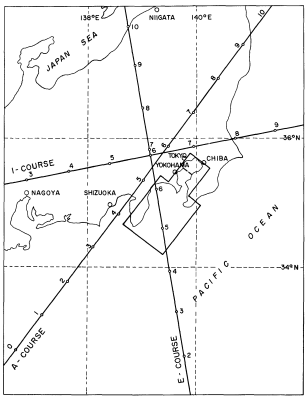

FIGURE 28: COURSE OF THE SIMULATED TYPHOON (ITO EN HINO 1964)

3.3.3.1.2 Results

Several relevant results from this simulation are shown in the figures below. It can be seen that the barrier is showing significant storm surge reduction of about 0.4 - 0.7 m already for the inner part of the barrier if the opening is 1000 m and no significant surge rise for the locations outside the barrier, see Figure 30[20]. Also the contribution of spring tide has been included in the simulation. The water level rise including spring tide is given in Figure 31. According to this simulation the superposition of the high tide level and the storm surge gives an overestimation of the final water level. Notice that this simulation is done 50 years ago, sea level have been rising in these 50 years and together with the possible typhoon intensification and further sea level rise, the absolute water level for a typhoon with the same return period as Ise-Bay typhoon will be higher in the future. But this simulation does give a good indication about the effectiveness of a storm surge barrier in Tokyo Bay. A more comprehensive description of the results of the simulation is given in Appendix 4.

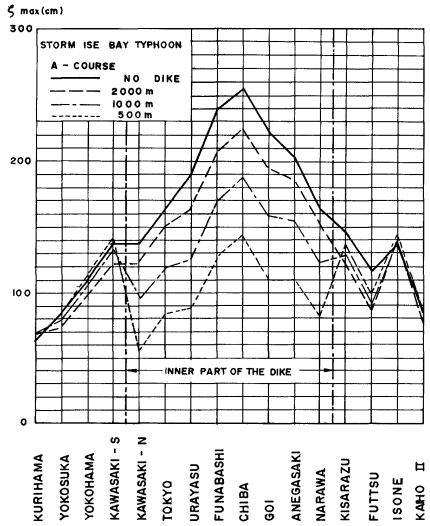

FIGURE 30: CALCULATED MAXIMUM SURGE ELEVATION ISE-WAN TYPHOON FOR DIFFERENT BARRIER OPENING WIDTHS (A-COURSE) (ITO EN HINO 1964)

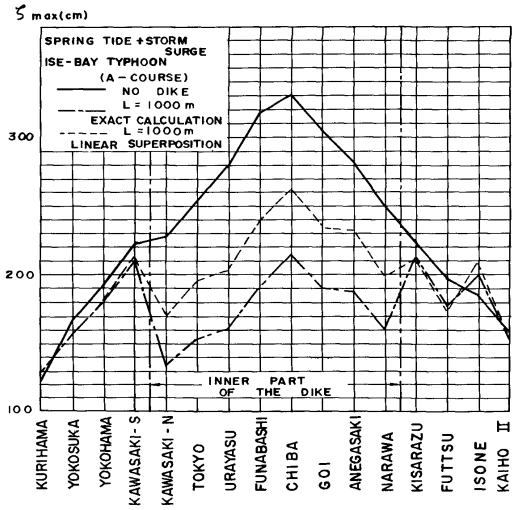

FIGURE 31: FINAL WATER LEVEL (INCLUDE SPRING TIDE), THE LINEAR SUPERPOSITION OF THE TIDE GIVE AN OVEREXTIMATION OF THE WATER LEVEL ACCORDING TOT HIS SIMULATION. (ITO EN HINO 1964)

3.3.4 CONCLUSION

By taking no protection measures the inundation risk by typhoon will be the same as elaborated in paragraph 3.2, which is unacceptable. Both dyke raising and storm surge barrier are considerable solutions. Since the dyke raising solution have already been investigated by S. Hoshino and not much research has been done to the storm surge barrier solution, it is interesting to investigate the effectiveness of a storm surge barrier. By this measure, the coastal protection length will be greatly reduced; saving a lot of indirect influenced and measures for the surrounding areas of the coastal dykes. Also the simulation done by Takeshi Ito in 1964 has shown great potential of constructing a storm surge barrier. Therefore the storm surge barrier is chosen to be further analysed in this thesis.

3.4 Summary

Tokyo Bay is considered most vulnerable to a tsunami caused the so called 'Genroku' earthquakes, located in the south of the Kanto region. The return period of such an earthquake is considered to be 2300 years. The Genroku Kanto earthquake originally happened in 1703, therefore the occurrence of such an earthquake within the design period of the barrier is considered to be very small.

Despite both simulations have shown a considerable water level elevation inside the bay caused by tsunamis, the chance of occurrence of such a tsunami is very small and the duration of the tsunami is really short. Also the chance of a tsunami attack during the maximum water level of the spring tide is considered negligible small. Therefor based on the result of the simulation it can be concluded that the risk caused by a tsunami attack on Tokyo and Kanagawa region is negligible small and the water level elevation caused by the tsunami won't be decisive for the design of the protection measure.

Global warming could lead to an increase of typhoon intensity and sea level rise in the future that could increase the chance of inundation in the low-lying areas around Tokyo Bay. The IPCC 5AR has shown a future projection of a worst scenario global sea level rise between 0.52 and 0.98 m higher than at present by the end of the 21st century. But Vermeer and Rahmstorf have argued a more extreme scenario of a sea level rise between the 0.81 and 1.90 m by the year 2100.

The Tokyo Bay has 150 km coastal dikes and 157 km river dikes, which 89% and 78% are sufficient respectively for the current design dike height. Of these dikes, 62% and 73% respectively of the coastal and river dike possesses earthquake resistance measures.

From the analysis and simulation results presented in paragraph 3.2, it can be concluded Typhoons can be considered as the main threat for the Tokyo and Kanagawa region. The possible intensification of the typhoons in the future and the sea level rise due to climate change makes the current coastal defence of the area insufficient for a large typhoon in the future. Together with the frequent occurrence of the typhoon in the area, it makes it the

main threat for the Tokyo and Kanagawa region and therefor decisive for the design of the possible protection measure.

Three possible protection measures for the Tokyo and Kanagawa region against future storm surges are considered:

- No measure
- Raise/build coastal dykes
- Storm surge barrier

By taking no measures, the incurred damage cost by Tokyo and Kanagawa is assumed to be the same as given in Figure 27.

For coastal dyke raise/rebuild, the total investments needed to make it sufficient for a 1 in 100 year typhoon with a 1.9 m sea level rise are given in Table 6.

By constructing a storm surge barrier, the coastal protection length will be greatly reduced, saving a lot of indirect influenced and measures for the surrounding areas of the coastal dykes. Since not much research has been done to this protection measure and the analysis done by Takeshi Ito in 1964 has shown great potential of constructing a storm surge barrier. Therefore the storm surge barrier is chosen to be further analysed in this thesis.

4 BARRIER LOCATION

In this chapter the location of the storm surge barrier will be determined. To be able to find the critical aspects for the barrier's cost-effectiveness, the important cost drivers have to be found. Based on these cost drivers various location alternatives will be compared and evaluated.

4.1 Cost drivers

The important cost drivers for a storm surge barrier barrier from a constructive point of view is given according to a formula drafted by van der Toorn (Vries 2014)

$$S_b = B_b * \Delta h_b * h_{c,b} * B_b * S_{U,b}$$

Where:

S_b	[€]	Total investment costs for the storm surge barrier
Δh_b	[m]	Maximum water level difference over barrier
$h_{c,b}$	[m]	Construction height barrier
B_b	[m]	Barrier span
$S_{U,b}$	[€/(m*m*m)]	Unit cost barrier

From this formula it can be seen that the cost of a storm surge barrier is mainly determined by the barrier height and the barrier length, which is basicly the area of the barrier. Note this is a first indication of the cost of the barrier, aspects like inexperience of working at a big depth will entail risk for a higher cost than that is expected.

4.2 Determination barrier location

To be able to find the most optimal location, 5 possible barrier locations are presented in Figure 32 and the subsoil of the bay is can be found in Appendix 5. The bathymetries of the considered barrier locations are shown in Figure 33 to Figure 37. They are based on a depth contour map provided by Miguel Estaban (M. Esteban 2014). For each location the advantages and disadvantages are given. These are presented in Table 7 to Table 11. A more comprehensive elaboration of the barrier locations are given in Appendix 5.

FIGURE 32: POSSIBLE BARRIER LOCATIONS (GOOGLE MAPS SD)

4.2.1 BARRIER LOCATION 1

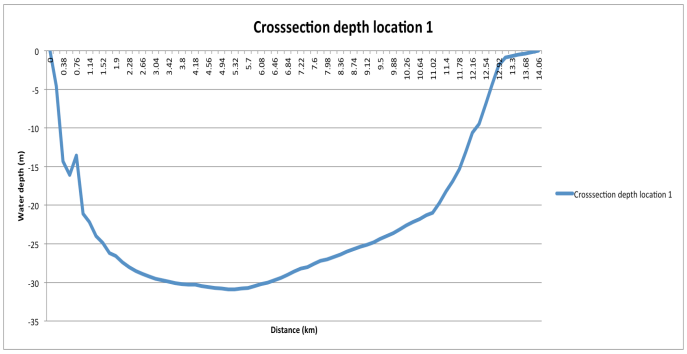

FIGURE 33: BATHYMETRY BARRIER LOCATION 1

TABLE 7: ADVANTAGE AND DISADVANTAGE BARRIER LOCATION 1

Advantage	Disadvantage
High effectiveness in surge height reduction at Tokyo	Largest cross-section area to be closed off, around 310000 m^2
Most shallow bathymetry of the considered locations	Longest span, around 14 km
	No protection to Yokohama
	Relatively weak subsoil (mud)

4.2.2 BARRIER LOCATION 2

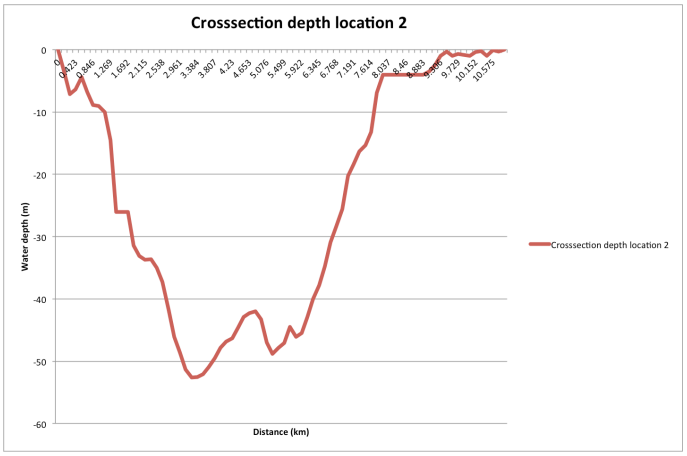

FIGURE 34: BATHYMETRY BARRIER LOCATION 2

TABLE 8: ADVANTAGE AND DISADVANTAGE BARRIER LOCATION 2

Advantage	Disadvantage
Protection Yokohama	Relatively long span, around 10.5 km
Avoiding the deep split at the mouth of the bay	Despite avoiding the deep split, still deep bathymetry
Less deep compared to similar locations	Relatively large area to be closed off, around 260000 m^2

4.2.3 BARRIER LOCATION 3

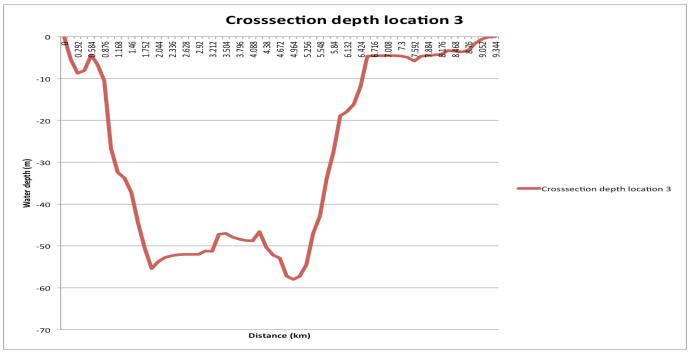

FIGURE 35: BATHYMETRY BARRIER LOCATION 3

TABLE 9: ADVANTAGE AND DISADVANTAGE BARRIER LOCATION 3

Advantage	Disadvantage
Protection Yokohama	Relatively short span, around 9.5 km
Avoiding the deep split at the mouth of the bay	Despite avoiding the deep split, still deep bathymetry
Flatter bottom compared to location 2, which makes it more suitable for construction	Relatively large area to be closed off, around 260000 m^2
	Deeper bathymetry compared to location 2

4.2.4 BARRIER LOCATION 4

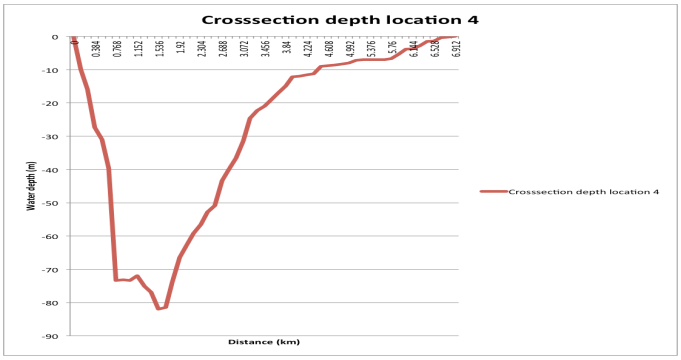

FIGURE 36: BATHYMETRY BARRIER LOCATION 4

TABLE 10: ADVANTAGE AND DISADVANTAGE BARRIER LOCATION 4

Advantage	Disadvantage
Smallest area to be closed off, around 200000 m^2	Barrier location with the greatest depth (81m)
Shortest span (6.9 km)	
Protection Yokohama and Yokosuka	
Relatively strong subsoil	
Relatively long shallow part suitable for moveable barrier construction, around 4 km	

4.2.5 BARRIER LOCATION 5

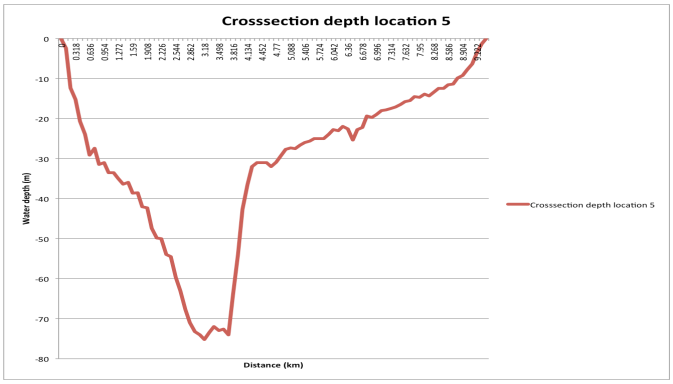

FIGURE 37: BATHYMETRY BARRIER LOCATION 5

TABLE 11: ADVANTAGE AND DISADVANTAGE BARRIER LOCATION 5

Advantage	Disadvantage
Protection Yokohama and Yokosuka	Large depth (74m)
Relatively shallow part (approximately 5 km) that is suitable for moveable barrier constructions.	Faced to the direction of the incoming waves from the sea, therefore probably suffer larger wave loads.
Relatively strong subsoil	Large 'to be closed' area, around 300000 m^2

4.2.6 EVALUATION

Since it would not be acceptable for the Japanese government not to protect Yokohama, barrier location 1 falls out the consideration immediately. As for the other four alternatives, it is assumed that the value of the protected area is approximately the same; therefore the choice will be based on the investment cost of the construction of the barrier. It is expected that the foundation cost will become decisive and a larger 'to be closed' area will generally lead to a higher cost. Therefore a short span and a small 'to be closed' area is preferable. This leads to barrier location 4. Compared to barrier location 2 and 3, the deepest point in barrier location 4 is indeed much deeper, but since it is only a small part of the bathymetry, it is expected that the extra cost of the greater depth will be smaller compared to the greater span and 'to be closed' area of location 2 and 3. Also location 4 has a relatively long shallow part in its bathymetry that makes it really suitable for moveable barrier constructions. This last one bears a great value considered the ecological value of the bay in the future. The bathymetry of barrier location 5 is similar to barrier location 4, except for it has a larger span and a much larger 'to be closed' area. Also it will probably suffer larger wave loads due to its position. Therefore barrier location 4 is the most preferable location to build the barrier and the further design considerations will be based on this location, see Figure 38 and Figure 39. A summary of the specifications of the barrier locations is given in Table 12.

TABLE 12: SUMMARY BARRIER LOCATION SPECIFICATIONS

	Barrie span	Largest depth	To be closed area	Protection Yokohama
Barrier location 1	14 km	31 m	310000 m²	No
Barrier location 2	10.5 km	52 m	260000 m²	Yes
Barrier location 3	9.5 km	58 m	260000 m²	Yes
Barrier location 4	6.9 km	81 m	200000 m²	Yes
Barrier location 5	9.5 km	74 m	300000 m²	Yes

FIGURE 38: BARRIER LOCATION 4 (GOOGLE MAPS SD)

FIGURE 39: LOCATION 4 DETAILED VIEW (GOOGLE MAPS SD)

4.3 Summary

The cost of a storm surge barrier is mainly determined by the barrier height and the barrier length, which is basicly the area of the barrier. Note this is a first indication of the cost of the barrier, aspects like inexperience of working at a big depth will entail risk for a higher cost than that is expected.

The span between Yokosuka and Futtsu (location 4) is the most suitable location for the placement of a barrier. This location has the shortest span between the two shores. Despite the large depth of this location (deepest point 81 m) it still has the smallest area to be closed off, which corresponds with the cost.

5 FUNCTIONAL REQUIREMENTS AND BOUNDARY CONDITIONS

In this chapter the functional requirements and the boundary conditions for the design of the typhoon barrier will be presented.

5.1 Functional requirements

This chapter a list of the functional requirements is given for the typhoon barrier in Tokyo Bay in order to function in a desirable manner, they serve as guidance throughout the design process. These requirements consists general requirements, nautical requirements, design requirements and operational requirements. Also a list of stakeholders is presented that are relevant to this project

5.1.1 GENERAL REQUIREMENTS

Inside the protected area by the barrier lies three major ports, which are port of Tokyo, port of Yokohama and port of Chiba, having a yearly arrival of around 32000, 65200 and 43000 vessels respectively. Therefor in normal condition a section of the barrier should be open in order to enable navigation in- and outward the bay. Also in order to maintain the ecological value of the bay, it is also desirable to maintain as much as possible water exchange between the bay and the sea when the barrier is open under normal condition.

5.1.2 NAUTICAL REQUIREMENTS

In order to maintain the current status of ports and not hinder its future development, the navigation opening in the barrier should have a high standard regarding the vessels that should be able to pass through. The port of Tokyo has at this moment the longest berth of these two ports and therefor the governing ship size for the port of Tokyo will be the governing size for the opening of the barrier. The governing ship for the port of Tokyo at this moment is the NYK OCEANUS (Jakota sd), which has a size of 336x46x14 m. But since the ship size will grow in the future and therefor also the size of the port. The size of current biggest ship is used as the governing size to calculate the width of the opening of the barrier, which is the Emma Maersk and has a size of 397x56x15.5 m.

5.1.2.1 Navigation channel dimensions

The minimum depth and width for the navigation opening in the barrier can be determined using the formulas developed by the PIANC group (Ligteringen 2009). By using the Emma Maersk as design ship, the required minimum depth and opening width of the navigation channel are given in Table 13. For an extensive calculation of the navigation channel dimensions see appendix 6.

TABLE 13: MINIMUM REQUIRED NAVIGATION CHANNEL DIMENSIONS

Minimum required depth	17.5 m
Minimum required width	465 m

5.1.2.2 Traffic intensity

The traffic intensity can be checked with the approximation of Groeneveld (Groeneveld 2002). The total amount of vessels is around 140200, which leads to an average of 384 vessels per day. It is of great importance that the current navigation not to be limited after the construction of the barrier. The calculation in Appendix 7 shows that the two one-way navigation channel does not result in delays for the navigation. This calculation is based on the traffic intensity calculation done for the Bolivar Road storm surge barrier in the master thesis done by Peter A.L. Vries (Vries 2014)

5.1.3 DESIGN REQUIREMENTS

This chapter contains the design requirements for the barrier, which are the requirements the barrier should be able to fulfil in the terms of safety level, lifetime, retaining character and the maximum overflow.

5.1.3.1 Safety level

The typhoon chosen as design standard for this barrier is the Ise-Wan typhoon in 1959, which is also the Japanese deterministic typhoon design standard. The properties of the typhoon are given in Table 14. The corresponding surge and wave heights are presented in the boundary conditions, see chapter 5.2.2.

TABLE 14: DATA ISE-WAN TYPHOON (1959) (MLIT SD)

Central pressure	929 hPa
Max wind speed	45 m/s

5.1.3.2 Barrier lifetime

The barrier will be designed for 100 years. This is shorter than the other large storm surge barriers like the Maeslantbarrier and Eastern Scheldt Barrier in the Netherlands, which have a design lifetime of 200 years. Due to the uncertainties regarding the sea level rise and typhoon intensification over 200 years, it is very difficult to determine the exact required retaining height. Also there is only information available for estimations of both aspects for only the coming 100 years. Therefor it is decided to design the barrier initially for 100 years and also in such way that after 100 years the retaining height could be increased in a relatively simple manner in order to be able to adjust to the uncertain water level until a lifetime of 200 years. This assumption is based on the assumed design lifetime for the Bolivar Road storm surge barrier in the master thesis done by Peter A.L. Vries (Vries 2014)

5.1.3.3 Barrier redundancy

It is required that the barrier must still be able to sufficiently reduce the surge if one or more gates fail to close. This number is assumed to be 10% of the total barrier gates. This requirement is adopted from the Eastern Scheldt Barrier design, which is still able to sufficiently block the surge in case 6 of 62 barrier doors (≈10%) fail to close in storm conditions. This assumption is based on the assumed redundancy for the Bolivar Road storm surge barrier in the master thesis done by Peter A.L. Vries (Vries 2014)

5.1.3.4 Allowed water level rise

The lowest dyke height at Tokyo is +3.466 T.P (Hoshino 2013). By assuming the worst-case scenario caused by the Ise-wan typhoon and barrier closure during low tide (+/- 0.966 m), the total allowed water level rise inside the bay over 100 years will be 4.432 m. Since a freeboard of around 0.5 m is preferred, the maximum allowed water level rise inside the protected area will be reduced to 3.932 m.

5.1.4 OPERATIONAL REQUIREMENTS

The arrival of a typhoon can be estimated quite accurately, people are warned well ahead of the arrival. The most industrial and nautical activities around the bay will come to a hold and the amount of ships passing by the barrier will be negligible. Therefor the influence of long closure duration on the navigation will be small and long closure duration is acceptable. It may be in the order of a few hours. This assumption is based on the assumption made for the Bolivar Road storm surge barrier in the master thesis done by Peter A.L. Vries (Vries 2014)

In case of a tsunami, in the worst-case scenario, the tsunami will arrive in the order of 10 minutes. It is impossible to react and close the barrier on time. And since the magnitude of the tsunami will largely reduce once it's inside the bay, it is decided to leave the barrier open during tsunami attacks and use the closure dam as a reduction barrier.

The barrier must also be accessible for inspection and maintenance.

5.1.5 STAKEHOLDERS

In order to create the largest added value out of this project, it is of importance to recognize and determine the stakeholders together with their interests and influence. In Table 15 a short list of the possible stakeholders is given together with their interests and influence.

TABLE 15: POSSIBLE STAKEHOLDERS

Stakeholders	Interests	influence
Government	Increase safety of residential area, protection economy and stimulation development of the protected area	+++
Environmentalist	Preservation of the bay's ecosystem	++
Coastal industrial	Protection against damage	++
Other business	Protection against damage	+
Inhabitants	Protection from disaster	+

5.2 Boundary conditions

In this paragraph the boundary conditions that govern in Tokyo and Tokyo Bay during various conditions are given. The barrier design must be compliance with these boundary conditions.

5.2.1 TOPOGRAPHIC BOUNDARY CONDITION

The inner bay area (shallow area) has an average depth of 30-40 m. At the mouth area of the bay there is a deep split of around 70-80 m and from this point there is a large increase in slope of the seabed, where the seabed gets much deeper. The bottom structure of the inner bay area is relatively flat with a mild slope; see Figure 40, so flow distortion caused by the bottom will be ignored in this research.

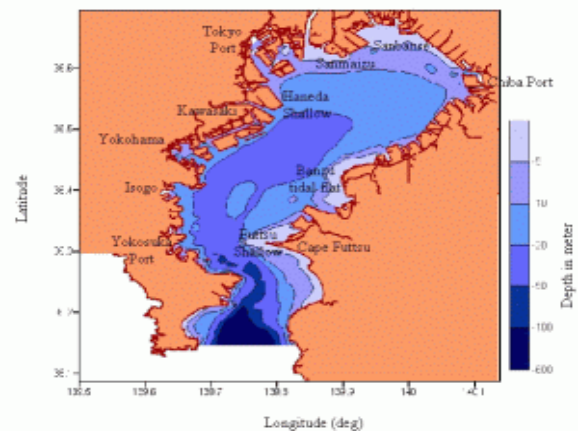

FIGURE 40: BATHYMETRY TOKYO BAY (EXTRA.SPRINGERS.COM SD)

5.2.2 HYDRAULIC CONDITIONS

For the hydraulic boundary conditions three conditions are recognized. These conditions are:

- Regular condition
- Typhoon condition
- Tsunami condition

Regular conditions gives the environmental conditions that are relevant for the barrier under normal circumstances, this includes the sea level rise estimation over 100 years. The typhoon condition is relevant for the circumstances under the design typhoon surge, which is the Ise-wan typhoon in 1959. Note that this design typhoon may not be correct regarding probability of occurrence, but due to the limit time given for a master thesis, the deterministic design typhoon in Japan with an assumed duration of 6 hours is taken as design standard. The theoretical background information regarding typhoons and surges generated by typhoons is given in appendix 8.

5.2.2.1 Regular conditions

Tides

Tokyo Bay has a semidiurnal tide and the average high tide that will be taken into account is T.P. +0.966 m.

Sea level rise

The upper value given by the prediction from IPCC 5AR is 0.98 m (Church 2013), which is approximately 1 m. For the simplification of further calculations, 1 m will be used as the expected sea level rise in year 2100

5.2.2.2 Typhoon condition

Pressure set-up

For the calculation of the pressure set-up, the formula of (Schloemer 1954) is used:

$$\Delta h_p = c_1 * (p_\infty - p_c)(1 - e^{-\frac{r_m}{r}})$$

Where:

Δh_p	[m]	Pressure set-up
c_1	[m/hPa]	Constant between 0.01 – 0.04
p_∞	[hPa]	Peripheral pressure
p_c	[hPa]	Pressure in the eye of the typhoon
r_m	[m]	Radius to maximum wind speed
r	[m]	Radius to particular location

The pressure set-up for this research will be based on Ise-wan typhoon for the worst-case scenario, which is the radius of the particular location is equal to the radius of the maximum wind speed. The constant c_1 is assumed as the average of the range values, which is 0.025. Filling in Schloemers formula gives:

$$\Delta h_p = 0.025 * (1000 - 929)(1 - e^{-1}) = 1.12\ m$$

Note in this thesis this value is assumed to be the same for both barrier location and Tokyo, which is a rather conservative assumption.

Wind set-up

For the calculation of the wind set-up, the quadratic relation of wind set-up and wind speed is used (Klaver 2005). The formula is given below:

$$\Delta h_w = F_{set-up} * c_2 * \frac{V_s^2}{gd}$$

Where:

Δh_w	[m]	Wind set-up
c_2	[-]	Constant between $2*10^{-6}$ - $4*10^{-6}$
V_s	[m/s]	Surface wind speed
F_{set-up}	[m]	Fetch length of wind set-up
d	[m]	Water depth
g	[m/s^2]	Gravitational acceleration

The maximum surface wind, V_s, used in this research will be the wind speed of the most severe typhoon suffered by Japan in the history, which is also the design typhoon for the Tokyo Bay set by the Japanese government. This wind speed is 45 m/s.

Wind set-up at Tokyo

For the calculation of wind set-up at Tokyo the fetch is taken as approximately the distance between Tokyo and Yokosuka, which is approximately 35 km. The average depth of the corresponding location is taken as 30 m. By filling in the same formulas gives a wind set-up at Tokyo of:

$$\Delta h_w = F_{set-up} * c_2 * \frac{V_s^2}{gd} = 35000 * 3 * 10^{-6} * \frac{45^2}{9.81 * 30} = 0.72\ m$$

Wind set up at barrier location

Since wind set-up has only large effects on shallow water, therefor only the shallow water part of the area in front of the barrier is taken as fetch, which is approximately 13 km. The average depth of corresponding location is taken as 50 m. Filling in the formula used earlier gives a wind set-up of:

$$\Delta h_w = F_{set-up} * c_2 * \frac{V_s^2}{gd} = 15000 * 3 * 10^{-6} * \frac{45^2}{9.81 * 50} = 0.16\ m$$

Wave height

The significant wave height at the barrier, based on the SBM-model, is given in the following equation (Klaver 2005):

$$H_s = \frac{V_s^2}{g} H_\infty \tanh\left(k_3 \left(\frac{dg}{V_s^2}\right)^{m_3}\right) \tanh\left(\frac{k_1 \left(\frac{F_{wave} g}{V_s^2}\right)^{m_1}}{\tanh\left(k_3 \left(\frac{dg}{V_s^2}\right)^{m_3}\right)}\right)$$

Where:

H_s = significant wave height
V_s = surface wind speed, which is 45 m/s
g = gravity acceleration
d = water depth
F_{wave} = Fetch length of waves
H_∞ = coefficient 0.283
k_1 = coefficient 0.0125
k_3 = coefficient 0.53
m_1 = coefficient 0.42
m_3 = coefficient 0.75

Wave height at Tokyo

For the calculation of the wave height at Tokyo the same fetch length is taken for the wind set-up calculation for Tokyo, which is 35 km. The wind speed is assumed as the maximum wind speed, which is 45 m/s. The water depth at shore of Tokyo is assumed to be 5 m (M. Esteban 2014) Filling in the formula gives:

$$H_s = 1.89\ m$$

Wave height at barrier location

Also here the same values for fetch and water depth as for the calculation of the wind set-up at the barrier location is used, which are 13 km and 50 m respectively. Filling in the equation gives a maximum wave height of

$$H_s = 3.95\ m$$

This value can be compared with the available wave records at Dai Ni Kaiho (Independent Administrative Institution, Port and Airport institute sd), which is a place nearby the barrier location. The available wave record of this location only stretches over -30 years of time. The maximum wave height recorded in Dai Ni Kaiho is 3.29 m. This height is in the same order of the calculated value. This confirms the validation of the used formula in this simulation. But due to the short wave record period, the available wave record doesn't contain waves due to a typhoon of the design typhoon magnitude; this is probably the reason why the maximum wave height given by the wave record is smaller than the calculated wave height. Therefor the calculated wave height will be used as design wave height.

5.2.2.3 Tsunami condition

Tsunami wave height at Tokyo

The chosen design tsunami will be the tsunami generated by the Genroku types of earthquakes as simulated by the Tokyo Metropolitan Government, see chapter 3.1.2. The maximum tsunami surge height (2.61 m) from this simulation is also taken as the tsunami boundary condition.

Tsunami wave height at barrier location

For the tsunami height ait the barrier location, the value indicated by Figure 12, which is approximately 0.8 m.

5.2.2.4 Summary hydraulic boundary conditions

Table 16 gives a summary of all hydraulic boundary conditions.

TABLE 16: HYDAULIC BOUNDARY CONDITIONS

Regular conditions	
Tide	+0.966 m TP
Sea level rise for the next 100 years	1 m
Typhoon conditions	
Maximum pressure set-up	1.12 m
Maximum wind set-up at Tokyo	0.72 m
Significant wave height at Tokyo	1.89 m
Maximum wind set-up at barrier location	0.16 m
Significant wave height at barrier location	3.95 m
Duration	6 hours
Tsunami conditions	
Tsunami wave height at Tokyo	2.61 m
Tsunami wave height at barrier location	0.8 m

5.2.3 GEOTECHNICAL BOUNDARY CONDITIONS

A sub-soil map of the Tokyo Bay can be found in Appendix 9.

5.2.4 DISCHARGE OF THE RIVERS THAT ARE CONNECTED WITH TOKYO BAY

There are mainly three rivers that contributes to the river discharge into the bay, which are the Tama river, Arakawa river and Edo river. Their discharges are:

- Tama river: 37 m^3/s
- Arakawa river: 30 m^3/s
- Edo river: 110 m^3/s

5.2.5 METEOROLOGICAL CONDITIONS AND RIVER DISCHARGES

The average annual maximum rainfall of Tokyo amounts around 180 mm (World weather and climate information 2013), which is during June. The rainfall during the 1959 Ise-wan typhoon amounts about 200 mm (Japan water forum 2005). Due to the large area of the Tokyo Bay, it is presumed that the rainfall does not cover the whole surface area of the bay. The peak rainfall will be spread out over the entire Bay resulting in just a slight increase of the water level. Therefor it is expected that the influence of the rainfall on the surge level inside the Bay will not be significant. Furthermore it is expected that the rainfall over the river basin will take quite some time to reach the Bay, and since the assumed duration of the typhoon will be around 6 hours, therefor it is presumed that the significant increase in river discharge at the bay will take place after the typhoon has passed by the bay. This assumption is based on the assumption made for the Bolivar Road storm surge barrier in the master thesis done by Peter A.L. Vries (Vries 2014)

5.2.6 EARTHQUAKE BOUNDARY CONDITIONS

The design earthquake is of a magnitude of 8.0 M_s, the earthquake of same magnitude as the Genroku earthquake (1703) and The great Kanto earthquake (1923). The Genroku earthquake is also the earthquake that will cause the most threatening tsunami for the Tokyo Bay.

6 SYSTEM LEVEL DESIGN: BARRIER SYSTEM

The typhoon barrier will first be designed on system level. In this chapter the retaining structure distribution of the barrier will be determined and a check will be perform regarding the possibility to leave the navigation channel permanent open.

6.1 Distribution of retaining structures

In this paragraph the distribution of the retaining structure will be determined. First the choice between fully closed barrier, fully moveable barrier or partly closed/partly moveable barrier will be elaborated in a global distribution analysis, while the exact distribution of the retaining structure will be further elaborated in a detailed distribution analysis.

6.1.1 GLOBAL DISTRIBUTION

In this paragraph three different alternatives of retaining structure distribution are considered. These alternatives are presented below.

- Alternative 1: The whole cross-section of the bathymetry will be closed off with a closure dam except for the opening for the navigation.
- Alternative 2: Moveable storm surge barriers will be build over the total span of the selected location.
- Alternative 3: The closure of the Tokyo Bay will be partly closure dam and partly moveable storm surge barrier.

Alternative 1 will have the biggest permanent closed area. So during tsunami attacks, this measure will effectively stop the tsunami wave from penetrating into the bay area. But due to the small opening that is left over, the water flow inward and outward the bay will be greatly hindered. This will have negative influences for the future ecological development of the area. This is exactly the other way around for alternative 2. The large opening over the total span will have a lot less influence on the inward and outward water flow, but as a result it will also allow a lot more water to penetrate into the bay during tsunami attacks. Therefore alternative 3 is the best overall choice for this situation. The relatively large opening at the barrier part of the span will allow enough water to flow inward and outward the bay, keeping the water inside the bay alive, while the closure dam area function as a reduction barrier during tsunami attacks, stopping a relatively large part of the water. A summary of the advantages and disadvantages of the alternatives is given in Table 17. The further analysis in this thesis will be based on the chosen alternative 3.

TABLE 17: SUMMARY ADVANTAGES AND DISADVANTAGES GLOABAL DISTRIBUTION OF RETAINING STRUCTURES

	Alternative 1	Alternative 2	Alternative 3
Advantage	Effectively stop tsunami wave penetration	Small influence for future ecological development of the area	Relatively small influence on future ecological development of the area Stopping relatively large part of the tsunami wave penetration
Disadvantage	Negative influence for future ecological development of the area	Large wave penetration during tsunami	

6.1.2 DETAILED DISTRIBUTION

In this paragraph two alternatives is considered for the detailed distribution of the barrier based on the analysis in the previous paragraph. Since the dam part of the barrier requires a lot of material due to the large depth at the barrier location. It will probably be the largest challenge of the project. Therefor the choice of the alternatives will be based on the saved material for the construction of the dam. Since this is a rough estimation of the material volume, the navigation depth is chosen to be 20 m and the non-navigation open area depth is chosen to 10 m. The two alternatives are presented below.

Alternative 1

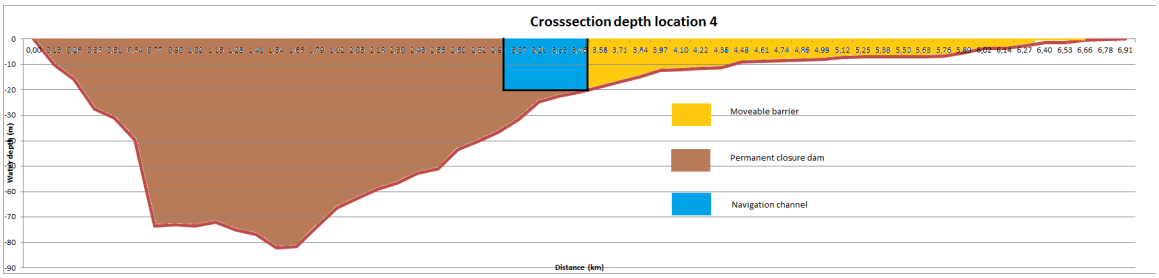

FIGURE 41: ALTERNATIVE 1 DETAILED DISTRIBUTION RETAINING STRUCTURES

Alternative 2

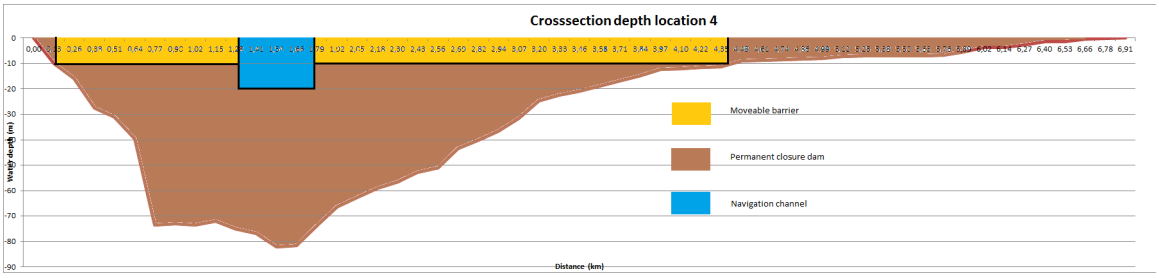

FIGURE 42: ALTERNATIVE 2 DETAILED DISTRIBUTION RETAINING STRUCTURES

From the calculations it has followed that alternative 2 with the moveable area in the middle of the bay saves the most material. The values are shown in Table 18.

TABLE 18: OVERVIEW ALTERNATIVE DAM VALUMES

	Original	Alternative 1	Alternative 2
Dam volume	33543759 m^3	31157362 m^3	20897662 m^3
Percentage original volume	100%	92.9%	62.3%

Based on this result, the further design of the barrier in this thesis will continue with the configuration of alternative 2, which is constructing the barrier at the deepest part of the cross-section. Note that the saved material volume might change due to the choices made for the dimensions of the moveable part of the barrier later in the design.

6.2 Water level inside the bay with permanent open navigation channel

Since the navigation channel requires a relatively large depth, and so does the moveable barrier gate for the channel, it is therefor interesting to check whether it is possible to keep the navigation channel permanent open.

The total water level rise inside the protected area by year 2100 also includes the following aspects.

- Pressure set-up (1.12 m)
- Wind set-up Tokyo (0.72 m)
- Sea level rise 2100 (1 m)
- River discharge (0.004 m)
- Wave overtopping (neglected in this stage)

It is assumed that the moveable barriers will be closed off at the moment when the water level inside the bay is at its lowest point. Since in this stage of the design it is not clear how many moveable barriers are going to be placed, the water level inside the bay will be checked assuming a permanently closed storm surge barrier with a permanently open navigation channel. Note that this assumption gives a much smaller allowable water level rise inside the bay compared to the actual situation with the moveable barrier due to the smaller tidal inlet.

For the calculation of the tidal inlet calculation the 'rigid-column approximation' (Labeur 2007) will be used. The obtained tidal inlet is 0.34 m, which is approximately 35% of the original tidal inlet. For an extensive calculation of the tidal inlet see appendix 10.

The minimum water level inside the bay is reached 0.6 hour before the start of the assumed typhoon condition. Since during this calculation the storm surge barrier is assumed to be

fully closed off except for the navigation channel, the water level inside the bay at the start of the typhoon is the same as the water level at the end of the tidal cycle. See Figure 43.

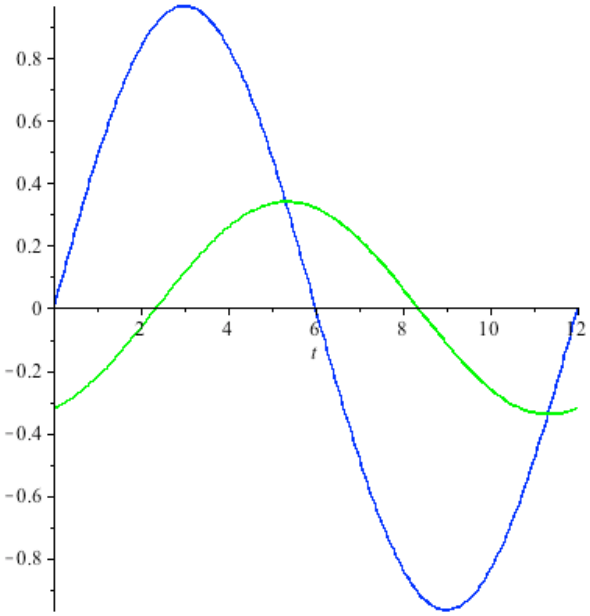

FIGURE 43: COMPARISON TIDAL LEVEL SEA SIDE (BLUE) WITH WATER LEVEL RISE INSIDE THE BAY (GREEN) WITH PERMANENT OPEN NAVIGATION CHANNEL, VERTICAL AXIS: WATER LEVEL RISE IN M, HORIZONTAL AXIS: TIME IN HOURS.

From this graph it can be seen that the water level inside the bay right before the assumed typhoon condition is 0.32 m under the mean water level inside the bay. The maximum allowed water level rise in the protected area caused by the flow through the permanent open navigation channel is then:

$$3.466 - 1.12 - 1 - 0.72 - 0.004 - 0.5 + 0.32 = 0.44\,m$$

Since the pressure set-up just inside and just outside the protected area is approximately the same, the maximum water head at the barrier during the typhoon is given in the equation below. Note that since this an initial estimation of the water level rise, the effect of wind set-down at the barrier is being neglected.

$$tide + wind\ set\ up + 0.32 = 0.966 + 0.16 + 0.32 = 1.44\,m$$

Also for this calculation the 'rigid-column approximation' (Labeur 2007) will be used. It is assumed that during storm surge the non-navigation parts of the barrier are fully retaining. The calculation results in a 0.41 m water level rise of the protected area inside the bay. For an extensive calculation of the water level rise see appendix 10.

The water level rise caused by the open navigation channel is below the maximal allowed water level rise. Therefor it is possible to keep the navigation channel permanent open during the design storm surge. The development of the assumed storm surge plus tide together with the corresponding water level rise inside the bay is plotted against time, in

Figure 44. Note in reality that the second part of the storm surge wave in the graph (after 6 hours) has a much smaller amplitude since it only contains the tide.

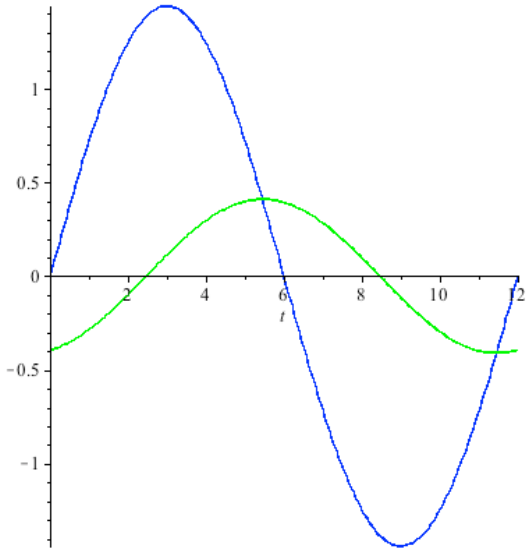

FIGURE 44: WATER LEVEL RISE STORM STORM SURGE (BLUE) COMPARISON WITH WATER LEVEL RISE INSIDE THE BAY (GREEN) WITH PERMANENT OPEN NAVIGATION CHANNEL, VERTICAL AXIS: WATER LEVEL RISE IN M, HORIZONTAL AXIS: TIME IN HOURS.

6.3 Summary

Considering the conservation of the environmental value of the Bay and the large depth of the chosen location, it appears that a barrier that is partly permanent closed and partly moveable is the most suitable choice for the situation. Also it appears that by placing the moveable barrier part at the deepest part of the span will save the largest volume of soil for the under water dam, which is 38.7% of the soil volume compared to fully closed off situation. This will also result in cost saving.

Based on calculations using the 'rigid column approximation' it can be concluded that the navigation channel can be left open during design typhoon conditions.

7 SUB-SYSTEM LEVEL DESIGN: MOVEABLE BARRIER

Because of the limited time provided for this master thesis it is decided to focus on the moveable part of the barrier, see Figure 45. It is presumed that earthquakes will be critical for this project the during the chosen design life. Therefor it is important to design a barrier that is earthquake resistant. Together with the fact that an under water closure dam is needed due to the great depth, a first look will be taken at the foundation types that is suitable for this situation. A comparison will be made between a bottom founded barrier and a new introduced concept, a floating barrier. After that several suitable barrier types will be presented and elaborated. The alternatives will be quickly assessed on their suitability to the situation.

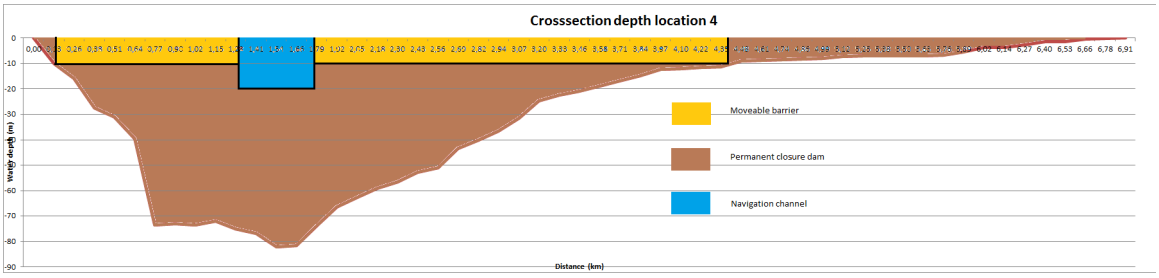

FIGURE 45: DISTRIBUTION RETAINING STRUCTURES STORM SURGE BARRIER

7.1 Bottom founded or floating

In this paragraph the bottom founded barrier will be compared to the floating barrier. For both types of barrier, the corresponding foundation alternatives will be presented with its advantages and disadvantages regarding the actual situation. Based on these characteristics a choice will be made between these two types of barriers and the suitable foundation types.

7.1.1 BOTTOM FOUNDED BARRIER (TRADITIONAL BARRIERS)

Bottom founded barriers are barrier that are situated on the ground. For the prescribed situation of this research, a bottom founded barrier will have to be situated on the under water dam. An impression of a bottom founded barrier is given in. Typical foundation types for bottom founded barriers are gravity based foundation and pile foundations.

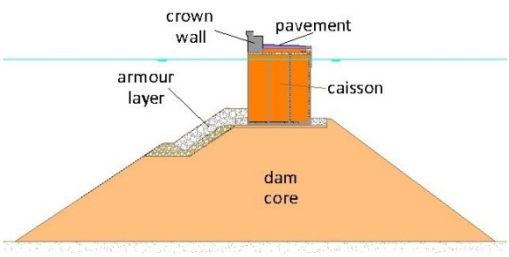

FIGURE 46: IMPRESSION BOTTOM FOUNDED BARRIER, CROSS-SECTINAL VIEW (FUENTES 2014)

7.1.1.1 Gravity based foundation

Gravity based foundation, or GBF, is a shallow foundation technic that is often used in the offshore industry. As the name already indicates, this type of foundation uses weight to maintain and support the upper structure. This is often done using big heavy concrete under structures. Due to its great size and weight, it is really difficult to make it on site. Therefor a GBF is often prefabricated and transported to site afterward. An impression of a GBF is shown in Figure 47, which is an foundation alternative during the design of the Eastern Scheldt storm surge barrier. A more comprehensive description of the gravity based foundation is given in Appendix 11.

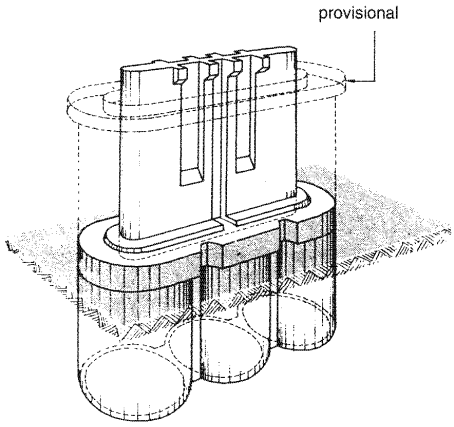

FIGURE 47: GRAVITY BASED FOUNDATION ALTERNATIVE EASTERN SCHELDT STORM SURGE BARRIER (A.A.BALKEMA 1994)

7.1.1.2 Pile foundation

Pile foundation is a deep foundations are foundations that are embedded deep into the soil. The main reason to choose a deep foundation over a shallow foundation is because of the large design load of the upper structure and poor soil quality at shallow depth. Piles are generally driven into the ground in situ, but it can also be put in place using drilling. The material used for the pile can vary from timber, steel, reinforced concrete and prestressed concrete. A more comprehensive description of the driven piles and drilled piles is given in Appendix 12.

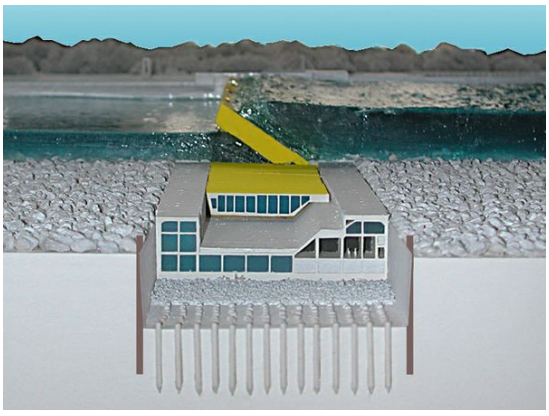

FIGURE 48: IMPRESSION PILE FOUNDATION MOSE BARRIER VENICE (RAUNEKK 2012)

7.1.1.3 Pros and cons

TABLE 19: PROS AND CONS BOTTOM FOUNDED BARRIER

Advantage	Disadvantage
Conventional way of installing barrier, more experience	Installation might affect adjacent structures
No extra floater needed	Installation might affect the strength of the under water dam
	Extra installation difficulties due to its placement on the under water dam
	Might need extra subsoil preparation before installation
	Under water dam probably needs to be designed with a higher standard since the stability the barrier is dependent on the stability under water dam, resulting in a higher cost of the under water dam
	Relatively more energy is being transferred from the sea bed to the barrier during earthquake

7.1.2 FLOATING BARRIER

Floating barriers is a new concept that is introduced in this thesis with the presumption that it posses a very promising earthquake resistant character. Floating barriers are just like the conventional bottom founded barriers, the only different is that they float and are fixed in its place by using mooring systems, see Figure 49. This mooring system technique is often used for station keeping of floating offshore platforms and recently it has also been applied to floating breakwaters. But is has never been applied on storm surge barriers. Since the working principles between a floating storm surge barrier and a floating offshore platform or a floating breakwater are approximately the same, it is assumes that this technique is also applicable for storm surge barriers. Mooring systems can be used for all water depths. The structure is fixed to the sea bed by using anchors and mooring lines.

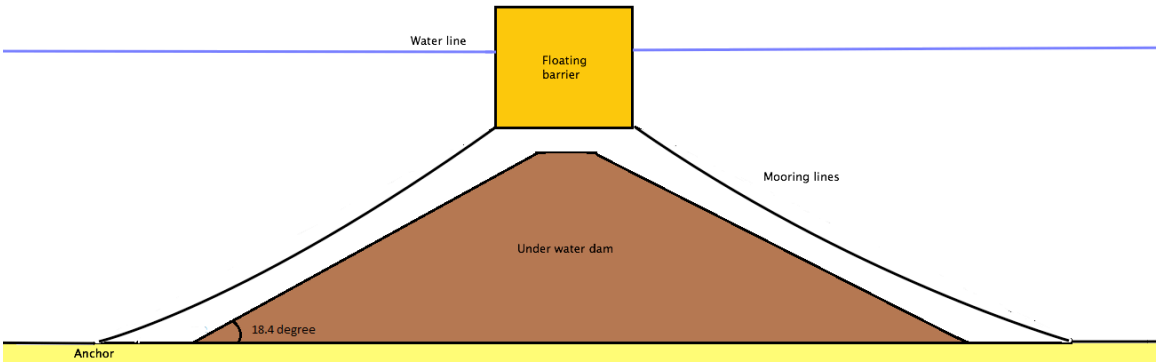

FIGURE 49: IMPORESSION CONCEPT FLOATING MOVEABLE BARRIER, CROSS-SECTIONAL VIEW

7.1.2.1 Types of Mooring Systems

In this paragraph three types of mooring systems are presented. They include:

- Catenary
- Taut leg
- Semi-taut

The catenary mooring system is often used in shallow water. The mooring line hangs free in water and changes its form when the upper structure moves. Because the mooring line lies horizontally at the seabed, its length has to be longer than the water depth. As the weight of the free hanging mooring lines increase faster with increasing depth than straight mooring lines, catenary systems becomes less economical as the water depth increases.

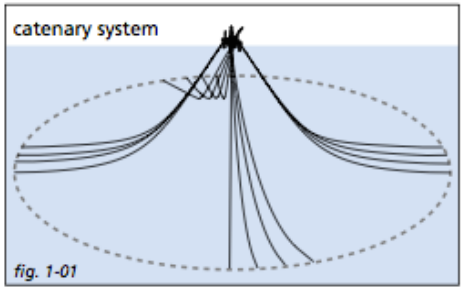

FIGURE 50: CATENARY MOORING SYSTEM (VRYHOF ANCHORS 2005)

The taut leg system typically uses polyester ropes that are pre-tensioned until taut. These ropes are connected to the anchors on the seabed under a 30 to 45 degree angle. For this type of mooring system both suction anchors and vertically loaded anchors can be used. When the upper structure moves due to waves or currents, the mooring lines stretch and set up an opposing force.

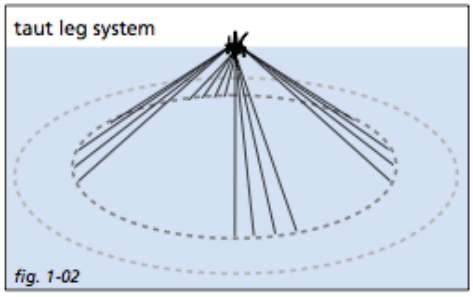

FIGURE 51: TAUT LEG MOORING SYSTEM (VRYHOF ANCHORS 2005)

The semi-taut system combines taut lines and catenary lines in one system. It is ideally used in deepwater.

7.1.2.2 Mooring line

The mooring line can be made from synthetic fiber rope, wire, chain or a combination of the three. Environmental factors like waves and currents determine which material for the mooring line is used. For shallow water up to 100 m depth, which is the situation of this

thesis, chain is often used for permanent mooring, whereas the other choices are more suitable for greater water depths.

FIGURE 52: MOORING FIBRE ROPE (LANKHORST ROPE 2012)

FIGURE 53: MOORING CHAIN (BLUE OCEAN TACKLE INC. SD)

FIGURE 54: MOORING WIRE (VRYHOF ANCHORS SD)

7.1.2.3 Anchors

The bearing capacity of the mooring system depends on the digging depth of the anchors and the surrounding soil properties. Anchor types include:

- Drag embedment anchors
- Suction piles
- Vertical load anchors

The drag embedment anchor is the most popular used anchor today, Figure 55. During anchoring it is being dragged along the seabed until it reaches the required depth in the soil. As it penetrates the seabed, it uses soil resistance to hold the anchor in place. The drag embedment anchor is mainly used for catenary mooring, where the mooring line arrives the seabed horizontally. The disadvantage of this type anchor is that it does not perform well under vertical forces.

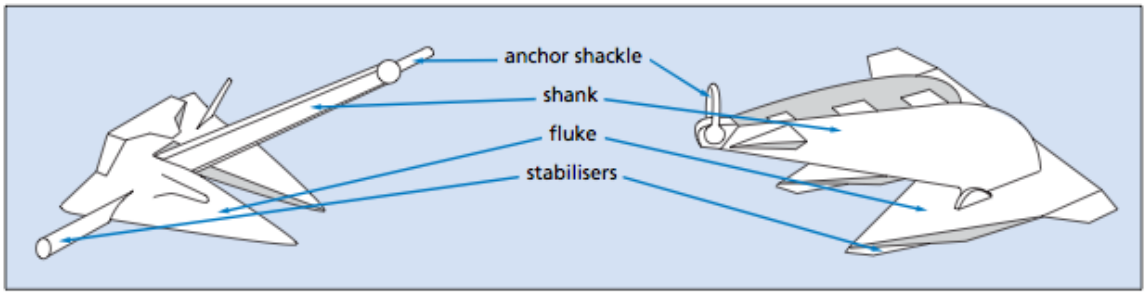

FIGURE 55: DRAG EMBEDMENT ANCHOR (VRYHOF ANCHORS 2005)

Suction piles anchors are tubular piles that are driven into the seabed, see Figure 56. The water is sucked out from the top of the pile by using a pump. This process pulls the pile further into the seabed. Suction piles can be used in sand, clay and mud soil, but not in gravel. This is due to the high permeability of the gravel where the water can flow through the ground during installation, which makes suction difficult. The pile is kept in place by the friction between the pile and the soil. It can resist both horizontal and vertical forces.

FIGURE 56: SUCTION PILE (INTERMOOR SD)

Vertical load anchors are similar to drag embedment anchors except for the greater weight that vertical load anchors possess, see Figure 57. Therefor vertical load anchors can withstand both horizontal and vertical forces. It is installed in the same way as the drag embedment anchors and is primarily used in taut leg mooring systems, where the mooring line arrives at an angle.

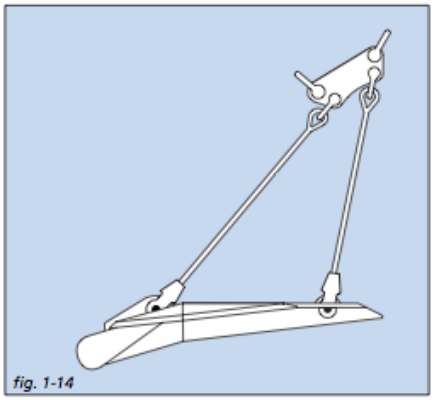

FIGURE 57: VERTICAL LOADED ANCHOR (VRYHOF ANCHORS 2005)

7.1.2.4 Pros and cons

TABLE 20: PROS AND CONS FLOATING BARRIER

Advantage	Disadvantage
Can be performed without subsoil improvements	Large number of anchors needed due to wave load and large size of the barrier
Barrier receives very small influence under earthquake situation	Barrier might move during the storm
Floating barrier can be disconnected from its location for maintenance or replacement	Gap between the floating barrier and the under water dam that might need to be closed off to limit the water inflow during the storm surge
Barrier stability independent of under water dam, no extra measure needs to be taken for the under water dam	Gap between floating barrier and the under water dam will probably induce large flow velocities that will lead to erosion problems
	Extra floater needed for the barrier
	Never been constructed before, no experience

7.1.3 EVALUATION

In this section, the pros and cons of both types of barriers will be compared with each other and evaluated. These pros and cons are again summarized in Table 21. It is presumed that the earthquake load will become decisive for the barrier design, therefor a barrier type that performs well under earthquake circumstances is preferred. In principle both bottom founded and floating types of barriers can be earthquake resistant. But because the stability of a bottom founded barrier is dependent on the under water dam and during earthquake significantly more energy is being transferred to the barrier, the floating barrier is more advantageous regarding earthquake resistance. Also a bottom founded barrier situated on the under water dam might influence the strength of the dam and due to its dependence on the under water dam, extra measures have to be taken during the design of the dam in order to maintain the stability of the moveable barrier above it. This might result in significantly higher cost for the dam due to its large volume. So by constructing a floating barrier, these extra costs can be prevented. On the other hand a floating barrier requires floaters in order to make the moveable barrier float. This will also lead to extra costs compared to the bottom founded barriers. Despite this fact, it is presumed that the costs for the floaters will be lower than the extra costs needed for the strengthening of the under water dam. Also the floating barrier consists the possibility to replace the barrier elements in a relatively easier way, making it more flexible than a bottom founded barrier. Other disadvantages of the floating barrier such as the movement of the moveable barrier during the storm and the gap between the under water dam and the moveable barrier can be solved with relatively easy measures. The movement of the barrier during storm can be controlled by controlling the length of the mooring lines and the gap between the under water dam and the moveable barrier can be closed of by using the principles of the ‘parachute barrier’. The barrier structure and the seabed will be connected using a synthetic rubber composite sheet (also used for bellows barriers) that will retain the water under the barrier structure. By using this method, the connection between the seabed and the barrier structure will maintain its flexibility, which will minimize the damage caused by the earthquake. Therefor it is chosen to continue with the floating barrier variant despite the fact that it has never been constructed before. In the following of this master thesis a conceptual design will be made of a floating moveable barrier. Note that the mooring system, mooring line and anchor types is not chosen yet. This will be evaluated later based on the preliminary design of the floating moveable barrier.

TABLE 21: COMPARISON PROS AND CONS BOTTOM FOUNDED AND FLOATING BARRIER

	Bottom founded barrier	Floating barrier
Advantage	Conventional way of installing barrier, more experience	Can be performed without subsoil improvements
	No extra floater needed	Barrier receives very small influence under earthquake situation
		Floating barrier can be disconnected from its location for maintenance or replacement
		Barrier stability independent of under water dam, no extra measure needs to be taken for the under water dam
Disadvantage	Installation might affect adjacent structures	Large number of anchors needed due to wave load and large size of the barrier
	Installation might affect the strength of the under water dam	Barrier might move during the storm
	Extra installation difficulties due to its placement on the under water dam	Gap between the floating barrier and the under water dam that might need to be closed off to limit the water inflow during the storm surge
	Might need extra subsoil preparation before installation	Extra floater needed for the barrier
	Under water dam probably needs to be designed with a higher standard since the stability the barrier is dependent on the stability under water dam, resulting in a higher cost of the under water dam	Gap between floating barrier and the under water dam will probably induce large flow velocities that will lead to erosion problems
	Relatively more energy is being transferred from the sea bed to the barrier during earthquake	Floating stability of the barrier has to be maintained
		Never been constructed before, no experience

7.2 Barrier alternatives evaluation

To determine the most suitable barrier gate for the floating moveable barrier, the alternatives will be judged based on a list of important criteria. They will be graded for each criteria from 1 to 3 with 3 is suitable and 1 not suitable. Also the criteria will be given a certain weight considering their importance. At the end, the barrier gate alternatives will be evaluated by using a Multi Criteria Analysis based on the given criteria and importance factors. For each barrier gate the grades will be multiplied with the corresponding criteria weight and summed up, giving a total score for the barrier. The barrier with the highest score will be chosen and a preliminary design will be made. For an extensive description of all barrier gate alternatives refer to Appendix 13.

7.2.1 EVALUATION CRITERIA

In this paragraph the considered number of criteria will be presented with their corresponding importance factor. For each criteria a short description will be given.

7.2.1.1 Adaptability to future water levels

This criterion judges the barrier by its flexibility to adapt to the uncertain water level rise in the future up to 200 years. Since this is one of the requirements for the barrier, it has an importance factor of 3.

7.2.1.2 Structure weight

Since it is chosen to build a floating barrier, it of importance to choose a barrier, which is as light as possible in order to limit the dead weight of the structure. Therefor it is chosen to also give this criterion an importance factor of 3

7.2.1.3 Space intake in open state

This criterion judges the barrier by its space intake in open state. It is preferred to keep as much of space open during open state regarding the preservation of the ecosystem inside the bay. Therefor the barrier will also be judged on this criterion. But because this criterion is only a preference in stead of a requirement, it is only given an importance factor of 1.

7.2.1.4 Maintenance of the barrier

Since the barrier is being design for really long time duration, the maintenance cost could be really significant; therefor it is important that maintenance needed is kept as low as possible. This criterion has been given an importance factor of 3.

7.2.1.5 Investment cost

This criterion is judging the barrier by its initial investment cost. Since the barrier will be build over a long span, it could lead to really large costs is a expensive barrier is chosen. Due to the importance to keep the initial cost as low as possible, this criterion is given an importance factor of 3. For barriers will be graded as following:

- Cost/m under 1 million: 3
- Cost/m under 2 million: 2

- Cost/m above 2 million: 1

For visor gates and barge gates no price has been found, so they have been graded with 2.

7.2.2 EVALUATION

Based on the above described criteria, and evaluation has been made in Table 22. It has been found that the inflatable rubber gate is the most suitable alternative. Its light weighted character and low initial investment cost made this type of barrier gate a very attractive choice for the floating barrier. But because the current existing inflatable barrier in Ramspol in the Netherlands is only 8.35 m high, it might needs to be scaled up to fulfil the minimal tidal inlet that is required for the bay. The only disadvantage of this alternative is its maintenance issues. Since it is made out of synthetic rubber material, it bears a higher chance for defection, especially in a relative rough environment like for the current situation. These rubber bellows might be replaced every 25 to 50 years. Despite this fact, it can also be seen as a chance to adjust the retaining height in the future if it's needed. Therefor it has scored a 2 for the adaptability for future water levels. Based on this evaluation it is decided to choose the inflatable rubber gate as barrier gate for the conceptual design of the floating moveable barrier

	Radial gates	Vertical lifting gates	Flap gates	Floating sector gates	Visor gates	Cylinder gates	Inflatable rubber gate	Barge gates	Horizontal sliding gate
Adaptability to future water level (3)	1	1	1	1	1	1	2	2	1
Weight of the structure (3)	1	1	3	2	1	2	3	2	1
Space intake in open state (1)	2	1	3	1	1	3	3	1	1
Maintenance of the barrier (3)	2	2	1	3	1	3	1	2	2
Investment cost (3)	3	3	1	2	2	1	3	2	2
Total score	23	23	21	22	16	24	30	22	19

TABLE 22: BARRIER EVALUATION NON-NAVIGATION GATE

7.3 Summary

It is presumed that earthquakes will be critical for this project the during the chosen design life. Therefor it is important to design a barrier that is earthquake resistant.

The bottom founded barrier is compared to the floating barrier. A floating moveable barrier has shown great potential regarding earthquake resistance due its independence of the stability of the under water dam and the small energy transfer from seabed to the moveable barrier during earthquake conditions. Despite the fact that this kind of barrier has never been made, it is considered technically feasible due to the comparable technique used for floating offshore platforms and floating breakwaters. Therefor it is chosen to continue with the floating barrier variant despite the fact that it has never been constructed before.

Considering the cost and the preferred weight and size of the gate for a floating moveable barrier, it appears that the inflatable rubber gate is the most suitable gate type to a floating moveable barrier.

8 PRELIMINARY DESIGN FLOATING MOVEABLE BARRIER

In this chapter a preliminary design will be made for the floating inflatable rubber barrier. This is divided into four elements, which are the Floating caisson (floater), inflatable rubber gate, anchors and mooring lines. As the design proceeds, certain design challenges might be revealed. Based on this a specific design aspect will be chosen and elaborated in further detail in the final design.

8.1 Design input and assumptions

8.1.1 DESIGN INPUT

In this paragraph a list of important design input will be presented. These design inputs are based on the information given in chapter 4.

- The maximum water level rise at the sea side during the assumed typhoon condition is 2.25 m above mean sea level. This value is gained by summing the pressure set-up. The wind set-up and the high tide level.
- Due the possible heave fluctuations of the floating barrier, it is chosen to increase the minimum depth of the navigation gate by 1 m, so the minimum navigation channel depth is now 18.5 m.
- The barrier must still be able to sufficiently reduce the surge if 10% of the barrier gates have failed to close. This requirement is adopted from the Eastern Scheldt Barrier design, which is still able to sufficiently block the surge in case 6 of 62 barrier doors (≈10%) fail to close in storm conditions.
- The horizontal wave loading on the barrier is based on the wave height presented in Table 16.
- The two way navigation channels must have a minimum width of 465 m.
- The surface of the floating structure where the inflatable rubber dam will be installed has to be above water without ballast. This way the maintenance of the rubber dam can be performed above water, making it a lot easier and cheaper.

8.1.2 ASSUMPTIONS

This preliminary design of the floating barrier is meant to give a first sense of the barrier dimensions and to recognize the possible critical issues. The calculation is done with the following assumptions.

- The inflatable rubber dam is installed on a semi-submerged caisson. The own weight if the rubber dam is assumed to be small compared to the caisson, therefor it is neglected in the pre-calculation.
- For the stability checks for working condition, the barrier is assumed to be moored on the seabed and translation of the barrier has not been taken into account. No mooring system has been chosen in this state, the mooring system is assumed to be stable and sufficient strong.
- In order to simplify the calculations, the influence of the mooring system on the stability of the floating barrier is during the floating stability check of the floating caisson.
- The calculations is done in the Serviceability Limit Stage (SLS). So safety factors for loads have not yet been taken into account. Only material factors for concrete strength properties are included in the calculation.
- Connections between barrier and anchor line is assumed to be sufficiently strong and will not be checked in this stage.
- Underseepage due to the hydraulic water head could result in groundwater flow or underseepage under the barrier has not been taken into account in the pre-calculation
- High velocities might occur around the barrier and might lead to scour holes around the anchors. These high velocities can occur during storm surge as well as in normal condition due to the constriction of the flow area. The effect of this phenomenon has not been included in the pre-calculation.
- The dynamic effects of earthquakes on the floating is neglected in this stage of the design.
- For the Floating caisson abutment a sloping plane of 45 degrees is assumed.

8.2 Configuration floating barrier concept

The floating barrier will be situated on top of the under water dam with a gap in between. The top of the under water dam is assumed to be 10 meters wide and the slope of the dam will be 1:3 (18.4 degrees). This is a quick assumption due to the limited time given for this master thesis. The configuration of the floating barrier and the under water dam is shown in Figure 58 and Figure 59.

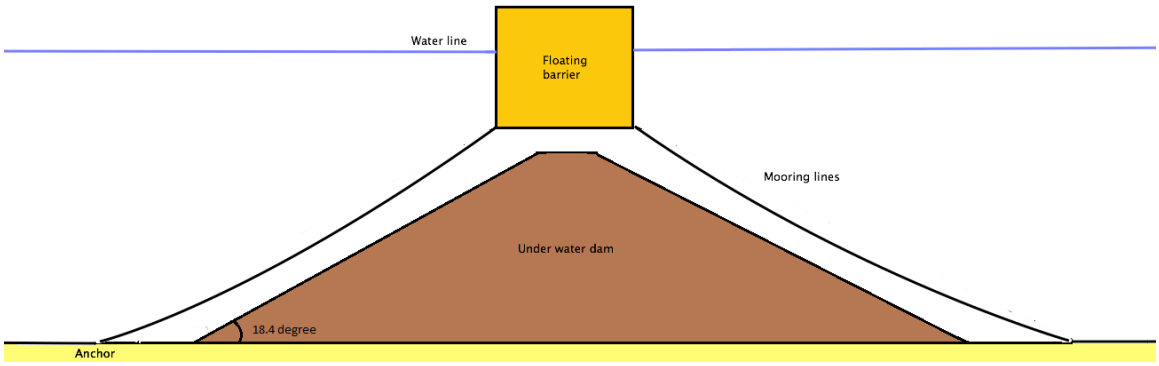

FIGURE 58: UNDER WATER DAM/FLOATING BARRIER CONFIGURATION, CROSS-SECTIONAL VIEW

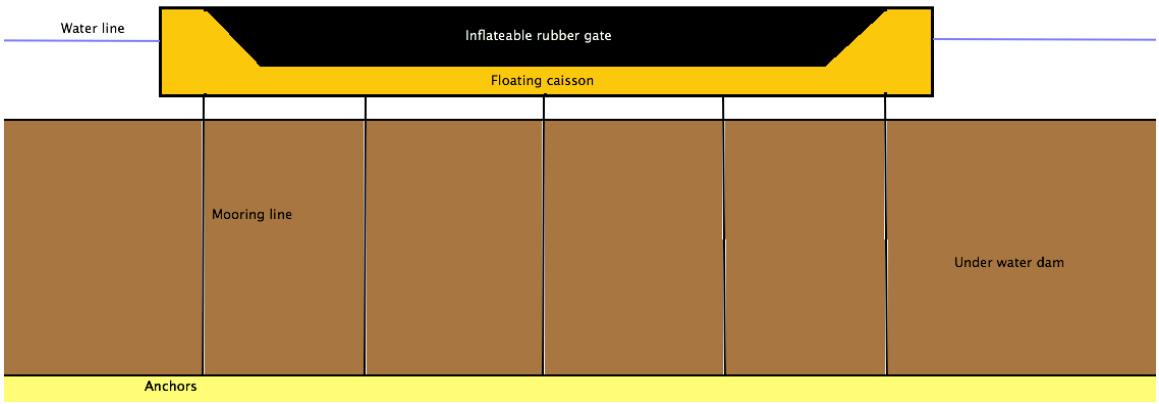

FIGURE 59: UNDER WATER DAM/FLOATING BARRIER CONFIGURATION, FRONT VIEW

8.3 Floating caisson design

This paragraph described the design of the floating where the inflatable rubber dam will be installed. First the caisson geometry will be defined. After the dimensions have been determined, different checks will be performed on the determined dimension

8.3.1 GEOMETRY DEFINITION

The will be separated into five parts, the central caisson and the two symmetrical abutments divided into two parts, one rectangular part and one trapezoid part, see Figure 60 The definition of these basic geometries are given in Appendix 14.

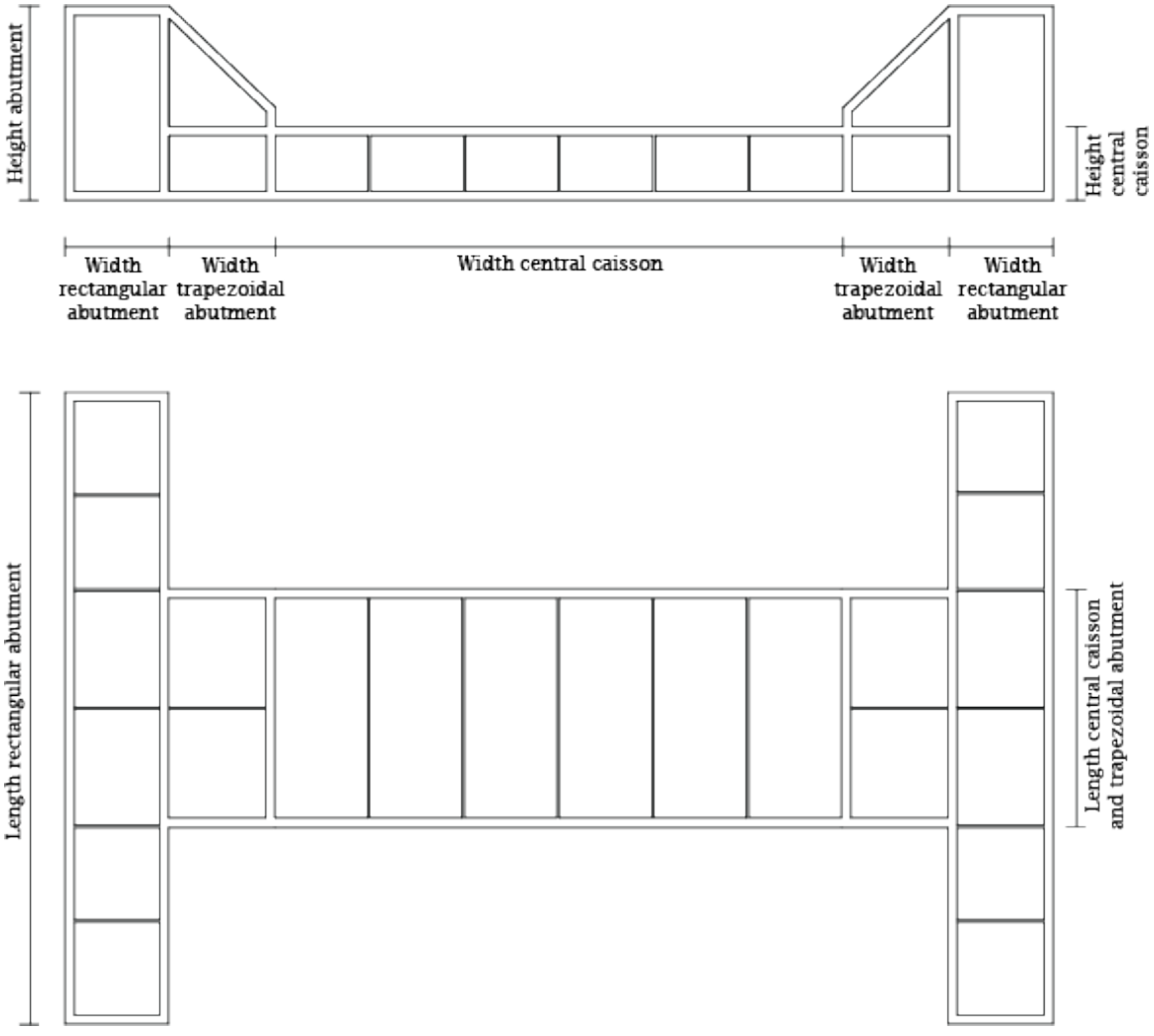

FIGURE 60: GEOMETRY FLOATING CAISSON, UPPER: FRONT VIEW, UNDER: UPPER VIEW

8.3.2 WEIGHT OF THE STRUCTURE

Before the weight of the structure can be defined, the volume of concrete has to be defined first. Since the weight of the inflatable rubber dam is neglected in open state (empty bellow), the weight of the caisson contains only the weight of the concrete and the weight of ballast.

The total volume of concrete can be defined by the following formula:

$$V_{concrete} = V_{cc} - V_{cc,in} + 2 * \left(V_{ab,rec} - V_{ab,rec,in}\right) + 2 * (V_{ab,tra} - V_{ab,tra,in})$$

Where:

$V_{concrete}$	[m³]	Volume of concrete
V_{cc}	[m³]	Volume central caisson
$V_{cc,in}$	[m³]	Total volume empty compartment central caisson
$V_{ab,rec}$	[m³]	Volume rectangular part abutment
$V_{ab,rec,in}$	[m³]	Total volume empty compartment rectangular abutment
$V_{ab,tra}$	[m³]	Volume trapezoid part abutment
$V_{ab,tra,in}$	[m³]	Total volume empty compartment trapezoid part abutment

The weight of the structure can then be simply determined by multiplying the volume by the volume weight of reinforced concrete, which is 25 kN/m³.

8.3.3 FLOATING CAPACITY

Before the floating capacity of the structure can be checked, the draft of the structure has to be determined first. The formula of the caisson's draft is determined as the following:

$$D_c = \frac{F_v}{\left(2 * W_{ab,rec} * L_{ab,rec} + 2 * W_{ab,tra} * L_{ab,tra} + W_{cc} * L_{cc}\right) * \rho_w}$$

Where:

D_c	[m]	Draft floating structure
F_v	[kN]	Total vertical load, in this case only the weight of the structure and Ballast.
ρ_w	[kN/m³]	Volume weight water
$W_{ab,rec}$	[m]	Width rectangular part abutment
$L_{ab,rec}$	[m]	Length rectangular part abutment
$W_{ab,tra}$	[m]	Width trapezoid part abutment
$L_{ab,tra}$	[m]	Length trapezoid part abutment
W_{cc}	[m]	Width central caisson
L_{cc}	[m]	Length central caisson

8.3.4 STATIC FLOATING STABILITY NORMAL CONDITION

The stability of floating caissons is maintained by keeping the metacenter of the caisson above the gravity center of the caisson by a minimum of 0.5 m see Figure 61. In the figure, M is the metacenter, G is the gravity center, B is the center of buoyancy and K is the reference point.

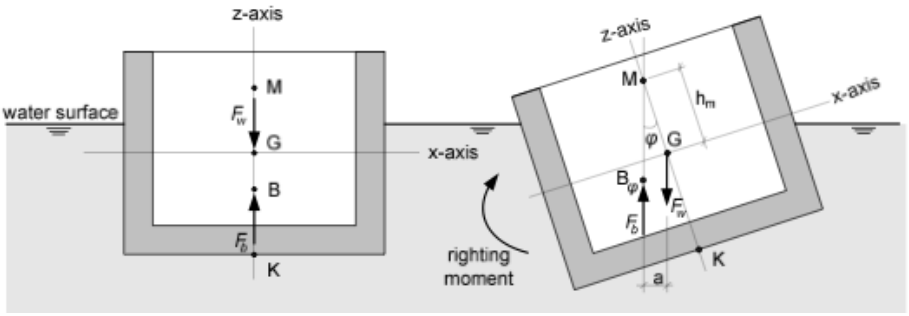

FIGURE 61: STATIC STABILITY SCHEME EMPTY CAISSON (TU DELFT 2011)

The distance between the metacenter and the gravity center can be determined as follows:

$$GM = BM + KB - KG$$

Where:

GM	[m]	Distance between metacentre and the gravity center
BM	[m]	Distance between metacenter and center of buoyancy
KB	[m]	Distance between center of buoyancy and reference point
KG	[m]	Distance between gravity center and reference point

A more comprehensive description of the static floating stability of the floating caisson during normal condition is given in Appendix 15.

8.3.5 STATIC FLOATING STABILITY STORM SURGE CONDITION

The same method can be used to calculate to static stability of the structure under storm surge condition. The only difference compared to the normal condition is that the rubber dam is now inflated with water and air, leading to an upward shift of the gravity centre of the structure, making it unstable. Also the water inside the bellow will cause sloshing during movement of the floating barrier. For the initial calculation of the storm surge situation, it is assumed the inflatable bellow is completely filled with water. To simplify initial calculation, the bellow is assumed to be a half cylinder over the whole span.

A more comprehensive description of the static floating stability of the floating caisson during storm condition is given in Appendix 16.

8.3.6 FLOATING CAISSON DIMENSIONS

By using the trial and error method it has been found that the gap between the under water dam and moveable barrier can be left open. In this paragraph the dimensions found for the floating caisson will be presented, which is based on the condition that without closing the

navigation opening and the gap between the under water dam, the water level rise will stay within the acceptable limits. This is constantly checked during an iteration proces of the caisson dimensions until it meets the requirements. The check for the waterlevel rise inside the protected area will be presented later in this report.

8.3.6.1 Input parameters

Due to the limited time provided for this thesis, no structural calculations are done. Assumptions have been made for the thickness of the walls and slabs in order to provide an initial indication for the dimensions and stability of the floating moveable barrier. The input parameters for the calculation is shown in Table 23. The retaining height of the inflatable rubber gate is chosen to be 3 m due to overtopping limitations. The effect of the overtopping to the water level rise inside the protected area will be checked later.

TABLE 23: FLOATING CAISSON INPUT PARAMETERS

Caisson inner space dimentions		
Central caisson empty width	60	m
Central caisson empty height	6	m
Central caisson empty length	25,25	m
Rectangular abutment empty width	10	m
Rectangular abutment empty height	19	m
Rectangular abutment empty length	65	m
Trapezoidal abutment empty width	10,5	m
Trapezoidal abutment triangle part empty height	12	m
Trapezoidal abutment total empty height	18	m
Storage height sheet inflatable rubber gate	2	m
Trapezoidal abutment empty length	25	m
Wall dimensions		
Outer wall thickness	1	m
Central caisson inner wall thickness	0,25	m
Abutment inner wall thickness	0,25	m
Abutment inner floor thickness	1	m
Number of compartments		
Number of compartment central caisson y-direction	6	-
Number of compartment trapezoidal abutment x-direction	2	-
Number of compartment rectangular abutment y-direction	1	-
Number of compartment rectangular abutment x-direction	6	-
Material densities		
Concrete weight	25	kN/m^3
Water weight	10	kN/m^3
Other inputs		
Minimum retaining height	3	m
Added water ballast volume	18200	m^3

8.3.6.2 Floating caisson dimensions

By using the assumed in internal dimensions of the floating caisson and wall thickness, the outer dimensions of the caisson elements are determined, see Table 24. By choosing a flow depth of 8 m for the moveable barrier, the required draught of the caisson after immersion is determined. Also the required maximum draught before immersion (no water ballast) is determined. This is to ensure that the surface of the central caisson, where the inflatable rubber gate will be installed, is above water. This way the maintenance of the rubber gate can be performed in dry conditions. Note that during the calculation, only the rectangular abutments are assumed to be filled with water ballast. The determined requirements are given in Table 25.

TABLE 24: FLOATING CAISSON DIMENSION RESULTS

Floating caisson dimension calculation		
Central caisson total width	61,25	m
Central caisson total height	8	m
Central caisson total length	27,25	m
Rectangular abutment total width	11,25	m
Rectangular abutment total height	21	m
Rectangular abutment total length	68,25	m
Trapezoidal abutment total width	11,5	m
Trapezoidal abutment total height	21	m
Trapezoidal abutment total length	27,25	m
Inflatable rubber gate height	11	m

TABLE 25: REQUIREMENTS FLOATING CAISSON DERIVED FROM INPUT PARAMETERS

Requirements		
Draught floating caisson	18	m
Maximum draught floating caisson before immersion	10	m

8.3.6.3 Draught calculation floating caisson

Based on the assumed input parameters and the determined caisson dimensions, the draught before and after the immersion can be calculated. These values are given in Table 26 and are checked with the required draughts in Table 25.

TABLE 26: FLOATING CAISSON DRAUGHT CALCULATION RESULT

Floating caisson draught calculation		
Total volume	55315,25	m^3
Total empty volume	40615	m^3
Total concrete volume	14700,25	m^3
Structural weight	367506,25	kN
Structural weight with ballast	549506,25	kN
Structural weight immersed	690014,0625	kN
Buoyancy force	38314,375	kN/m
Draught before immersion	9,591863367	m
Draught after immersion	18,00927361	m

8.3.6.4 Floating stability check

The floating stability of the floating caisson is checked based on the formulas given in paragraph 8.3.4 and 8.3.5. Note that the floating stability is only checked for storm condition after immersion. This is because this condition is the most unfavourable and unstable condition and thus the governing condition for the floating stability of the caisson. The results of the floating stability check are presented in Table 27.

TABLE 27: FLOATING STABILITY CALCULATION RESULTS

Weight floating caisson elements		
Weight central caisson	106562,5	kN
Weight rectangular abutment	188703,125	kN
Weight trapezoidal abutment	92793,75	kN
Weight water ballast	182000	kN
Weight water inside inflatable rubber gate	113564,4416	kN
Added water ballast height	14	m
Eccentricity floating caisson elements		
e central caisson	4	m
e rectangular abutment	10,25	m
e trapezoidal abutment	7,946751315	m
e water ballast	8	m
e water inside inflatable rubber gate	13,7595188	m
e floating caisson resultant	8,071162179	m
Displaced water floating caisson		
Displaced water weight submerged rectangular abutment	138206,25	kN
Displaced water weight submerged trapezoidal abutment	47142,5	kN
Displaced water weight submerged central caisson	133525	kN
Total volume of displaced water floating caisson	50422,25	m^3
Buoyancy floating caisson elements		
Bouyancy center rectangular abutment	9	m
Bouyancy center trapezoidal abutment	7,755298651	m
Bouyancy center central caisson	4	m
Moment of inertia floating caisson		
Ixx submerged	128493,9538	m^4
Iyy submerged	827230,9043	m^4
Floating stability storm condition floating caisson		
KG	9,203434847	m
KB	7,443183978	m
BM Ixx	2,548358191	m
BM Iyy	0,788107322	m
GM Ixx	16,40606883	m
GM Iyy	14,64581797	m

8.3.6.5 Final dimensions floating caisson

From the tables above it can be seen that the assumed caisson dimensions provides sufficient stability during storm condition and meets the required draughts. The final dimensions of the floating caissons and the flow area per caisson are presented in Table 28.

TABLE 28: FINAL DIMENSIONS FLOATING CAISSON

Final dimensions floating caisson		
Floating caisson total width	106,75	m
Floating caisson total height	20,5	m
Floating caisson total length	68,25	m
Flow area per Floating caisson	574	m^2

8.3.7 CHECK WATER LEVEL RISE INSIDE THE PROTECTED AREA

The 'rigid-column approximation' will again be used for the check of the water level rise inside the protected area of the bay caused by the gap between the floating barrier and the under water dam. For description of the theory see paragraph 6.2. Before the maximum amount of floating barriers can be calculated and the water level rise can be checked, the gap height between the floating barrier and the under water dam and the contribution of the wave overtopping have to be determined first.

8.3.7.1 Gap height between the floating barrier and the under water dam

Due to the consideration of the heave motion of the waves and the possible heave motion of the under water dam during earthquake, a gap height of 3 m between the under water dam and the floating barrier is guaranteed during normal condition without any tide. So the under water dam is at a depth of 21 m (before sea level rise). The maximum gap height is chosen to be 5 m. With this maximum gap height the floating barrier can move freely with the daily tides even after a SLS of 1 m without the mooring lines being tensioned. Note that due to the limited time given for the master thesis, this quick assumption is made with the believe that this gap height is sufficient for the heave motions of the waves and earthquake.

8.3.7.2 Water level rise caused by overtopping

For the determination of the water level rise caused by wave overtopping the approximation given by the hydraulic engineering manual is used (TU Delft 2011). Since the configuration of the floating barrier is different for the scenarios 'right after construction' and 'year 2100', the freeboard of floating barrier is also different, which are 2.75 m and 1.75 m for the scenarios 'right after construction' and 'year 2100' respectively. Also for the calculation of the overtopping the slope steepness of the under water dam is assumed to be 1:3 and the wave attacks are assumed to be perpendicular to the floating barrier. Using the approximation provided by the hydraulic engineering manual the water level rise caused by wave overtopping can then be determined, see Table 29. For an extensive calculation of the wave overtopping see appendix 17.

TABLE 29: WATER LEVEL RISE CAUSED BY WAVE OVERTOPPING

Scenario right after installation	0.0004 m
Scenario year 2100	0.006 m

8.3.7.3 Floating barrier numbers and water level rise inside the protected area during storm

The water level rise is being checked with the 'rigid column approximation' and the assumed contribution for the water level rise at Tokyo by year 2100 beside the water flow through the open navigation channel and the gap between the under water dam and the floating barrier are summarized in Table 30.

TABLE 30: CONTRIBUTION WATER LEVEL RISE BESIDE FLOW THROUGH OPEN NAVIGATION CHANNEL AND GAP BETWEEN UNDER WATER DAM AND FLOATING BARRIER.

Contribution water level rise	
Pressure set-up	1.12 m
Wind set-up	0.72 m
River discharge	0.004 m
Wave overtopping right after barrier construction	0.0004 m
Wave overtopping year 2100	0.006 m
Sea level rise	1 m

After an iterative calculation process is has been concluded that by choosing in total 5 moveable floating barriers the gap and the navigation channel can be left open permanently without the water level rise exceeds the allowed limit. The total length of the moveable barrier plus the open navigation channel will be approximately 1 km. It is worth to note that even only 5 floating moveable barrier are placed, the soil volume needed for the permanent closure dam is still 29% less than placing the moveable barriers directly on the seabed at the shallow areas of the span. The configuration of the storm surge barrier is illustrated in Figure 62.

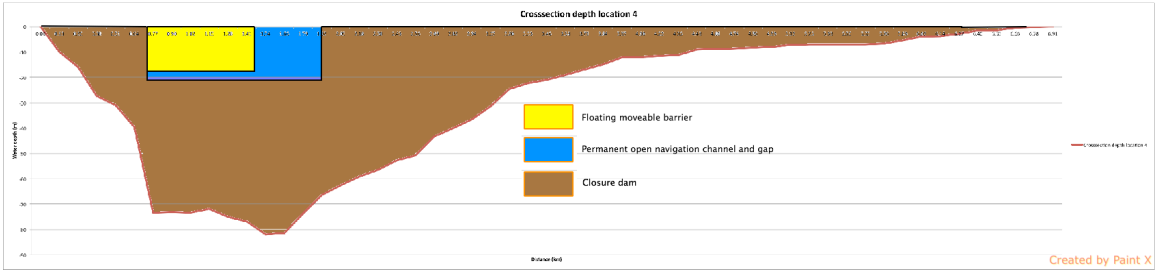

FIGURE 62: DISTRIBUTION FLOATING MOVEABLE BARRIER

For the scenario right after the barrier construction, because there is no sea level rise yet for this scenario, it is chosen to close the barrier gates at neutral tide conditions in order to guarantee a minimum gap height of 3 m during the whole storm duration. By counting in the contribution of the wave overtopping, the maximum allowed water level rise inside the protected area due to the open navigation channel and gap after closing the barrier gate without tide becomes:

$$3.466 - 0{,}5 - 1.12 - 0.72 - 0.004 - 0.0004 = 1.12\,m$$

And for the scenario year 2100, due to the 1 m SLR it is chosen to close the barrier during lowest water level inside the bay which corresponds to a water level of 0.48 m below mean sea level. For the assumed typhoon condition (spring tide + storm surge) this water level inside the bay is reached 1 hour before the start of the storm surge. Since the gape between the floating moveable barrier and the under water dam and the navigation channel has been left open, the water level rise inside the bay over the period between the barrier closure and the start of the storm surge have been approximated by the water level rise caused by the tide between the moment of the lowest water level inside the bay and 1 hour after when only the gap and the navigation channel is left open. This results in a 0.05 m water level rise inside the bay. See also Figure 63.

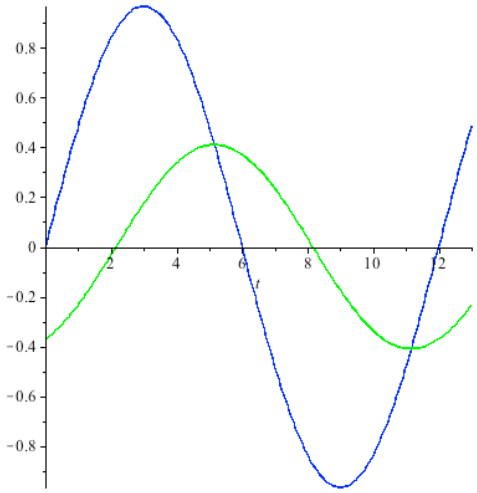

FIGURE 63: COMPARISON WATER LEVEL RISE TIDE (BLUE) WITH WATER LEVEL RISE INSIDE THE BAY (GREEN) WITH PERMANENT OPEN NAVIGATION CHANNEL AND OPEN GAP, VERTICAL AXIS: WATER LEVEL RISE IN M, HORIZONTAL AXIS: TIME IN HOURS.

Therefor the maximum allowed water level rise inside the protected area due to the open navigation channel and gap after closing the barrier gate at low tide becomes:

$$3.466 + 0.48 - 0.05 - 0{,}5 - 1 - 1.12 - 0.72 - 0.004 - 0.006 = 0.55\ m$$

The corresponding water level rise during the design typhoon condition due to flow through the gap and the open navigation channel is 0.45 m for the scenario right after the barrier construction and 0.54 m for the scenario year 2100. By including the requirement with 10% gate closure failure, which corresponds with approximately 1 gate, the water level rise contribution inside the protected area becomes 0.47 m and 0.56m respectively for the right after construction and year 2100 scenarios. So for both scenarios, during situations where no gate closure failure occurs, the water level rise caused by the gap and the open navigation channel is within the allowed limit. When including the gate failures, the water level rise for the scenario right after barrier construction is still well within limit while for the scenario year 2100 the water level rise is above the allowed limit. Since the chance of occurrence of the gate failure and the design typhoon situation at the same time is considered very small, this exceedance of the allowed water level rise can be retained by the 0.5 m freeboard that

has been taken into account. In this case extra wave overtopping protection measures can be taken at the coastal dykes. This reinforcement of the coastal dykes is outside the scope of this research. The development of the assumed storm surge plus tide together with the corresponding water level rise inside the bay is plotted against time. See Figure 64. Note the water levels given in the graph are with respect to the water level inside the bay at the start of the storm surge (0.43 m below mean sea level), also in reality the second part of the storm surge wave in the graph (after 6 hours) has much smaller amplitude since it only contains the tide.

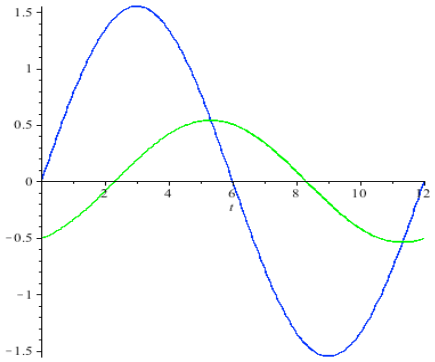

FIGURE 64: COMPARISON WATER LEVEL RISE STORM SURGE (BLUE) WITH WATER LEVEL RISE INSIDE THE BAY (GREEN) WITH PERMANENT OPEN NAVIGATION CHANNEL AND OPEN GAP, VERTICAL AXIS: WATER LEVEL RISE IN M, HORIZONTAL AXIS: TIME IN HOURS.

In next paragraphs different water levels with the corresponding gap heights are presented for both normal and storm conditions for the scenarios right after the construction of the barrier and by year 2100.

8.3.7.3.1 Scenario tight after barrier construction

During normal condition right after the construction of the floating barrier, the gap between the floating barrier and the under water dam is 3 m and the mooring lines contains a small sag. See Figure 65.

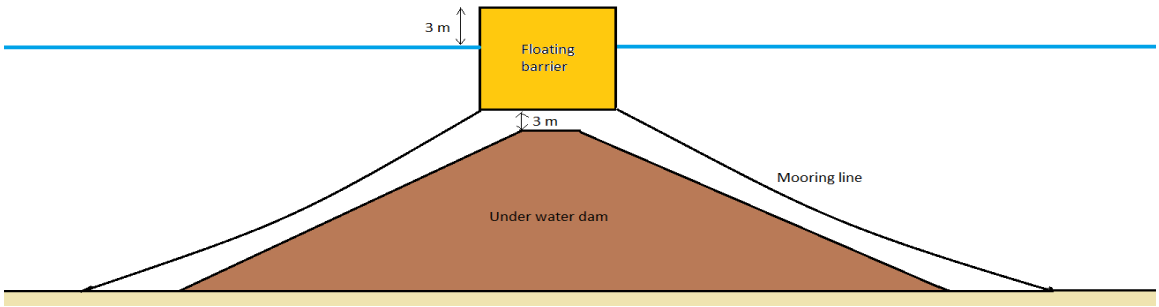

FIGURE 65: NORMAL CONDITION SCENARIO RIGHT AFTER INSTALLATION

During storm conditions the moveable barriers are closed during normal tide. The water level rise at sea side is the tide height, the pressure set-up and the wind set-up:

$$0.966 + 1.12 + 0.16 = 2.246\,m$$

The water level rise at the bay side is only the pressure set-up, which is 1.12 m, creating a maximum water head of 1.126 m, see Figure 66.

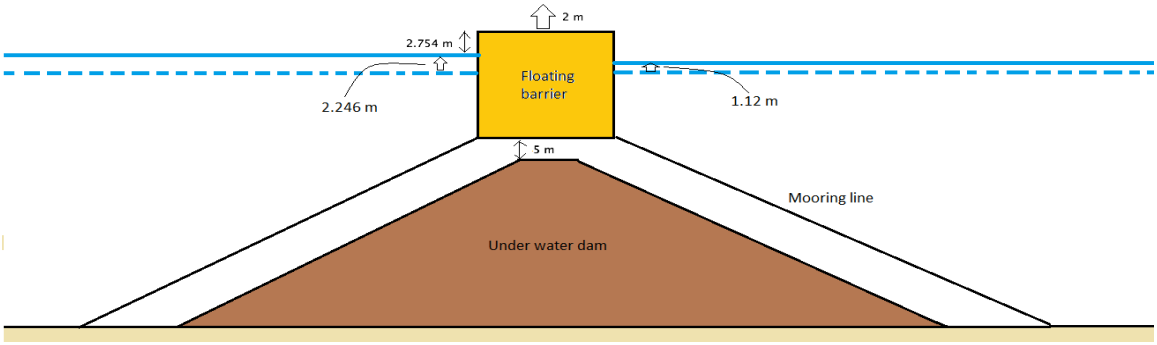

FIGURE 66: STORM CONDITION SCENARIO RIGHT AFTER INSTALLATION

8.3.7.3.2 Scenario year 2100

During normal condition by the year 2100 the gap between the floating barrier and the under water dam will increase to 4 m due to a sea level rise of 1 m. The mooring lines contain small sag. See Figure 67.

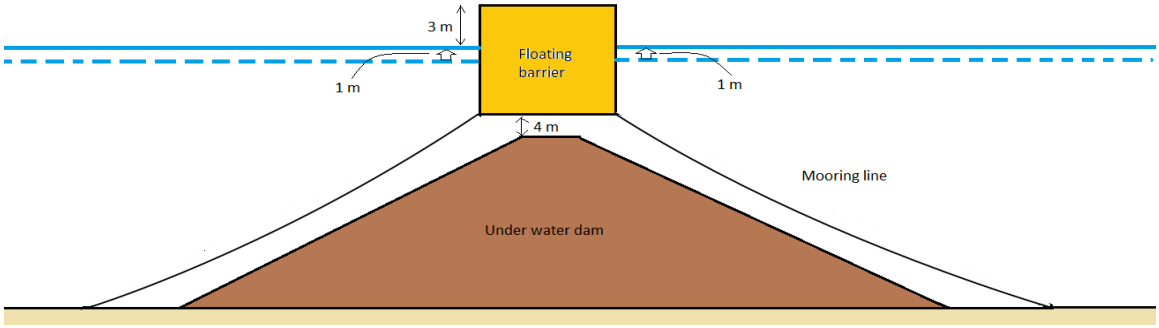

FIGURE 67: NORMAL CONDITION SCENARIO YEAR 2100 (WITH 1 M SLR)

Due to the 1 m SLR it is chosen to close the barrier at the moment when the water level inside the bay is at its lowest point, therefor the gap height between the floating barrier and the under water dam becomes 3.52 m and there will be a small sag in the mooring lines, see Figure 68.

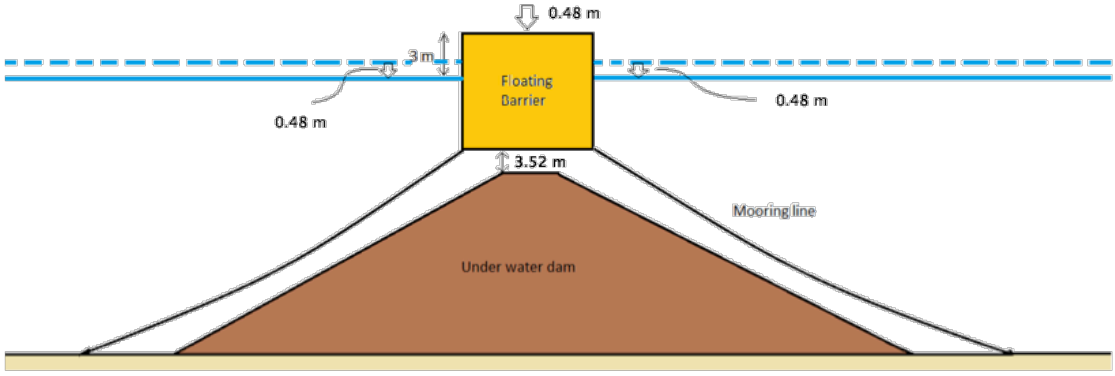

FIGURE 68: SCENARIO YEAR 2100 (WITH 1 M SLR), RIGHT BEFORE BARRIER GATE CLOSURE (LOW TIDE)

During storm condition, the total water level rise at the seaside is therefor the following

$$0.966 + 0.48 + 1.12 + 0.16 = 2.726\ m$$

The water level rise at the bay side is the pressure set-up and the water level rise caused by the tide between barrier closure and the start of the storm surge, which is 1.17 m, creating a maximum water head of 1.55 m. The mooring lines are fully stretched out in this condition. See Figure 69.

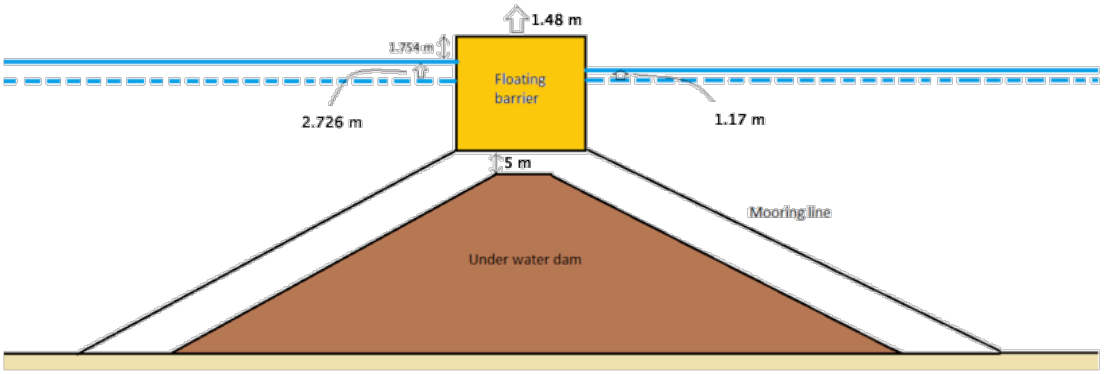

FIGURE 69: STORM CONDITION SCENARIO YEAR 2100 (WITH 1 M SLR)

8.3.7.4 Check tidal inlet

The tidal inlet can also be checked with the same method used for the determination of the water level rise inside the bay area. With the assumed number of floating barriers and gap height, the corresponding tidal inlet is 50% of the original tidal height for both scenarios.

8.3.7.5 Evaluation

From this analysis it is found that the water level rise inside the bay is very sensitive to the moment of barrier closure because of the large permanent open area. So when the barrier is closed has a large influence on the magnitude of the water level rise inside the bay. Since this is not preferable for the functionality of the barrier, it can be chosen to close off the gap between the floating barrier and the under water dam to make the water level rise inside the bay less sensitive to the moment of barrier closure. Also by closing off the gap more floating moveable barriers can be placed over the span. This will result in a larger tidal inlet, which will again lead to more water exchange during normal condition and higher allowed water level rise limit inside the bay during storm surge and thus a higher safety level. One of the possibilities to close off the gap is to use synthetic rubber sheets, this way the floating barrier can still move freely, this especially important for earthquake conditions. Another possibility is to add a certain layer between the floating barrier and the under water dam to neutralize the impact when the floating barrier collides with the under water dam. Note that with this latter possibility the gap is not closed off, but the gap height can be decreased to limit the flow during storm conditions. Due to the limited time provided for this thesis this gap closure is not further investigated and the 5 floating barriers will be assumed for further design.

8.4 Mooring lines

In this paragraph a preliminary design will be made for the mooring lines of the floating barrier. First the governing load on the floating barrier will be determined. After that the appropriate type and number of mooring lines will be chosen.

8.4.1 LOADS

For the design of the mooring lines three load cased are considered, which are the typhoon load case, the tsunami load case and the earthquake load case. From the obtained results of each load case calculation appendix 18, it can be concluded that the typhoon load case is the governing load case for both horizontal and vertical loads. Therefor the loads caused during the design typhoon condition will be used for the design of the mooring lines. The governing loads are given in Table 31.

TABLE 31: GOVERNING LOAD ON FLOATING BARRIER

Horizontal load	69525 kN/barrier
Vertical load	70382 kN/barrier

8.4.2 MOORING LINES DESIGN

It is assumed that the center of the floating barrier is situated exactly above the center of the under water dam. It is chosen to have the floating barrier fixed with in total 14 mooring chains, 7 mooring chains each side of the floating barrier. The chosen mooring chain is R4-RQ4 studless type of chain with diameter of 178 mm. The proof load of the chosen mooring chain is 18018 kN, see Table 32.

TABLE 32: PROEF/BREAK LOAD MOORING CHAINS (VRYHOF ANCHORS 2005)

diameter	Proof load						Break load				Weight	
	R4-RQ4		R3S		R3	RQ3-API	R4-RQ4	R3S	R3	RQ3-API		
	stud	studless	stud	studless	stud-studless	stud-studless	stud and studlless				stud	studless
mm	kN	kN	kN	kN	kN	kN	kN	kN	kN	kN	kg/m	kg/m
105	8478	7497	7065	6829	6123	5495	10754	9773	8753	8282	241	221
107	8764	7750	7304	7060	6330	5681	11118	10103	9048	8561	251	229
111	9347	8265	7789	7529	6750	6058	11856	10775	9650	9130	270	246
114	9791	8658	8159	7887	7071	6346	12420	11287	10109	9565	285	260
117	10242	9057	8535	8251	7397	6639	12993	11807	10574	10005	300	274
120	10700	9461	8916	8619	7728	6935	13573	12334	11047	10452	315	288
122	11008	9734	9173	8868	7950	7135	13964	12690	11365	10753	326	298
124	11319	10009	9432	9118	8175	7336	14358	13048	11686	11057	337	308
127	11789	10425	9824	9497	8515	7641	14955	13591	12171	11516	353	323
130	12265	10846	10221	9880	8858	7950	15559	14139	12663	11981	370	338
132	12585	11129	10488	10138	9089	8157	15965	14508	12993	12294	382	348
137	13395	11844	11162	10790	9674	8682	16992	15441	13829	13085	411	375
142	14216	12571	11847	11452	10267	9214	18033	16388	14677	13887	442	403
147	15048	13306	12540	12122	10868	9753	19089	17347	15536	14700	473	432
152	15890	14051	13241	12800	11476	10299	20156	18317	16405	15522	506	462
157	16739	14802	13949	13484	12089	10850	21234	19297	17282	16352	540	493
162	17596	15559	14663	14174	12708	11405	22320	20284	18166	17188	575	525
165	18112	16016	15094	14590	13081	11739	22976	20879	18699	17693	596	545
168	18631	16474	15525	15008	13455	12075	23633	21477	19234	18199	618	564
171	19150	16934	15959	15427	13831	12412	24292	22076	19771	18707	640	585
175	19845	17548	16538	15986	14333	12863	25174	22877	20488	19386	671	613
178	20367	18010	16972	16407	14709	13201	25836	23479	21027	19896	694	634
180	20715	18318	17263	16687	14961	13427	26278	23880	21387	20236	710	648
185	21586	19088	17989	17389	15590	13991	27383	24884	22286	21087	750	685

The 14 mooring chains are installed parallel with the slope of the under water dam. 4 on the abutments both side of the floating barrier in the width direction and 10 on the central

caisson. The two on the abutment are again 60 degrees tilted in the width direction of the floating barrier to resist possible forces in that direction. The configuration of the mooring chains are shown in Figure 70 and Figure 71.

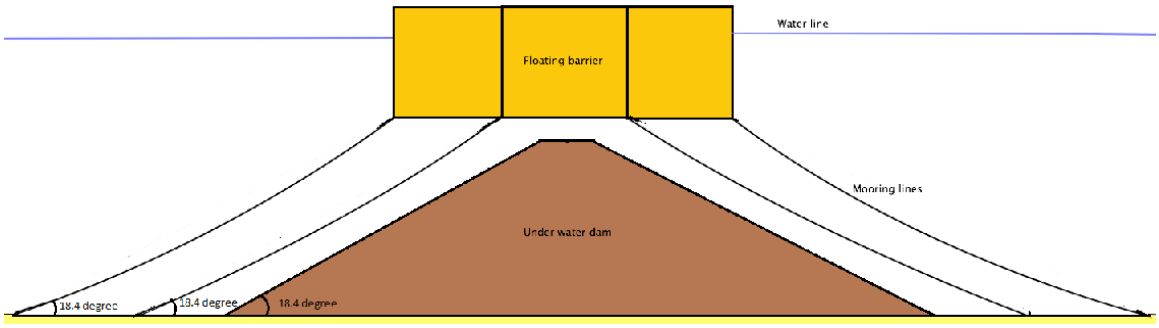

FIGURE 70: UNDER WATER DAM/FLOATING BARRIER CONFIGURATION, CORSS-SECTIONAL VIEW

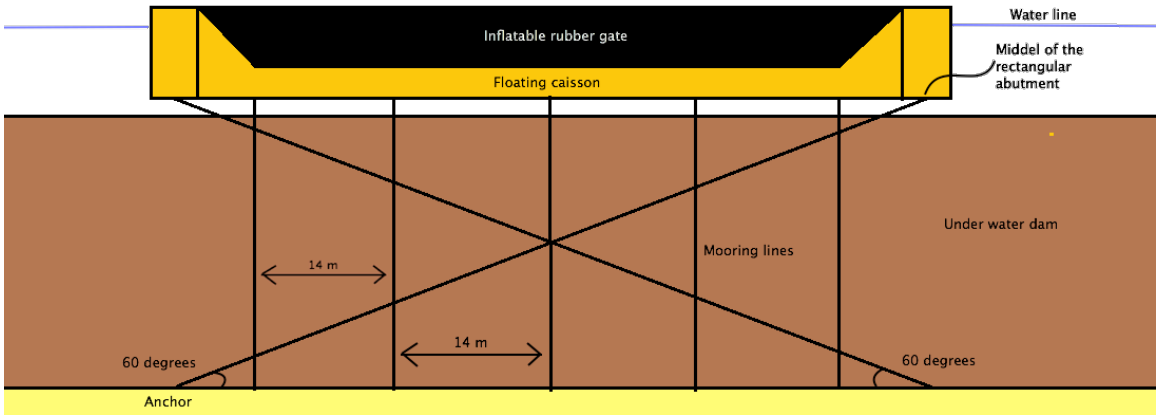

FIGURE 71: UNDER WATER DAM/FLOATING BARRIER CONFIGURATION, FRONT VIEW

The resistance of mooring chains are calculated as the following:

Mooring chains on the central caisson:

$$F_{h,c} = 18018 * \cos(18.4) = 17089\ kN/chain$$
$$F_{v,c} = 18018 * \sin(18.4) = 5684\ kN/chain$$

Mooring chains on the abutment:

$$F_{h,a} = 16016 * \sin(60) * \cos(18.4) = 14800\ kN/chain$$
$$F_{v,a} = 16016 * \sin(60) * \sin(18.4) = 4923\ kN/chain$$

The total resistance of the mooring chains amounts 115045 kN in the design wave direction (perpendicular to the width of the floating barrier) and 76541 kN in the vertical direction. This is 45521 kN and 6160 kN more than the required reistance force for the horizontal and vertical load repectively. This done by intention to keep the floating barrier in its position during the design typhoon condition even after one of the mooring chains is broken.

8.5 Inflatable rubber gate

In this paragraph a preliminary design will be made for the inflatable rubber gate. Due to the limited time given for a master thesis, only a number of basic properties of the inflatable rubber gate will be discussed and elaborated. The descriptions given in this paragraph is based on the master thesis of M. Breukelen (Breukelen 2013). A more comprehensive elaboration of the design and upscaling of the inflatable rubber gate can be found in the master thesis of M. Breukelen (Breukelen 2013)

8.5.1 ONE AND TWO SIDED CLAMPED INFLATABLE DAM

An inflatable rubber gate consists of a rubber sheet that is connected to a supporting structure. It can be closed by inflating the rubber sheet using a filler e.g. air and/or water. Two types of inflatable rubber gates can be distinguished, which are one sided clamped and two sided clamped rubber gates.

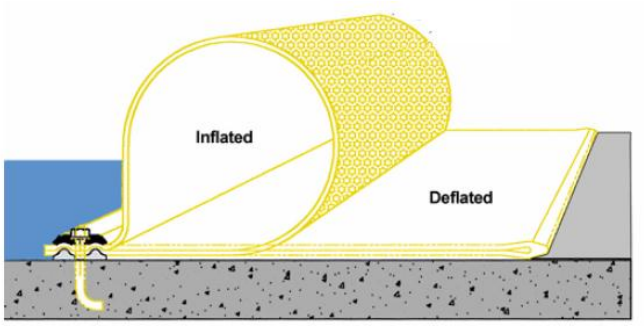

FIGURE 72: ONE-SIDED CLAMPED RUBBER SHEET (BOUWDIENST RIJKWATERSTAAT EN WL| DELFT HYDRAULICS 2005)

8.5.1.1 One sided clamped rubber gate

For a one sided clamped rubber gate, both long sides of the sheet are clamped in the same clamping line, see Figure 72. Normally a one sided clamped inflatable rubber gate is used as a weir, because a weir only need to retain water in one direction.

8.5.1.2 Two sided clamped rubber gate

For a two sided clamped rubber gate, the long sides of the sheet are separately clamped in the supporting structure, so there are two clamping lines, see left figure of Figure 73. Both clamping lines continues to the abutment and comes together above the waterline. Two sided clamped inflatable rubber gates are normally used as storm surge barriers.

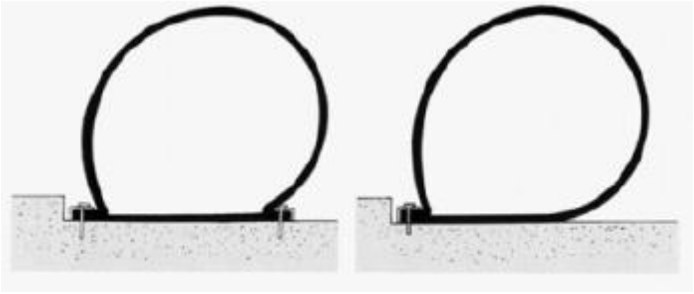

FIGURE 73: LEFT: TWO-SIDED CLAMPED RUBBER SHEET, RIGHT: ONE-SIDED CLAMPED RUBBER SHEET (BREUKELEN 2013)

For the situation considered in this thesis a two sided clamped sheet with a symmetrical design relative to the longitudinal axis needs to be applied in order to prevent suddenly and uncontrolled flipping of the rubber sheet during the storm surge, therefor the two sided clamped inflatable rubber gate is considered suitable for this situation

8.5.2 FILLER OF THE INFLATABLE RUBBER GATE

Filler of the inflatable rubber gate can consist of air, water or a combination of air and water; it determines a large part of the deformation capacity and force transfer of the rubber gate. Different fillers provide different behaviour of the rubber gate and results therefor in a different load distribution. The difference between internal and external pressure directly influences the stiffness of the rubber gate. For the selection of the filler the following aspects have to be considered.

1. The required crest height of the barrier, the circumferential length of the sheet and the internal pressure required to achieve this crest height.
2. Speed of the opening and closing of the gate and therefor the required pump power. This aspect is important for storm surge barriers.
3. The magnitude of the load in the sheet and foundation floor. This load depends on the internal pressure, external pressure and the self-weight of the sheet.
4. Stability of the rubber gate.
5. Weather conditions.
6. Degree of fluctuating loads
7. The influence of the compressibility of the filler on the stiffness and dynamic behaviour of the inflatable rubber gate.

In Table 33 a comparison has been made between the fillers: air, water, water and air, based on the aspects mentioned above.

TABLE 33: COMPARISON FILLER INFLATABLE RUBBER GATE (BREUKELEN 2013)

Aspects	Air	Water	Air and water	Elaboration
1	--	-	+	An air filled rubber gate needs a larger internal pressure to withstand the external loads and therefor a larger total internal pressure to achieve the required crest height. In case of a water filled gate a much lower internal pressure is needed, but it requires a larger circumferential length. Therefor a combination of air and water gives the best solution for this aspect.
2	+	--	0	Air requires less energy and time to pump in than water. For the combination of air and water, water can flow into the rubber gate by gravity after the first air supply. During deflation the water must be pumped out.
3	--	-	+	For an air filled rubber gate the tension is high and its own weight is low. For a water filled rubber gate the tension is lower and its own weight much higher. With a combination of both water and air it's in between.
4	--	-	-	An air filled dam has the tendency to V-notching. A water filled dam could move along with waves. A combination of water and air may cause sloshing in the dam due to the free water surface.
5	+	-	-	In theory the water could freeze when the temperature drops below zero and the air could expand when the temperature rises. The first is case is less favourable than the last one since it can cause a loss of flexibility.
6	0	0	+	A water filled rubber gate could move along with waves. A water and air filled dam can withstand several load combinations.
7	-	+	++	For the combination of water and air, the amount of air pressure can be adjusted.
Result	Negative	Negative	Positive	

Disadvantages of a water filled inflatable rubber gate (Breukelen 2013):

- A larger dynamic load (due to the large pivoting water);
- A smaller retaining height (due to sagging of the dams by the water weight);
- A large pressure in the supporting structure will be present.

Disadvantages of an air filled inflatable dam (Breukelen 2013)

- Sensitive for vibration in a spillway situation;
- V-notch phenomenon that occurs when the internal pressure is reduced and the water flows over the dam; the plunging jet might affect the bottom protection.

Advantages of a combination of water and air are (Breukelen 2013):

- For closing the inflatable dam only compressors for air are needed, the water flows naturally in the rubber gate;
- The shape and the pressure of the inflatable rubber gat fits itself to the changing water levels; this is because the interior of the rubber gate is connected with the upstream water;
- The inflatable rubber gate is during wave loads stiffer than a completely filled dam with air;
- Only water pumps required for deflation of the inflatable rubber gate; the air is pushed out of the rubber gate due to the external water pressure.

From this analysis it can be concluded that the combination of air and water is the most preferable filler for the inflatable rubber gate.

8.6 The Anchors

Due to the limited time provided for the master thesis, only the type of anchor to be chosen will be qualitatively elaborated. Three general types of anchors were introduced in paragraph 7.1.2.3, which are:

- Drag embedment anchors
- Suction piles
- Vertical load anchors

The working principles of drag embedment anchors and vertical load anchors are similar. Both uses soil resistance to hold the anchor in place. During storm surge condition, the floating moveable barrier will be exposed to a considerable amount of vertical load due to the water surge at the seaside of the barrier. Since the drag embedment anchors does not perform well under vertical forces and the vertical load anchors can withstand both horizontal and vertical forces due to its greater weight, the vertical load anchor is preferred over drag embedment anchors. A more comprehensive description of the background theory of design the drag embedment anchors and vertical load anchors is given in (Vryhof anchors 2005).

Suction piles are also able to resist both horizontal and vertical loads. But because the anchor strength of the suction pile is based on suction and since the soil of the seabed might be shaken loose after an earthquake, it is unsure what the influence of the shaken soil will be on the anchor strength of the suction piles. Therefor more research needs to be done on the anchor strength of the suction piles under earthquake condition before a comparison can be made between the suction piles and the vertical load anchors. Both of these anchors are possible solutions for this situation.

8.7 Impression drawings

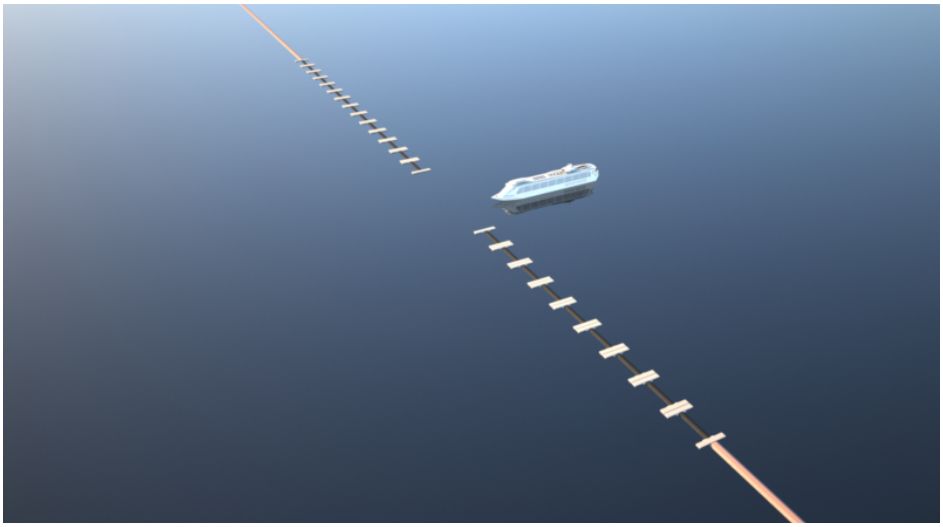

FIGURE 74: IMPRESSION DRAWING, BIRD VIEW

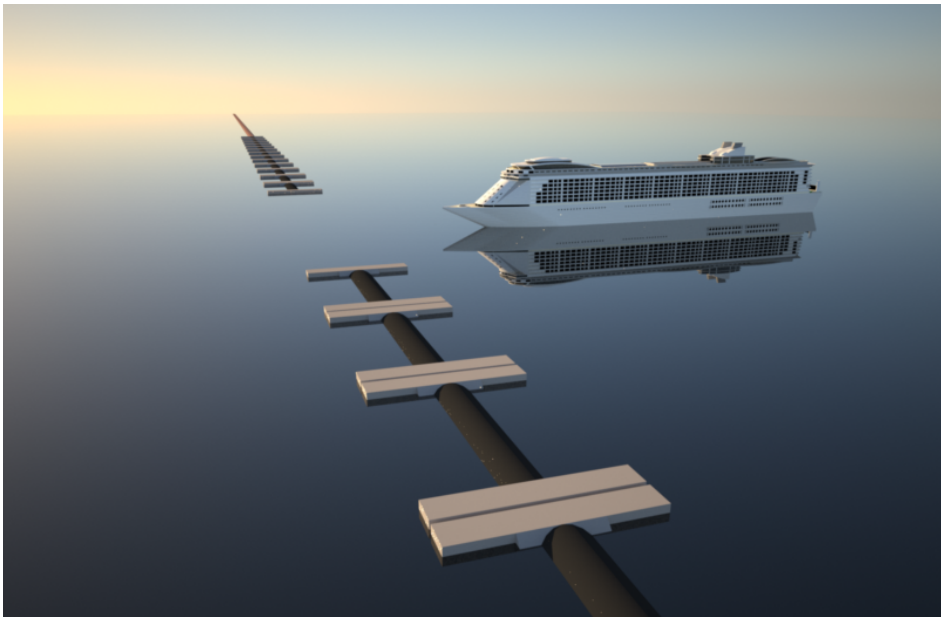

FIGURE 75: IMPRESSION DRAWING, SIDE VIEW

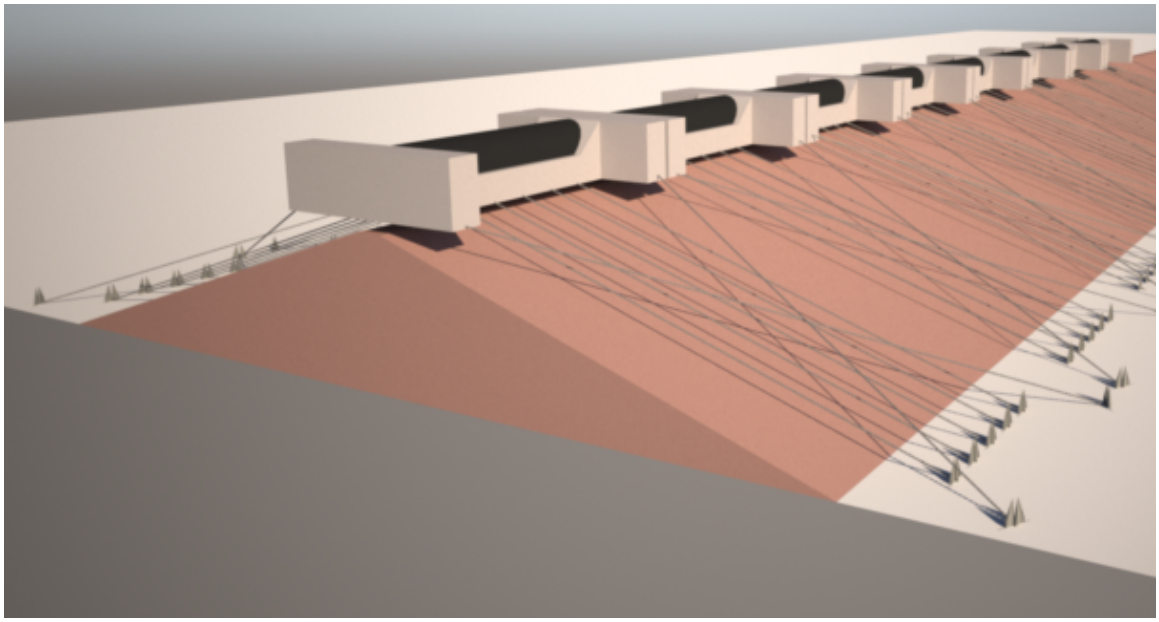

FIGURE 76: IMPRESSION DRAWING CROSS-SECTIONAL VIEW

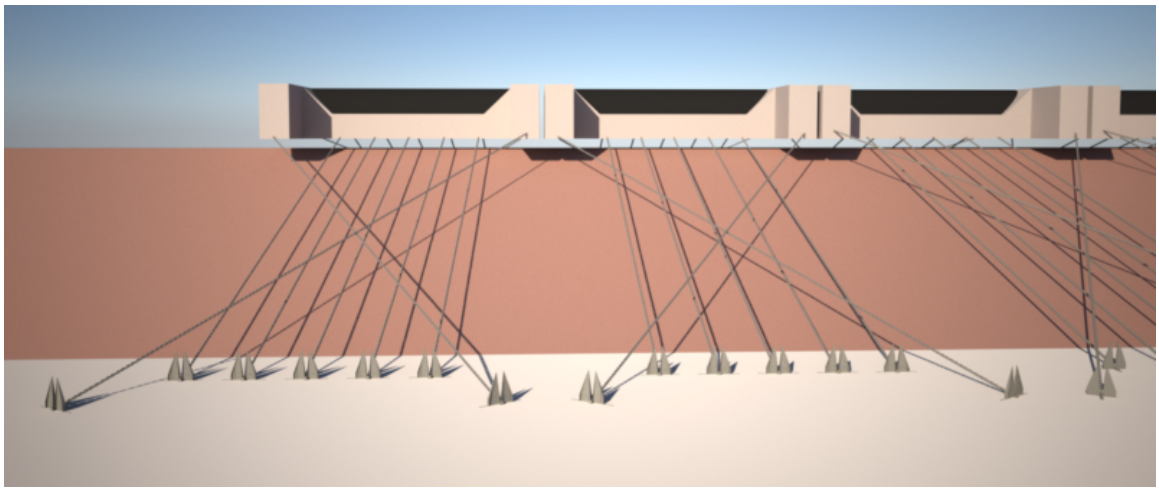

FIGURE 77: IMPRESSION DRAWING, FRONT VIEW

8.8 Summary

The geometry of the Floating caisson that will function as the floater of the floating moveable barrier is shown in Figure 78

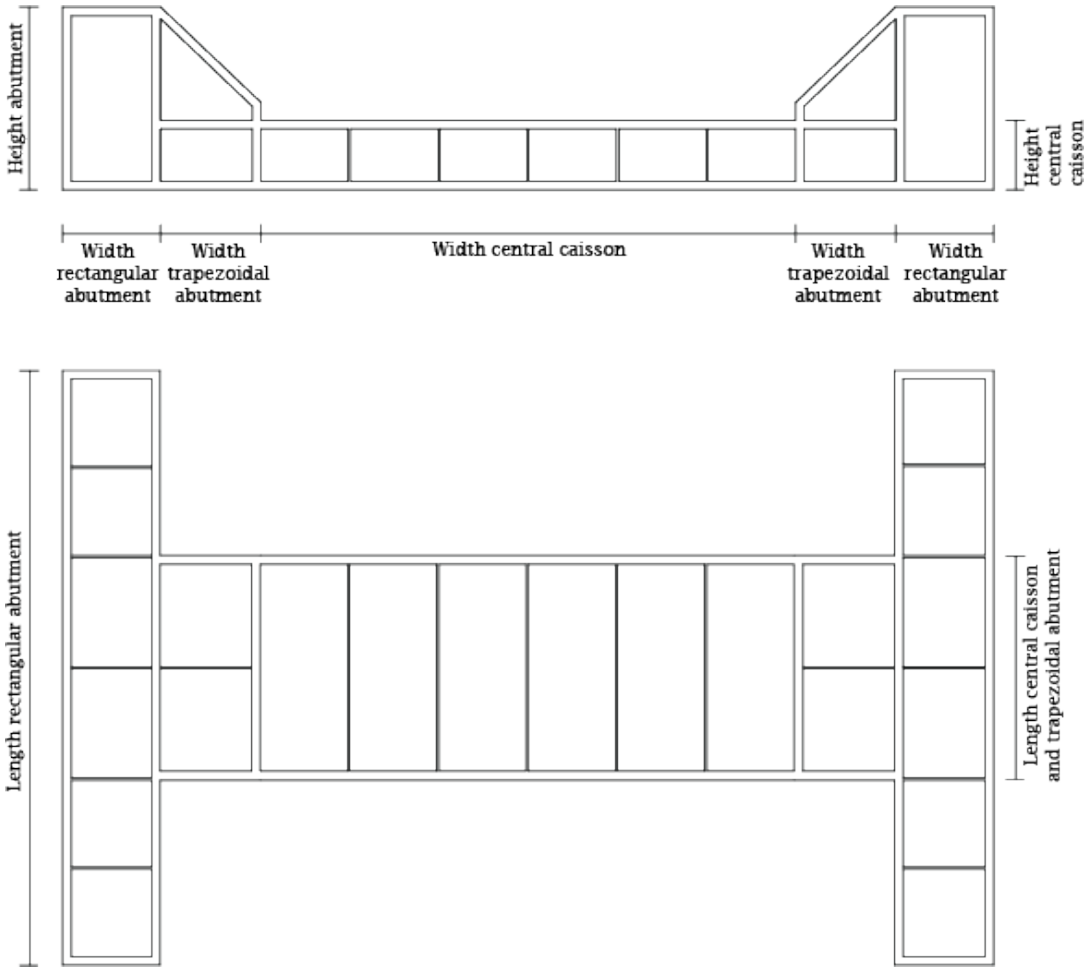

FIGURE 78: GEOMETRY FLOATING CAISSON

The final dimensions of the floating caissons and the flow area per caisson are presented in Table 28.

TABLE 34: FINAL DIMENSIONS FLOATING CAISSON

Final dimensions floating caisson		
Floating caisson total width	106,75	m
Floating caisson total height	20,5	m
Floating caisson total length	68,25	m
Flow area per Floating caisson	574	m^2

With these dimensions the floating caisson is considered stable in both normal and storm conditions. In total 5 floating moveable barriers will be placed. The maximum gap between the floating barrier and the under water dam has been chosen to be 5 m. After check with the 'rigid column approximation' it was concluded that with this number of floating barriers both this gap and the navigation channel can be left open without the water level rise inside the protected area exceed its acceptable limit even after 10% of the number of floating barriers (1) fails to close. The tidal height inside the bay after constructing the barrier will be 50% of the original tidal height.

From this analysis it is found that the water level rise inside the bay is very sensitive to the moment of barrier closure because of the large permanent open area. Since this is not preferable for the functionality of the barrier, it can be chosen to close off the gap between the floating barrier and the under water dam to make the water level rise inside the bay less sensitive to the moment of barrier closure. Also by closing off the gap more floating moveable barriers can be placed over the span. This will result in a larger tidal inlet, which will again lead to more water exchange during normal condition and higher allowed water level rise limit inside the bay during storm surge and thus a higher safety level. Due to the limited time provided for this thesis this gap closure is not further investigated and the 5 floating barriers will be assumed for further design.

Both the horizontal and vertical load on the floating barrier are governed by the load generated during the design typhoon. The top of the under water dam is assumed to be 10 meters wide and the slope of the dam will be 1:3 (18.4 degrees). It is chosen to have the floating barrier fixed with 7 mooring chains each side of the floating barrier. The chosen mooring chain is R4-RQ4 studless type of chain with diameter of 178 mm. The proof load of the chosen mooring chain is 18018 kN. The number of mooring chains is chosen such that the floating barrier will still be kept in its position during the design typhoon scenario even after one of the mooring chains is broken.

For the situation considered in this thesis a two sided clamped sheet with a symmetrical design relative to the longitudinal axis needs to be applied in order to prevent suddenly and uncontrolled flipping of the rubber sheet during the storm surge. Also from analysis it can be concluded that the combination of air and water is the most preferable filler for the inflatable rubber gate.

Both suction piles and vertical load anchors are possible solutions for the situation. But because it is unsure what the influence of the possible shaken soil after during earthquake will be on the anchor strength of the suction piles. More research is needed on the anchor strength of the suction piles under earthquake condition before choice can be made between the two anchors types.

9 EARTHQUAKE RESISTANCE FLOATING MOVEABLE BARRIER

In this chapter the possible failure mechanisms of the floating barrier will be recognized and the resistance regarding dynamic resonance of the floating moveable barrier during earthquake scenarios will be checked. First the earthquake ground motion frequencies and amplitudes will be elaborated. After that a dynamic model will be made for the floating barrier and the stability of the floating barrier will be analysed based on its resonance area and the frequencies of the earthquake ground motions.

9.1 Floating barrier failure mechanisms

A number of recognized failure mechanisms of the floating barrier are listed below:

- **Dynamic instability during earthquake, this failure regards the occurrence of dynamic resonance during earthquake conditions.**
- Hydrodynamic instability, this failure regards the occurrence of resonance under hydrodynamic conditions.
- Failure of the anchor due to design load exceendance during typhoon conditions.
- Failure of anchor due to earthquake.
- Failure of the mooring lines due to design load exceendance during typhoon conditions.
- Collision of the floating barriers against each other.
- Collision of ships against the floating barriers.
- Collision of the floating barrier against the under water dam.
- Failure of the inflatable rubber gate.

Due to the limited time provided for this master thesis, only 1 failure mechanism is chosen to be further analysed. Since the main advantage of the floating barrier over the bottom founded barriers during the comparison in paragraph 7.1 was the presumption of its great earthquake resistant character. Therefor the stability regarding resonance occurrence during earthquakes is chosen for further investigation.

9.2 Earthquake ground motion frequencies and amplitudes

Both frequencies and amplitudes of the ground motion during an earthquake depend on the type of earthquake and the intensity of the earthquake. Earthquakes have a large range of ground motion frequencies, the so-called short period frequencies and long period frequencies. The short period ground motions are often relative mall, which are in the order

of 10 cm with a period in the range of seconds or even smaller. The long period ground motions are spread over a longer period, varying between several seconds and one minute depending on the earthquake. Typical maximum amplitude of such long period ground motion of a severe earthquake is in the order of 0.4 m to above 1 m. In Figure 79 a ground motion measured during the Niigata earthquake (1964) is shown. The maximum displacements are in the range of 30-40 cm with a 'long period motion' period in the order of 7 seconds, while the 'long period motion' period measured during the Tohoku earthquake (2011), shown in Figure 80 is in the order of 1 minute. Also the maximum displacement measured from the Tohoku earthquake is much larger than the one measured from Niigata earthquake. From the ground motion measured from the 2011 Tohoku earthquake it can be clearly seen that there are 'short period' ground motions riding along the 'long period' ground motions. From these two given example it can be seen that the characteristic ground motion frequency and amplitude of an earthquake is really dependent on the type and intensity of the earthquake.

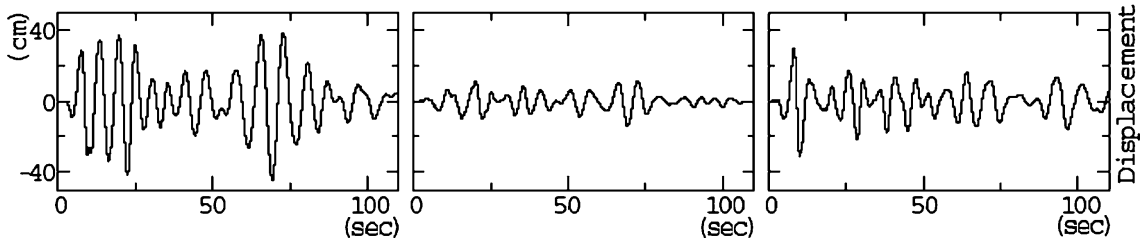

FIGURE 79: GROUND DISPLACEMENTS NIIGATA EARTHQUAKE (1964, M7.6) MEASURED AT 50 KM FROM EPICENTER, FROM LEFT TO RIGHT, NORTH/SOUTH, UP/DOWN, EAST/WEST (KOKETSU EN MIYAKE 2008)

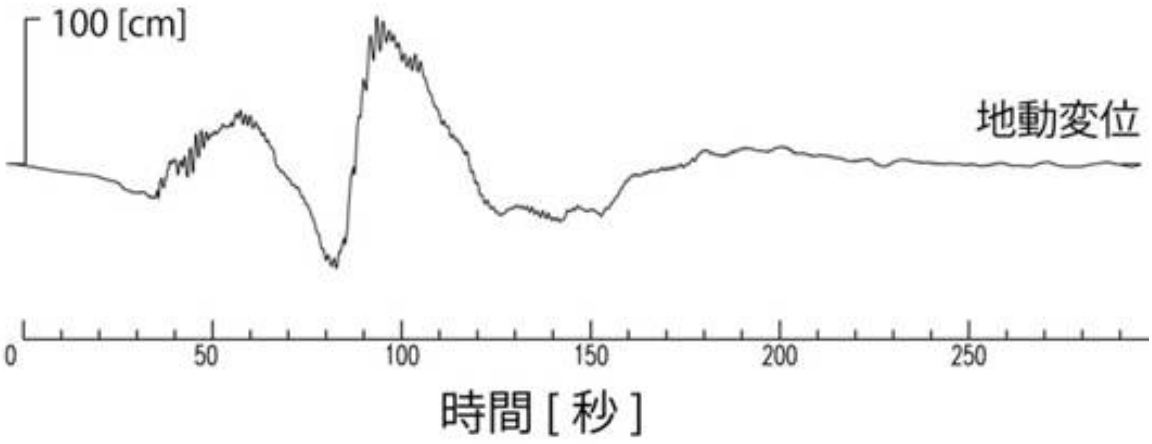

FIGURE 80: GROUND DISPLACEMENT TOHOKU EARTHQUAKE (2011, M9.0) MEASURED AT ISHINOMAKI, NORTH/SOUTH MOTION. HORIZONTAL AXIS TIME IN SEC AND VERTICAL AXIS DISPLACEMENT IN CM (OUTREACH AND PUBLIC RELATIONS OFFICE 2012)

9.3 Dynamic model floating barrier

To simplify the situation, the floating moveable barrier is being modelled as a rectangular block with springs. See Figure 81.

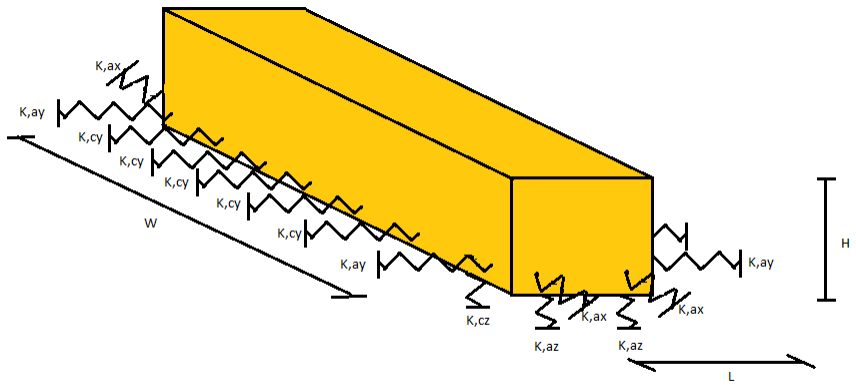

FIGURE 81: DYNAMIC MODEL FLOATING BARRIER

The dimension of the rectangular block is being approached as the following:

$$W = W_{fb}$$
$$H = \frac{H_{cc} + H_{ab,rec}}{2}$$
$$L = \frac{L_{cc} + L_{ab,rec}}{2}$$

Where:

W	[m]	Width rectangular model
H	[m]	Height rectangular model
L	[m]	Length rectangular model
W_{fb}	[m]	Width floating barrier (106.75 m)
H_{cc}	[m]	Height of the central caisson (8 m)
$H_{ab,rec}$	[m]	Height of the rectangular abutment (21 m)
L_{cc}	[m]	Length of the central caisson (27.25 m)
$L_{ab,rec}$	[m]	Length of the rectangular abutment (68.25 m)

Filling in the values gained from paragraph 8.3.6, the simplified dimensions of the floating barrier are:

W = 106.75 m
H = 14.5 m
L = 47.75 m

9.3.1 MASS MATRIX

The mass matrix of the dynamic model is constructed as the following:

$$M := \begin{bmatrix} m & 0 & 0 & 0 & 0 & 0 \\ 0 & m & 0 & 0 & 0 & 0 \\ 0 & 0 & m & 0 & 0 & 0 \\ 0 & 0 & 0 & J1 & 0 & 0 \\ 0 & 0 & 0 & 0 & J2 & 0 \\ 0 & 0 & 0 & 0 & 0 & J3 \end{bmatrix} \begin{bmatrix} z'' \\ y'' \\ x'' \\ xr'' \\ yr'' \\ zr'' \end{bmatrix}$$

Where

$$J1 = \frac{m}{12} * (L^2 + H^2)$$
$$J2 = \frac{m}{12} * (W^2 + H^2)$$
$$J3 = \frac{m}{12} * (L^2 + W^2)$$

With

J1	[kg*m^2]	Rotational moment of inertia around the x-axis
J2	[kg*m^2]	Rotational moment of inertia around the y-axis
J3	[kg*m^2]	Rotational moment of inertia around the z-axis
m	[kg]	Mass of the floating barrier (5.6e7 kg)

Filling in the equations gives:
J1 = 1.16*10^{10} kgm^2
J2 = 5.42*10^{10} kgm^2
J3 = 6.38*10^{10} kgm^2

9.3.2 STIFFNESS MATRIX

The dynamic system of the floating barrier under earthquake circumstances is assumed to be an undamped single mass spring system connected to the seabed with harmonic prescribed displacements in all x, y and z directions, which are in the direction of the length, width and height of the floating barrier respectively. The mooring chains are being modelled as springs and projected in all the three directions. For the spring stiffness of the chains, the Law of Hooke is being used, Note the sag in the mooring line has been neglected to simplify the model. Since the water depth varies over the span of the floating barrier, the 2 sets of spring stiffness are calculated, which are of the barrier at the deepest (+/-72 m) and the shallowest depth (+/-64 m).

$$k = \frac{EA}{L_m}$$

Where

E	[N/m^2]	Elasticity modulus (210000000)
A	[m^2]	Mooring chain cross section area (2*0.178^2*0.25*3.14=0.05 m^2)
L_m	[m]	Length mooring chain (deepest depth: 171 m for chain connected to central caisson and 197 m for chains connected to the abutments, shallowest depth: 145 m for chain connected to central caisson and 168 m for chains connected to the abutments)

Filling in the formula gives for the floating barrier at the deepest depth:

k_a = 53026471 N/m
k_c = 61088975 N/m

and for the shallowest depth:

k_a = 62179850 N/m
k_c = 72042861 N/m

Where:

k_a	[N/m]	Spring stiffness mooring chain connected to abutment
k_c	[N/m]	Spring stiffness mooring chain connected to central caisson

The spring stiffness projected in the considered directions are calculated as the following:

$$k_{c,z} = \sin(18.4) * k_c$$
$$k_{c,y} = \cos(18.4) * k_c$$
$$k_{a,z} = \sin(60) * \sin(18.4) * k_a$$
$$k_{a,y} = \sin(60) * \cos(18.4) * k_a$$
$$k_{a,x} = \cos(60) * k_a$$

Where

$k_{c,z}$	[N/m]	Spring stiffness central caisson mooring chain in z direction
$k_{c,y}$	[N/m]	Spring stiffness central caisson mooring chain in y direction
$k_{a,z}$	[N/m]	Spring stiffness abutment mooring chain in z direction
$k_{a,y}$	[N/m]	Spring stiffness abutment mooring chain in y direction
$k_{a,x}$	[N/m]	Spring stiffness abutment mooring chain in x direction

The water spring stiffness k_w can be calculated using the buoyancy principles. The displaced water weight per m draught is the water weight multiplied with the water cutting area of the floating caisson. Since this area varies with varying draught due to the slope of the abutment, the averaged bottom area of the abutment is used as the water cutting area.

$$k_w = \rho * g * 2 * (L_{ab,rec} * W_{ab,rec} + L_{ab,tra} * \frac{W_{ab,tra}}{2})$$

Filling in the equations gives:

	Deepest depth	Shallowest depth
$k_{c,z}$	19282661 N/m	22740241 N/m
$k_{c,y}$	49808129 N/m	68359748 N/m
$k_{a,z}$	12455327 N/m	16997466 N/m
$k_{a,y}$	37442128 N/m	51096315 N/m
$k_{a,x}$	22781970 N/m	31089972 N/m
k_w	18138690 N/m	18138690 N/m

FIGURE 82: SPRING STIFFNESS

By using the displacement method, forces on the floating barrier during the different motions can be determined. For each motion, the equation of motion is determined, see appendix 19. Based on these equations of motion the stiffness matrix of the dynamic model can be constructed, see below:

$$K := \begin{pmatrix} 10\cdot Kcz + 4\cdot Kaz + Kw & 0 & 0 & 0 & 0 & 0 \\ 0 & 5\cdot Kcy + 2\cdot Kay & 0 & (5\cdot Kcy + 2\cdot Kay)\cdot a & 0 & 0 \\ 0 & 0 & -w^2\cdot m + 2\cdot Kax & 0 & 2\cdot Kax\cdot a & 0 \\ 0 & (5\,Kcy + 2\,Kay)\cdot a & 0 & \frac{Kw\cdot L^2}{12} + (5\cdot Kcy + 2\cdot Kay)\cdot a^2 + \frac{(5\cdot Kcz + 2\,Kaz)\cdot L^2}{4} & 0 & 0 \\ 0 & 0 & 2\cdot Kax\cdot a & 0 & \frac{Kw\cdot B^2}{12} + 2\cdot Kcz\cdot 14^2 + 2\,Kcz\cdot 28^2 + 2\cdot Kaz\cdot\frac{B^2}{4} & 0 \\ 0 & 0 & 0 & 0 & 0 & -2\cdot Kcy\cdot 14^2 + 2\,Kcy\cdot 28^2 + 2\cdot Kay\cdot\frac{B^2}{4} \end{pmatrix} \begin{bmatrix} z \\ y \\ x \\ xr \\ yr \\ zr \end{bmatrix}$$

9.3.3 EIGEN FREQUENCY

The equation of motion of the system without earthquake load is presented in the form:

$$M\ddot{X} + KX = 0$$

By assuming a harmonic movement of the floating caisson with angular frequency ω, the displacement X can be expressed with:

$$X = \hat{X}\sin(\omega t)$$

Substituting
into the mass matrix and the stiffness matrix, the mass-stiffness matrix can be constructed, see below:

$$MK := \begin{pmatrix} -w^2\cdot m + 10\cdot Kcz + 4\cdot Kaz + Kw & 0 & 0 & 0 & 0 & 0 \\ 0 & -w^2\cdot m + 5\cdot Kcy + 2\cdot Kay & 0 & (5\cdot Kcy + 2\cdot Kay)\cdot a & 0 & 0 \\ 0 & 0 & -w^2\cdot m + 2\cdot Kax & 0 & 2\cdot Kax\cdot a & 0 \\ 0 & (5\,Kcy + 2\,Kay)\cdot a & 0 & -w^2\cdot J1 + \frac{Kw\cdot L^2}{12} + (5\cdot Kcy + 2\cdot Kay)\cdot a^2 + \frac{(5\cdot Kcz + 2\,Kaz)\cdot L^2}{4} & 0 & 0 \\ 0 & 0 & 2\cdot Kax\cdot a & 0 & -w^2\cdot J2 + \frac{Kw\cdot B^2}{12} + 2\cdot Kcz\cdot 14^2 + 2\,Kcz\cdot 28^2 + 2\cdot Kaz\cdot\frac{B^2}{4} & 0 \\ 0 & 0 & 0 & 0 & 0 & -w^2\cdot J3 + 2\cdot Kcy\cdot 14^2 + 2\,Kcy\cdot 28^2 + 2\cdot Kay\cdot\frac{B^2}{4} \end{pmatrix} \begin{bmatrix} z \\ y \\ x \\ xr \\ yr \\ zr \end{bmatrix}$$

Where

ω	[rad/s]	Angular frequency

The eigen frequency of the floating barrier can be determined by solving the determinant of the mass-stiffness matrix to zero. Solving these equations gives six eigen frequencies for each barrier. The obtained eigen frequencies for the barrier at the deepest and shallowest depth are shown in Table 35 and Table 36.

TABLE 35: EIGEN FREQUENCY FLOATING BARRIER DEEPEST DEPTH

Eigen frequency different directions	ω	f	T
ω in Z-direction	2.19 rad/s	0.38 Hz	2,64 s
1st ω in coupled movement in Y and Xr direction	1.13 rad/s	0.18 Hz	5.56 s
2nd ω in coupled movement in Y and Xr direction	2.70 rad/s	0.43 Hz	2.33 s
1st ω in coupled movement in X and Yr direction	0.96 rad/s	0.15 Hz	6.54 s
2nd ω in coupled movement in X and Yr direction	3.44 rad/s	0.55 Hz	1.82 s
ω in Zr direction	2.38 rad/s	0.35 Hz	2.87 s

TABLE 36: EIGEN FREQUENCY FLOATING BARRIER SHALLOWEST DEPTH

Eigen frequency different directions	ω	f	T
ω in Z-direction	2.37 rad/s	0.38 Hz	2.65 s
1st ω in coupled movement in Y and Xr direction	1.22 rad/s	0.19 Hz	5.14 s
2nd ω in coupled movement in Y and Xr direction	2.93 rad/s	0.47 Hz	2.14 s
1st ω in coupled movement in X and Yr direction	1.04 rad/s	0.17 Hz	6.04 s
2nd ω in coupled movement in X and Yr direction	3.70 rad/s	0.59 Hz	1.70 s
ω in Zr direction	2.58 rad/s	0.41 Hz	2.43 s

9.3.4 DYNAMIC RESPONSE TO HARMONIC MOTION

The resonance response graph of the dynamic system can be plotted by solving the mass-stiffness for a certain load in a degree of freedom. It is assumed that during an earthquake only ground motions in the x, y and z will occur. For each of these ground motions the resonance response graph has been plotted. For all the ground motions an amplitude of 1 meter has been assumed.

9.3.4.1 Ground motion in Z-direction

The equation of motion with a harmonic ground motion in Z-direction due to earthquake is given as:

$$M * \ddot{x} + \left(10 * k_{c,z} + 4 * k_{a,z} + k_w\right) * (z - u_z * \sin(\omega t)) = 0$$

It can be rewritten as:

$$M * \ddot{x} + \left(10 * k_{c,z} + 4 * k_{a,z} + k_w\right) * z = u_z * \sin(\omega t) * \left(10 * k_{c,z} + 4 * k_{a,z} + k_w\right)$$

Where:

u_z [m] Earthquake ground motion in Z-direction

Since motion is not coupled with motions in other directions, it only induces motions in the Z-direction. For both considered floating barriers, the resonance response graph for a ground motion in the Z-direction is shown in Figure 83 and Figure 84. As it can be seen the resonance angular frequency corresponds with the angular eigen frequency of the floating barrier given in Table 35 and Table 36. And when the frequency is goes to zero, the amplitude of the barrier motion becomes the same as the amplitude of the ground motion.

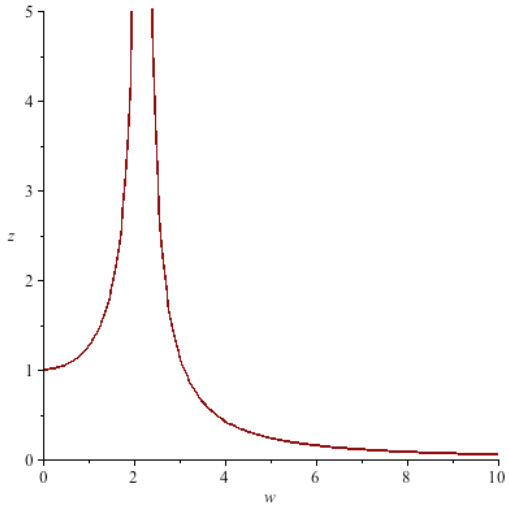

FIGURE 83: DEEPEST DEPTH: RESONANCE RESPONSE GRAPH FLOATING BARRIER DEEPEST DEPTH IN Z-DIRECTION BY GROUND MOTION IN Z-DIRECTION, VERTICAL AXIS: AMPLITUDE BARRIER MOTION IN M, HORIZONTAL AXIS: MOTION FREQUENCY RAD/S

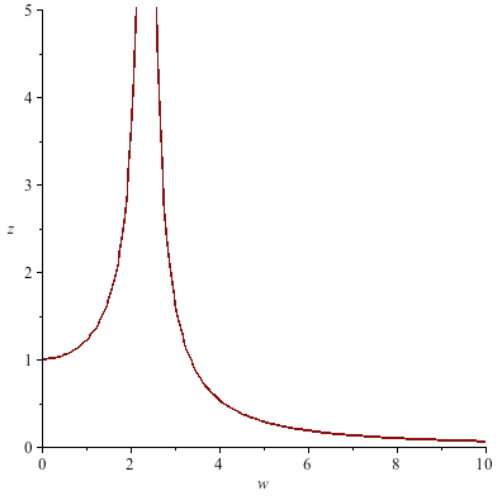

FIGURE 84 SHALLOWEST DEPTH: RESONANCE RESPONSE GRAPH FLOATING BARRIER IN Z-DIRECTION BY GROUND MOTION IN Z-DIRECTION, VERTICAL AXIS: AMPLITUDE BARRIER MOTION IN M, HORIZONTAL AXIS: MOTION FREQUENCY RAD/S

9.3.4.2 Ground motion in Y-direction

The equation of motion with a harmonic ground motion in Y-direction due to earthquake is given as:

$$M * \ddot{x} + \left(5 * k_{c,y} + 2 * k_{a,y}\right) * \left(y - u_y * \sin(\omega t)\right) + \left(5 * k_{c,y} + 2 * k_{a,y}\right) * (x_r - u_{xr} * \sin(\omega t)) * a = 0$$

It can be rewritten as:

$$M * \ddot{x} + \left(5 * k_{c,y} + 2 * k_{a,y}\right) * y + \left(5 * k_{c,y} + 2 * k_{a,y}\right) * x_r * a = u_y * \sin(\omega t) * \left(5 * k_{c,y} + 2 * k_{a,y}\right) + u_{xr} * \sin(\omega t) * \left(5 * k_{c,y} + 2 * k_{a,y}\right) * a$$

Where:

u_y	[m]	Earthquake ground motion in Y-direction
u_{xr}	[rad]	Barrier rotational motion in the Xr-direction induced by the earthquake ground motion in Y-direction

Since forces in the Y-direction is coupled with the rotational motion in the Xr-direction, it also induces motions in the Xr-directions. For both considered floating barriers, the resonance response graph for a ground motion in the Y-direction is shown in Figure 85 to Figure 88. As it can be seen the resonance angular frequencies corresponds with the angular eigen frequency of the floating barrier given in Table 35 and Table 36. Also when the frequency is goes to zero, the amplitude of the barrier motion in Y-direction becomes the same as the amplitude of the ground motion in Y-direction and the rotational amplitude of the barrier goes to zero.

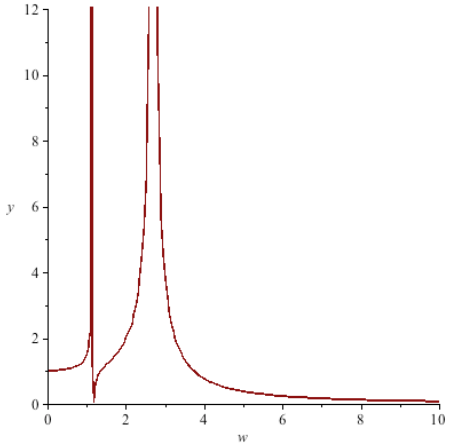

FIGURE 85: DEEPEST DEPTH: RESONANCE RESPONSE GRAPH IN Y-DIRECTION BY GROUND MOTION IN Y-DIRECTION, VERTICAL AXIS: AMPLITUDE BARRIER MOTION IN M, HORIZONTAL AXIS: MOTION FREQUENCY RAD/S

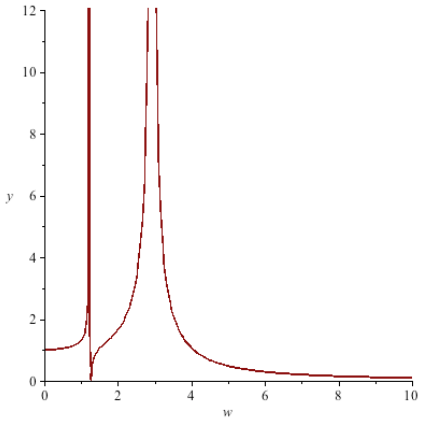

FIGURE 86: SHALLOWEST DEPTH: RESONANCE RESPONSE GRAPH IN Y-DIRECTION BY GROUND MOTION IN Y-DIRECTION, VERTICAL AXIS: AMPLITUDE BARRIER MOTION IN M, HORIZONTAL AXIS: MOTION FREQUENCY RAD/S

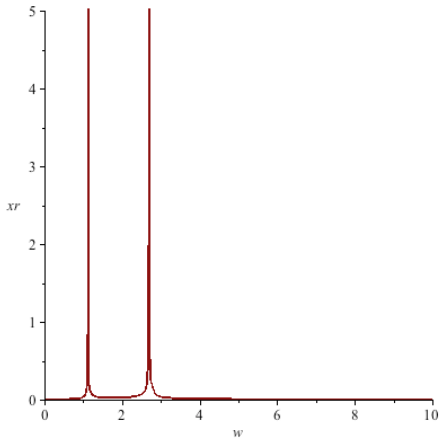

FIGURE 87: DEEPEST DEPTH: RESONANCE RESPONSE GRAPH IN XR-DIRECTION BY GROUND MOTION IN Y-DIRECTION, VERTICAL AXIS: AMPLITUDE BARRIER ROTATIONAL MOTION IN RAD, HORIZONTAL AXIS: MOTION FREQUENCY RAD/S

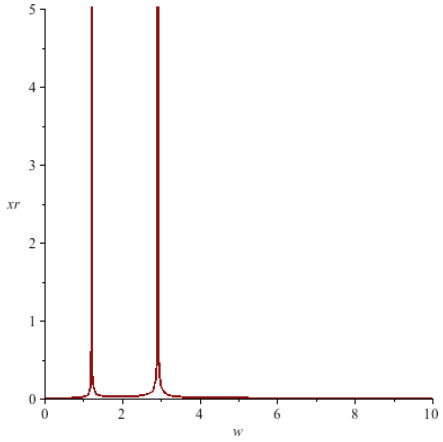

FIGURE 88: SHALLOWEST DEPTH: RESONANCE RESPONSE GRAPH IN XR-DIRECTION BY GROUND MOTION IN Y-DIRECTION, VERTICAL AXIS: AMPLITUDE BARRIER ROTATIONAL MOTION IN RAD, HORIZONTAL AXIS: MOTION FREQUENCY RAD/S

9.3.4.3 Ground motion in x-direction

The equation of motion with a harmonic ground motion in Y-direction due to earthquake is given as:

$$M * \ddot{x} + 2 * k_{a,x} * (x - u_x * \sin(\omega t)) + 2 * k_{a,x} * (y_r - u_{yr} * \sin(\omega t)) * a = 0$$

It can be rewritten as:

$$M * \ddot{x} + 2 * k_{a,x} * x + 2 * k_{a,x} * y_r * a = u_x * \sin(\omega t) * 2 * k_{a,x} + u_{yr} * \sin(\omega t) * 2 * k_{a,x} * a$$

Where:

u_x	[m]	Earthquake ground motion in X-direction
u_{yr}	[rad]	Barrier rotational motion in the Xr-direction induced by the earthquake ground motion in Y-direction

Since forces in the X-direction is coupled with the rotational motion in the Yr-direction, it also induces motions in the Yr-directions. For both considered floating barriers, the resonance response graph for a ground motion in the X-direction is shown in Figure 89 and Figure 92. As it can be seen the resonance angular frequencies corresponds with the angular eigen frequency of the floating barrier given in Table 35 and Table 36. Also when the frequency is goes to zero, the amplitude of the barrier motion in X-direction becomes the same as the amplitude of the ground motion in X-direction and the rotational amplitude of the barrier goes to zero. Note that in Figure 89 the resonance response for the angular frequency 3.44 rad/s seems to stop at certain amplitude. This is probably due to the limited calculation step size used by the calculation program. So the calculation step where the response goes to infinity is skipped during the calculation due to the minimum size of the calculation step is too large for the required calculation step. In reality the response should go to infinity.

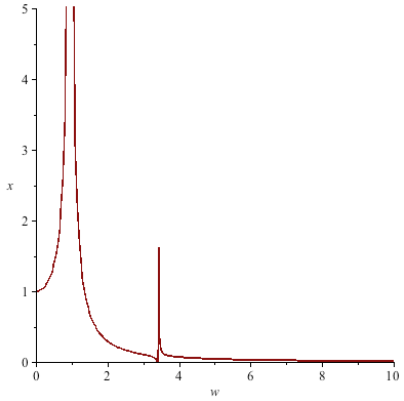

FIGURE 89: DEEPEST DEPTH: RESONANCE RESPONSE GRAPH IN X-DIRECTION BY GROUND MOTION IN X-DIRECTION, VERTICAL AXIS: AMPLITUDE BARRIER MOTION IN M, HORIZONTAL AXIS: MOTION FREQUENCY RAD/S

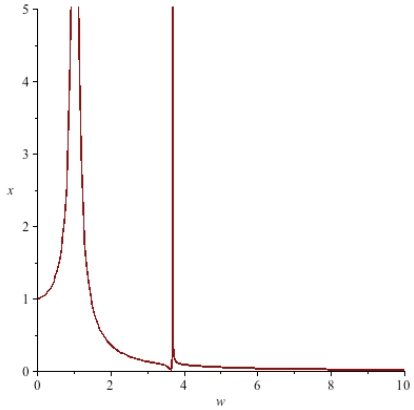

FIGURE 90: SHALLOWEST DEPTH: RESONANCE RESPONSE GRAPH IN X-DIRECTION BY GROUND MOTION IN X-DIRECTION, VERTICAL AXIS: AMPLITUDE BARRIER MOTION IN M, HORIZONTAL AXIS: MOTION FREQUENCY RAD/S

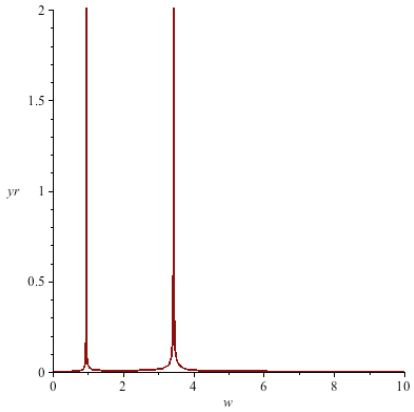

FIGURE 91: DEEPEST DEPTH: RESONANCE RESPONSE GRAPH IN YR-DIRECTION BY GROUND MOTION IN X-DIRECTION, VERTICAL AXIS: AMPLITUDE BARRIER ROTATIONAL MOTION IN RAD, HORIZONTAL AXIS: MOTION FREQUENCY RAD/S

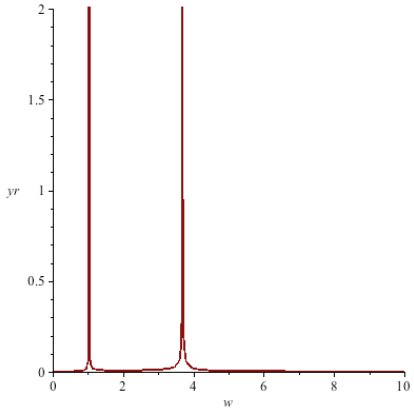

FIGURE 92: SHALLOWEST DEPTH: RESONANCE RESPONSE GRAPH IN YR-DIRECTION BY GROUND MOTION IN X-DIRECTION, VERTICAL AXIS: AMPLITUDE BARRIER ROTATIONAL MOTION IN RAD, HORIZONTAL AXIS: MOTION FREQUENCY RAD/S

9.4 Evaluation stability floating barrier during earthquake

From the results gained from the previous paragraph it has been determined that the floating barriers have a natural frequency range between 0.15 Hz and 0.59 Hz depending on the water depth. It can be seen that the natural frequency increases with decreasing water depth. Figure 93 presents the spectrum of several past earthquakes in Japan (personal communication Miguel Esteban, 27-05-2014), the red lines indicate the resonance frequency range of the floating barriers at various depth. It can be seen that for all spectrums the natural frequencies of the floating barriers are outside the frequency range of the earthquake that contains the most energy. It is also found that for floating barriers at a water depth larger than 30 m, its maximum natural frequency is still below 1 Hz, which is just outside the area that contains the most energy. But since this consideration is only based on spectrum of 3 of the past earthquakes, no hard conclusion can be made for the stability of floating barrier during earthquakes. So the question arises:

What is the chance that the natural frequency of the floating barrier coincides with the high-energy frequencies of the earthquake?

Since this is a quite time consuming research, it is not investigated in this thesis. But there is still another question, which is:

What if an earthquake occurs from which the high-energy frequency area coincides with the natural frequencies of the barrier?

Judging from the situation, for the assumed model the damping effect of the seawater and the sag in the mooring lines haven't been taken into account during the dynamic analysis of the floating barrier. Water damping will decrease the magnitude of response of the floating barrier during resonance. While the sag in the mooring lines will decrease the stiffness of the floating barrier, resulting in lower natural frequencies. So judging from the earthquake spectrum in Figure 93, the resonance frequency range of the floating barrier will be further away from the earthquake frequency range that contains the most energy. Also since resonance will occur at really low frequency and the duration of an earthquake is between 30 sec and 1 minutes, the number of cycles which resonance occur will be limited and thus the maximum displacement of these floating barriers is expected to be limited. Therefor even if the earthquake frequency coincides with the natural frequency of these floating barriers at depth deeper than 30 m, it does not have to lead to instability of these barriers.To validate this reasoning more research regarding the dynamic behaviour of the floating barrier is needed. If the floating barriers appears to be unstable after the validation, the sag of the mooring line can be changed to adjust the stiffness of the system.

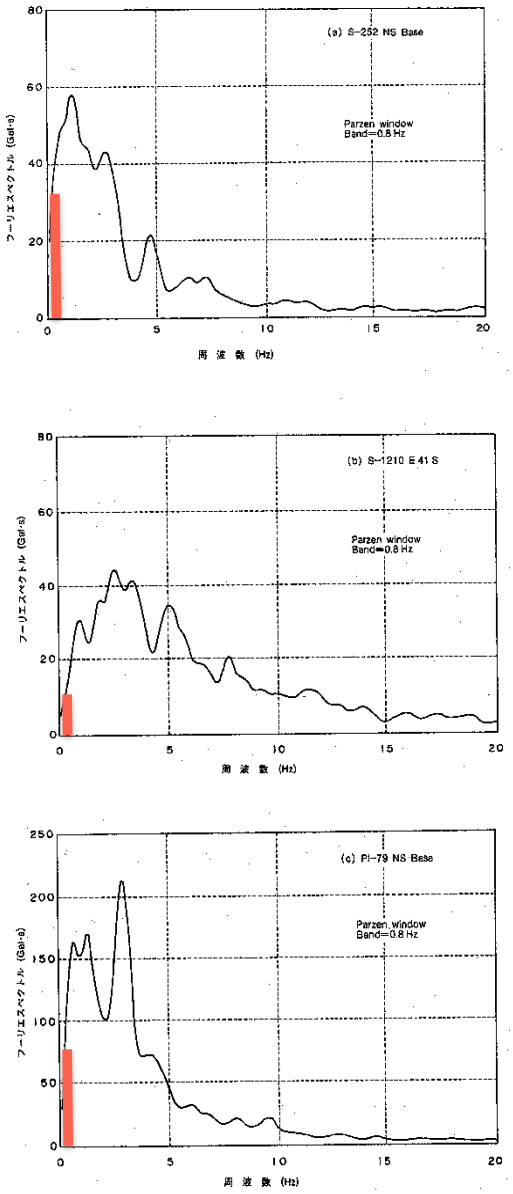

FIGURE 93: EARTHQUAKE SPECTRUM OF SEVERAL PAST EARTHQUAKES IN JAPAN.THE RED LINES INDICATE THE RESONANCE FREQUENCY RANGE OF THE FLOATING BARRIERS (M. ESTEBAN 2014)

10 CONCLUSION AND RECOMMENDATION

In the first section of this chapter the conclusions of this study are presented. In the second section several recommendations are given.

10.1 Conclusion

In this research a conceptual design of a typhoon barrier at the Tokyo Bay to reduce the flooding risk of Tokyo and Kanagawa region is investigated. The following conclusions are drawn from the investigation.

10.1.1 RISK TOKYO AND KANAGAWA REGION BY TSUNAMIS AND TYPHOONS

- An existing simulation of the tsunami caused by a Genroku type of earthquake (M8.0) has shown that the maximum water level rise inside the bay due to such a tsunami attack is in the order of 2 m. Since the chance of occurrence of such a tsunami is very small and the duration of the tsunami is really short, the chance of a tsunami attack during the maximum water level of the spring tide is considered negligible small. Therefor based on the result of the simulation it can be concluded that the risk caused by a tsunami attack on Tokyo and Kanagawa region is negligible small.
- Typhoons are considered as the main threat for the Tokyo and Kanagawa region. The possible intensification of the typhoons in the future and the sea level rise due to climate change makes the current coastal defence of the area insufficient for a large typhoon in the future. Together with the frequent occurrence of the typhoon in the area, it makes it the main threat for the Tokyo and Kanagawa region.

10.1.2 BARRIER DESIGN

- The span between Yokosuka and Futtsu (location 4, see paragraph 4.2) is the most suitable location for the placement of a barrier. This location has the shortest span between the two shores. Despite the large depth of this location (deepest point 81 m) it still has the smallest area to be closed off, which corresponds with the cost.
- Considering the conservation of the environmental value of the Bay and the large depth of the chosen location, it appears that a barrier that is partly permanent closed and partly moveable is the most suitable choice for the situation. Also it appears that by placing the moveable barrier part at the deepest part of the span will save the largest volume of soil for the under water dam, which is 38.7% of the soil volume compared to fully closed off situation. This will also result in cost saving.
- Earthquake loads might become decisive for the moveable barrier considering its design lifetime. A floating moveable barrier has shown great potential regarding

earthquake resistance due its independence of the stability of the under water dam and the small energy transfer from seabed to the moveable barrier during earthquake conditions. Despite the fact that this kind of barrier has never been made, it is considered technically feasible due to the comparable technique used for floating offshore platforms and floating breakwaters.

- Considering the cost and the preferred weight and size of the gate for a floating moveable barrier, it appears that the inflatable rubber gate is the most suitable gate type to a floating moveable barrier.
- Based on calculations using the 'rigid column approximation' it can be concluded that the navigation channel and the gap between the floating moveable barrier and the under water dam can be left open during design typhoon conditions. The water level rise caused by the flow through these openings is considered acceptable.
- It has been found that for water depth deeper than 30 m the maximum natural frequency is below 1 Hz, which is just outside the frequency ranges that contain the most energy for the presented earthquakes spectrums. Because the comparison is only based on 3 of the past earthquakes, no hard conclusion can be drawn from these results. But judging from the actual situation, seawater and sag in the mooring line will contribute to the stability by decreasing the response magnitude and lowering the natural frequency of the floating barrier. Therefor even if the earthquake frequency coincides with the natural frequency of these floating barriers at depth deeper than 30 m, it does not have to lead to instability of the barrier. To validate this reasoning more research regarding the dynamic behaviour of the floating barrier is needed. If the floating barriers appears to be unstable after the validation, the sag of the mooring line can be changed to adjust the stiffness of the system.

MAIN CONCLUSION

In this master thesis a new concept of moveable barrier type, the floating moveable barrier, has been proposed as solution of the risk reduction of hazards caused by typhoon and tsunami on the Tokyo and Kanagawa region. After this research, the new concept has been considered technically feasible and has shown great potential in its effectiveness regarding the earthquake resistance and flexibility in maintenance and replacement. Therefor this new concept is considered worthy for further investigation.

10.2 Recommendation

The research done in this master thesis is based on a number of assumptions that are discussed throughout the report. Therefor the result obtained from this research has its limitations and a number of further investigations are recommended here below.

10.2.1 PROBLEM ANALYSIS

- No probabilistic analysis has been done for the future occurrence of typhoons with certain intensity. So a probabilistic analysis about this occurrence is recommended for future investigation. Based on the result a more accurate judgement can be made on the acceptable design typhoon and a probabilistic design of the protection measure can be made instead of a deterministic design.
- No accurate cost analysis of the possible protection measures has been made. Therefor it is recommended for future investigation to analyse of costs of the possible protection measures for certain design typhoon level. Based on this analysis a better judgement can be made on the best to be taken protection measure.
- Due to lack of data, a lot of assumptions have been made for the functional requirements and boundary conditions; these ambiguities should be further investigated.

10.2.2 BARRIER DESIGN

- No strength check has been made during the preliminary design of the floating caisson. So this still needs to be done for future research.
- For the design of the floating caisson, concrete was chosen as construct material. It is also interesting to investigate the possibilities of using other types of materials such as steel or a combination of different materials. It might lead to better results.
- Due to the relative small opening of the gap between the floating barrier and the under water dam, high-speed flow will probably occur during storm conditions. Analysis of the erosion problems and the bank protection measures of the under water dam is therefor recommended.
- The water level rise inside the protected area is checked using a simplified approximation, the 'rigid column approximation'. To have a more accurate result regarding the water level rise, a numerical simulation is recommended.
- During the design of the mooring lines, no sag has been determined for the mooring lines. The sag in the mooring lines can compensate the fluctuations of the movements of the floating barrier due to wave motions. Therefor an accurate determination of the sag is recommended.
- Due to limited time given for this master thesis, no anchor design has been done. So for future investigation this still has to be done.
- Due to the uncertainty of behaviour of suction piles under earthquake conditions, traditional anchors has been chosen for the preliminary design of the anchor system.

Therefor it is recommended to also investigate the strength behaviour of the suction piles under earthquake conditions.

- Strength of the mooring lines has not been checked for earthquake conditions and possible tsunami impact afterwards, so for future investigation this still has to be done.
- Since the large ground motions during an earthquake have a large range of possible frequencies, it is recommended to have further investigations on this subject.
- Connections between the floating moveable barriers have not been analysed. Since connections can provide more stability for the floating movable barrier, further investigations on this subject is recommended.
- It is recommended to investigate the possibilities for gap closure.
- The dynamic behaviour of the floating barrier under earthquake conditions has only been analysed based on a simplified model without taken into account the water damping and sag of the mooring lines. Therefor it is recommended to create a more accurate dynamic model by including the water damping and the sag in the mooring lines and by creating a more accurate approximation of the mass and stiffness matrix of the system. Also it is interesting to have investigations on the dynamic behaviour of the floating barrier under different hydraulic conditions.
- For this master thesis, only the resistance of the floating moveable barrier to earthquakes has been analysed. It is recommended to have further investigation on he other possible failure mechanisms. Also it is interesting to analyse the possible solutions for these failure mechanisms.

11 BIBLIOGRAPHY

A.A.Balkema. *Design plan Oosterchelde Storm-surge barrier, Overall design and design philosophy.* A.A.Balkema, 1994.
A3M Mobile Personal Protection GmbH. *A3M Mobile Personal Protection GmbH.* 2012. http://www.tsunami-alarm-system.com/en/faq/faqs.html (accessed 09 2014).
Blue ocean tackle Inc. *Blue ocean tackle Inc.* http://www.blueoceantackle.com/anchors_for_marine_industry.htm (accessed 2014).
Bouwdienst Rijkwaterstaat en WL| Delft Hydraulics. *Hydraulische aspecten van balgstuwen en balgkeringen,.* Bouwdienst Rijkswaterstaat, 2005.
Breukelen, M. Van. *Improvement and upscaling of an inflatable rubber storm surge barrier for Texas, USA.* Delft: TU Delft, 2013.
Bryant, E. *TSUNAMI: The Underrated Hazard.* Cambridge: Cambridge University Press, 2001.
Church, John A. *IPCC 5AR climate change 2013: The physical science basis, chapter 13.* Cambridge: Cambridge University Press, 2013.
Esteban, M., interview by Kaichen Tian. (27 05 2014).
Esteban, Miguel, interview by Kaichen Tian. *Depth map Tokyo Bay* (9 01 2014).
Extra.springers.com. http://www.google.nl/url?sa=i&rct=j&q=&esrc=s&source=images&cd=&docid=2yNL3LmKgc6puM&tbnid=0IHmBWLdFJBByM:&ved=0CAUQjhw&url=http%3A%2F%2Fextras.springer.com%2F2006%2F978-1-4020-3654-5%2Ftokyo2%2Findex.htm&ei=V1clVPeKBMnLPbQU&bvm=bv.76247554,d.ZWU&psig=AFQjCNGeDrnpzMDm-oHkl7llrWE1kJc_5w&ust=1411819733489194 (accessed 2014).
Fuentes, M.J. Ruiz. *Storm surge barrier Tokyo Bay, Analysis on a system level and conceptual design.* Delft: TU Delft, 2014.
Goda, Y. (1985). Random seas and design of maritime structures. University of Tokyo Press: Tokyo. .
Goda, Y. *Random seas and design of maritime structures* . Tokyo: University of Tokyo, 1985.
Google maps. https://www.google.nl/maps/place/Tokio,+Japan/@35.4935295,139.925308,10z/data=!4m2!3m1!1s0x605d1b87f02e57e7:0x2e01618b22571b89 (accessed 2014).
Groeneveld, R. *Inland Waterways: Ports, Waterways and Inland Navigation. Lecture Notes CT4330. .* Delft: TU Delft, 2002.
Hays, Jeffrey. *Facts and Details.* 2009. http://factsanddetails.com/japan/cat26/sub160/item2768.html (accessed 2014).
Hoshino, S. *Estimation of Storm Surge and Proposal of the Coastal Protection Method in Tokyo Bay, Waseda University, Feb 2013.* Tokyo: Waseda University, 2013.
Independent Administrative Institution, Port and Airport institute. *NOWPHAS (1979-1999).* ndependent Administrative Institution, Port and Airport institute, Japan.
Intermoor. *Intermoor.* http://www.intermoor.com/information-center-23/press-releases-24/intermoor-wins-design-fabrication-installation-and-hook-up-contract-with-llog-in-the-gulf-of-mexico-737 (accessed 2014).
Ito, Takeshi, and Mikio Hino. "Numerical prediction of typhoon tide in Tokyo Bay." *Proceedings of 9th conference on coastal engineering, Lisbon, Portugal*, 1964.
Jakota. *FleetMon.* http://www.fleetmon.com/en/ports/Tokyo_Ko_10674 (accessed 2013).
Japan water forum. *Typhoon Isewan (Vera) an its lessons.* Tokyo: Japan water forum, 2005.
Klaver, Elwyn N. *Probalistic analysis of typhoon induced hudraulic boundary conditions for Sou-nada Bay.* Delft: TU Delft, 2005.
Koketsu, Kazuki, and Hiroe Miyake. *A seismological overview of long period ground motion.* Tokyo: University of Tokyo, 2008.
Labeur, R.J. *Open Channel Flow. Lecture Notes CT3310. .* Delft: TU Delft, 2007.
Lankhorst Rope. *Lankhorst Rope.* 12 01 2012. http://www.lankhorstropes.com/Offshore/news_media/page_4/Lankhorst-Ropes-awarded-polyester-mooring-rope-contract-for-Lucius-spar (accessed 2014).

Ligteringen, H. *Lecture notes CIE4330 and CIE 5306: Ports and Terminals.* Delft, 2009.
MLIT. "MLIT." *MLIT.* http://www.mlit.go.jp/river/trash_box/paper/pdf_english/15.pdf (accessed 2014).
National police agency of Japan. "Damage Situation and Police Countermeasures associated with 2011Tohoku district - off the Pacific Ocean Earthquake." 2014.
Outreach and Public Relations Office. *Outreach and Public Relations Office.* 2012. http://outreach.eri.u-tokyo.ac.jp/eqvolc/201103_tohoku/eng/#aftershock%20past%20quake.
PIANC . "Mitigation of tsunami disasters in ports." 2010.
Plas, T. van der. *A STUDY INTO THE FEASIBILITY OF TSUNAMI PROTECTION STRUCTURES FOR BANDA ACEH & A PRELIMINARY DESIGN OF AN OFFSHORE RUBBLE- MOUND TSUNAMI BARRIER* . Delft: Tudelft, 2007.
Pricewaterhouse Coopers. *Pricewaterhouse Cooper* . 2009. http://www.pwc.com/ .
Raunekk. *bright hub engineering.* 15 11 2012. http://www.brighthubengineering.com/hydraulics-civil-engineering/56319-venice-tide-barrier-project/ (accessed 09 16, 2014).
Schloemer, R.W. "Analysis and synthesis of hurricane wind patterns over Lake Okeechobee." *Hydrometeorological Report, USWB, No. 31, pp. 1-49* , 1954.
Shima, Etsuzo, Manabu Komiya, and Keiji Tonouchi. *Estimation of strong ground motion in the Tokyo metropolitan area during the 1923 great Kanto earthquake.* Paper, Tokyo: University of Tokyo, 1988.
Takagi, H. (01 11 2013).
Tanimoto, K. *On the Hydraulic Aspects of Tsunami Breakwaters in Japan* . Tokyo: Terra Scientific Publishing Company , 1981.
TU Delft. *Manual hydraulic structures CT3330.* Delft: TU Delft, 2011.
Vermeer, M., and S. Rahmstorf. *Global sea level linked to global temperature.* Helsinki: Helsinki University of Technology, 2009.
Vries, Peter A.L. de. *The Bolivar Roads Surge Barrier: A conceptual design for the envi- ronmental section* . Delft: Tu Delft, 2014.
Vryhof anchors. *Vryhof anchor manuals* . Vryhog anchors, 2005.
—. *Vryhof anchors.* http://www.vryhof.com/products/mooring_lines.html (accessed 2014).
Wikipedia. http://en.wikipedia.org/wiki/Tokyo_Bay#mediaviewer/File:Tokyobay_area.png (accessed 2014).
—. *Wikipedia.* http://en.wikipedia.org/wiki/Sumida_River (accessed 2013).
World weather and climate information. *World weather and climate information.* 2013. http://www.weather-and-climate.com/average-monthly-Rainfall-Temperature-Sunshine,Tokyo,Japan (accessed 11 10, 2013).
Wu, Y. "Numerical tsunami propagation of 1703 Kanto earthquake." Tokyo, 2012.
Yasuda, Tomohiro. *Projection of future typhoons landing on Japan basd on a stochastic typhoon model utilizing AGCM projections.* Kyoto: J-Stage, 2010.

LIST OF FIGURES

LIST OF TABLES

ography